NASA SP-5098

TECHNOLOGY UTILIZATION

POWDER METALLURGY IN AEROSPACE RESEARCH

A SURVEY

NATIONAL AERONAUTICS AND SPACE ADMINISTRATION

NASA SP-5098

POWDER METALLURGY IN AEROSPACE RESEARCH

A SURVEY

By
H. W. Blakeslee

PREPARED UNDER CONTRACT FOR NASA BY
FRANKLIN INSTITUTE RESEARCH LABORATORIES
Philadelphia, Pennsylvania

Technology Utilization Office 1971
NATIONAL AERONAUTICS AND SPACE ADMINISTRATION
Washington, D.C.

For sale by the Superintendent of Documents,
U.S. Government Printing Office, Washington, D.C. 20402
Price $1 Stock number 3300-0397
Library of Congress Catalog Number 71-611991

Foreword

A program has been established by the National Aeronautics and Space Administration to collect the results of aerospace-related research, and to evaluate, organize, and disseminate them for the benefit of the industrial and educational communities of the Nation. Other Governmental organizations also benefit from this dissemination process, at state and local levels. The new technology so collected and prepared for different audiences is described and announced in appropriate documents issued by the Technology Utilization Office of NASA and made available to potential users. These documents describe the nature of, and uses for, the latest developments in materials, processes, management systems, products, and design methodology.

In this document, one of a series dealing with specialized processes, the methodology and results of powder metallurgy are described so potential users can evaluate their worth in non-aerospace applications. Since the process is one by which many parts can be made that are not practical to produce by other methods, by which metals can be worked at temperatures lower than would otherwise be required, and which is of value in designing parts for particularly severe service conditions, NASA has had a major interest in its development. Others have also contributed, and the field is one of the most rapidly growing methods for the production of metallic parts and composites.

This report discusses the various techniques by which powders can be produced, as pure metals or as alloys; it explains the methods by which these powders can be formed into the final parts, and further processing that may be necessary to meet the specific requirements spelled out by the user. The NASA developments are detailed, and references are provided for those who wish to obtain further information characteristic of any methodology. Compiled by experts associated with the Franklin Institute Research Laboratories, the document should be of value to manufacturing establishments, and to investigators in such areas as high strength, high temperature service, or the resistance of materials to cryogenic temperatures.

Director
Technology Utilization Office

Acknowledgments

The author is indebted to Dr. Henry H. Hausner, internationally recognized authority on powder metallurgy, with whom he spent many hours discussing and editing the manuscript. The assistance of many NASA Headquarters personnel is also gratefully acknowledged. In particular, the author acknowledges the assistance of Edward N. Case, Special Assistant to the Director for Publications, Technology Utilization Office, NASA Headquarters.

Personnel at several NASA Centers have been very helpful, providing information and data on their projects. These include:

Lewis Research Center—Harrison Allen, Jr., John Weeton, John Freche, Robert Hall, John Kazaroff, and Gordon Watson.

Langley Research Center—Paul Kurbjun, Marion Seyffert, John Buckley, Thomas Bales, Clyde Thiele, Charles King, Robert Little, John Morgan, Al Burbas, and Edgar Kastelberg.

Marshall Space Flight Center—H. L. Martin, Eugene McKannon, Orvil Reece, and Marshall King.

Space Nuclear Propulsion Office—Samuel Snyder, Walter Scheib, and Harold Hessing.

The author would also like to thank Mark Klein and Kathleen Mason of Science Information Services, The Franklin Institute Research Laboratories, for their aid.

Contents

	Page
Chapter 1. INTRODUCTION	1
Chapter 2. SELECTED POWDER METALLURGY PROCESSES	5
Powder Production	5
Powder Blending	13
Powder Compaction	15
Sintering	28
Post-Sintering Processes	31
Safety in Handling Powders	35
Chapter 3. POWDER METALLURGY OF SPECIFIC METALS	39
Light Metals	39
Common Metals	55
Refractory Metals	62
Chapter 4. POWDER REINFORCED COMPACTS	73
Nickel	79
Chromium	83
Cobalt	87
Tungsten	87
Iron and Copper	89
Chapter 5. FIBER REINFORCED COMPACTS	93
Copper-Infiltrated Tungsten Wires	94
Tungsten Wire Properties	101
Tungsten Wire in Noncopper Matrices	107
Whisker-Reinforced Composites	113
Oxide Fiber Reinforcement	114
Chapter 6. SOME SPECIAL POWDER METALLURGY PRODUCTS	121
Porous Materials	121
Materials for Electrical Applications	129
Sintered Bearings	134
Nuclear Materials	144
REFERENCES	157

Introduction

Powder metallurgy has been a viable metalworking technique since antiquity because of its ability to form metal objects without fusion. In prehistoric times, iron and copper were formed by reducing ores with charcoal and pounding the resulting spongy mass into shapes. With the advent of better furnaces, this technique was replaced by smelting, but powder metallurgy continued to be the only way to form the higher melting refractories and ceramics. By the 20th century, furnaces had been developed so that platinum (melting point 3224° F) could be fused. The trend has continued and now powder metallurgy's hold on the refractory metals tungsten and molybdenum is being threatened. Despite this, powder metallurgy is increasing in importance in industry because of several other inherent advantages. For example, it can be used to form certain materials such as:

- Fully dense objects having close dimensional tolerances and complex shapes without machining; for example, gears, cams, and bushings.
- Porous materials with controllable porosity ranging from above 60% to less than 1%.
- Composites of two or more materials with widely disparate properties; for example, an alloy where one metal melts above the boiling point of the other.
- Materials with extremely fine grain structures.
- Alloys which cannot be fused because of deleterious reactions such as carbide precipitation.
- Metals which cannot be fused because of the formation of a weak lattice structure upon solidification, such as beryllium.

The basic process of powder metallurgy is repeated by every child making snow balls. A finely powdered starting material is pressed and sintered into a dense compact. The snow never reaches the melting point and yet a solid is produced. The pressing and sintering take place simultaneously, as do they in the industrial process of hot-pressing, powder extrusion, powder rolling, and powder forging. Metal powders formed by grinding or chemical reduction of metallic compounds are pressed into the de-

sired shape by hydraulic presses. The degree of particle surface roughness and the compaction pressure determine the "green strength" of the compact which has to hold together during sintering. Sintering takes place below the melting point of the material, and is the process whereby the multiparticle compact is converted into a uniform solid. Variations in press and sinter techniques include isostatic compaction, where a rubber mold is filled with powder and then subjected to gas or hydraulic pressure; slip casting, a molding technique; and loose powder sintering, often used to form porous materials.

Smooth spherical powders can be produced by dispersing a molten metal or alloy into fine droplets which harden while suspended in a gas stream. High-purity materials can be obtained, but when compacted they have very low green strength. For this reason, the techniques mentioned earlier that combine compaction and sintering are used. Often, the powders are enclosed in metal cans under vacuum before these operations. In addition to compaction and sintering, the metal is extruded, rolled, and forged to impart higher strength and better homogeneity to the final product. Consequently, pressed and sintered compacts are also often postformed.

The powder metallurgy techniques presented in this Special Publication are not the typical processes described above but rather adaptations of these techniques as applied to modern aerospace problems. Here is positive proof of the vitality of powder metallurgy: in some cases, it is the only means possible, and in others, it is the best means of obtaining special alloys and properties. Examples of these include:

- Superalloys that exhibit superplasticity at 2000° F
- Dispersion-strengthened composites which retain usable strength at temperatures close to the melting point of the metallic matrix
- Fiber-reinforced composites containing fibers produced *in situ* during the forming process
- Metal-carbide-graphite composites having usable strength at 6000° F

The techniques used to make these materials are as interesting as the materials themselves. A few examples are:

- Ball-milling powders down to particles as fine as those in cigarette smoke
- Explosive compaction of powder
- Hot-isostatic compaction with gas pressures of 15 000 psi and 1600° F
- Extrusion at temperatures up to 5000° F.

This document on powder metallurgy, as used by the National Aeronautics and Space Administration, should be particularly useful to workers in materials engineering and powder metallurgy fields. It contains material not usually found in the technical or trade literature because industrial researchers are not encouraged to publish details of new commercial developments for obvious, proprietary reasons. On the other hand, reports describing NASA research and developments are openly distributed except when restricted for reasons of national security. Thus, this publication can guide interested readers to detailed NASA reports, proceedings of conferences, and articles describing the techniques and processes mentioned here. In addition, a section covers industrial hazards of handling powders. NASA's interest in this is twosided because of the potential use of pyrophoric powders as fuels, and because of the dangers to personnel working with these materials.

Page intentionally left blank

CHAPTER 2

Selected Powder Metallurgy Processes

In 1958, powder metallurgy was defined by the American Society for Testing and Materials as "the arts of producing metal powders and of the utilization of metal powders for the production of massive materials and shaped objects." Powder metallurgy today has become more than just an art, and the many NASA contributions to the fundamentals of this technique have considerably advanced its development into a science.

Powder metallurgy consists basically of the steps of compaction and sintering, apparently simple operations, but this is only part of the picture. The complexity and expense of the process go up as the requirements of strength and dimensional tolerances are increased (fig. 1) (ref.1). Also, there are important criteria for the production, characterization, and mixing of the metal powders, which must be considered. Thus, it soon becomes evident that powder metallurgy consists of a series of complex operations, each of which is vitally important to the success of the final product.

POWDER PRODUCTION

The first consideration in powder metallurgy is, of course, the powder itself. There are almost as many ways to produce powders as there are metals from which they are produced, but basically, there are seven general methods. These include atomization of molten metals, chemical reduction of metallic compounds, and mechanical comminution of solid metals. Some commercial methods together with raw materials, product characteristics, advantages, and disadvantages of each are listed in table I. Typical applications of the powders resulting from each of these methods are listed in table II.

Most of the metal powders used in industrial powder metallurgy range in size from 4 to 200 microns. During the last few years, however, powders of submicron size have been developed by NASA and used for various purposes, one of the most important being the application of "ultrafine" particles to dispersion-strengthened materials (chapter 4). Metal powders with particles

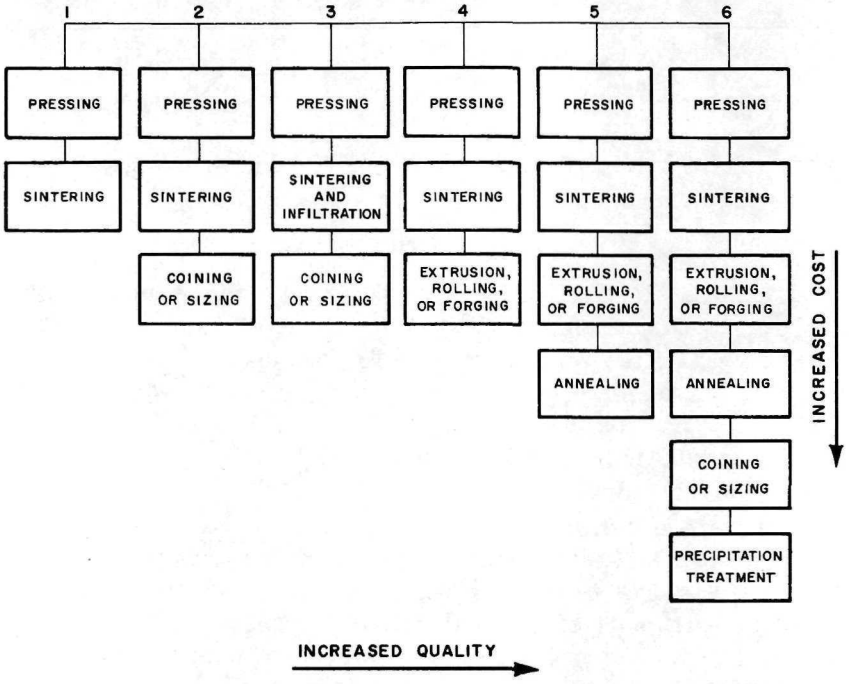

FIGURE 1.—Various common processes for the manufacture of sintered structural parts (ref. 1).

in the size of 0.01 to 1 micron are used for the production of these alloys, but they offer many difficulties. For example, they do not flow in any standard equipment, they agglomerate easily, the loose powder density is very low, there is high friction between the particles, they oxidize readily with the atmosphere and are difficult to reduce without bonding together, and they change their characteristics when stored. The advantages are the very fine grain sizes possible in the dispersed phase and the good dispersion itself. In other applications, extremely fine particles sinter readily at lower temperatures and in shorter times than are required by their coarser counterparts.

The methods developed by NASA to produce ultrafine powders include ball-milling (refs, 2, 3, and 4) and various reduction processes (refs. 5, 6, and 7). In ball-milling, grinding is usually accompanied by particle welding and agglomeration. In the past, this has made the milling of ductile metals difficult (ref. 8). The ultimate particle size obtained levels off when the grinding rate equals the particle-welding rate. Liquid-grinding aids have been used to reduce this welding tendency, by reducing the final parti-

cle size (ref. 9). These are generally surfactants which tend to create surface charges on the particles, holding them apart. Quatinetz, Schafer, and Smeal of the Lewis Research Center found that various inorganic salts in alcohol were far more effective as grinding aids (ref. 2). Powders of copper, chromium, iron, silver, and nickel were successfully ground to less than 1 micron in size using these aids. The mechanism for this effect was not understood until recently through work by Arias, also at Lewis (ref. 3). It is now felt that chemical reactions occurring at the surface of the particles during grinding enable the production of extremely fine particle sizes.

Brittle materials, such as glass, can be pulverized readily by hammering. The impact of the blows breaks the particles into smaller pieces. Ductile metals such as iron or copper cannot be fractured as readily, but more brittle ones, such as chromium, can be ground in this manner. Chromium is brittle down to a particle size roughly approximating its grain size and is ductile below this size. Thus, the brittleness appears to be due to intergranular cleavage. The particle size reached by ball-milling chromium in an inert environment is about 0.5 micron; in a reactive environment, however, particle sizes below 0.06 micron can be acheived.

A variety of grinding liquids has been found to produce pressure increases during ball-milling which have been attributed to temperature rise. Chromium milled in water, however, produces too large a pressure to be explained in this way, and mass spectroscopy has shown the gas produced to be hydrogen. As the metal is being ground, the fresh surfaces react with the water to form a layer of chromium oxide and hydrogen. This protective layer hinders the freshly cleaved surface from welding together, and consequently, finer particles are produced. Some agglomeration still occurs, so the resulting powder has some oxide trapped inside the particles as well as on the surface, making cleaning more difficult. The reaction occurring at room temperature is predominantly: $2Cr(solid) + 3H_2O(liquid) = Cr_2O_3(solid) + 3H_2(gas)$. This reaction had not been observed previously because chromium is normally covered by a thin oxide layer, but ball-milling either flattens or breaks up the particles, exposing fresh surfaces. Only these exposed surfaces react with water at room temperature.

In practice, flake chromium powder was hammer-milled to pass through a 30-mesh screen. All subsequent processing was done under an atmosphere of argon gas. The ball mill, illustrated in figure 2, has a volume of 1580 cm^3 and is pressure tight. Four hun-

TABLE I.—*Comparison of Principal Commercial*

	Atomization	Gaseous reduction of oxides	Gaseous reduction of solutions
Raw materials	Scrap or virgin melting stock or metal or alloy powder desired	Oxides of metals such as Cu_2O, NiO, Fe_3O_4	Ore for leaching or other metal salt solution
Type of powders produced	Stainless steel, brass, bronze, other alloy powders, aluminum, tin, lead, iron, zinc	Iron, copper, nickel, cobalt, tungsten, molybdenum	Nickel, cobalt, copper
Typical purity*	High, 99.5+	Medium, 98.5 to 99.0+	High, 99.2 to 99.8
Particle shape	Irregular to smooth rounded dense particles	Irregular, spongy	Irregular, spongy
Meshes available	Coarse shot to 325 mesh	Usually 100 mesh and finer	Usually 100 mesh and finer
Compressibility (softness)	Low to high	Medium	Medium
Apparent density	Generally high	Low to medium	Low to medium
Strength	Generally low	High to medium	High
Advantages	Best method for alloy powders. Applicable to any metal or alloy melting below 3000° F.	Easy to control particle size of powder. Good compacting powder.	Ore can be used. Purification during leaching. Fine particles.
Disadvantages	Wide range of particle sizes, not all salable. Particles too spherical for some applications.	Requires high grade oxides. Restricted to reducible oxides.	Applicable to few metals such as nickel, cobalt, copper

* Purity varies with metal powder involved; estimates are typical purity.

dred 12.6-mm stainless-steel balls in 750 ml of degassed water provided the grinding medium for 150 g of powder, and milling was done at 100 rpm in time periods ranging from 2 to 32 days. In the longest period, the average particle size of the resulting powder was 0.031 micron. Its oxygen content was very high, representing 58% Cr_2O_3, and it appeared that if ball-milling had been continued, the metal would have been totally oxidized. The iron content of the powder increased steadily with the milling time, representing metal picked up from the balls and the body of the mill. This effect was tested in a subsequent project by running the ball mill without an initial powder charge (ref. 4). Powder was produced at a rate of 2.5 mg/hr, and this powder was also oxidized by the water to produce hydrogen.

Powders of zirconium, tantalum, iron, stainless steel, nickel,

Methods of Producing Metal Powders

Reduction with carbon	Electrolytic	Carbonyl decomposition	Grinding
Ore or mill scale	Soluble anodes	Selected scrap, sponge mattes	Brittle materials such as beryllium, high sulfur nickel, high carbon iron, antimony, bismuth, iron and manganese cathode
Iron	Iron, copper, nickel, silver	Iron, nickel, cobalt	Iron, beryllium, manganese, nickel, antimony, bismuth
Medium, 98.5 to 99.0+	High, + 99.5+	High, 99.5+	Medium, 99.0+
Irregular, spongy	Irregular, flaky to dense	Spherical	Flaky and dense
Most meshes from 8 down	All mesh sizes	Usually in low micron ranges	All mesh sizes
Medium	High	Medium	Medium
Medium	Medium to high	Medium to high	Medium to high
Medium to high	Medium	Low	Low
Low cost. Control of particle size. Controlled variation in properties possible.	High purity of product. Easy to control.	Produces fine, pure powders	Controlled size of powder
Requires high grade ore or mill scale. Applicable mainly to iron.	Limited to few metals, high cost.	Limited to few powders, high cost.	Limited to brittle or embrittled materials. Quality of powder limits use. Slow.

copper, and silver were also ball-milled in water. Of these metals, only zirconium, tantalum, iron, and stainless steel, whose oxides are more stable than water, were reduced to the desired ultrafine particle size. The remaining metals, nickel, copper, and silver, were not comminuted, nor did they react with the water. If oxygen gas were added to the system, nickel and copper could then also be comminuted.

The major problem with this ball-milling technique is the excessive amount of oxide produced in the final powder. In some cases it exceeds 50% of the final product and is dispersed throughout the particles. Reducing these oxides has been done with hydrogen (refs. 10 and 11), or with reactive metals (ref. 6). However, the temperatures needed to reduce oxides of nickel and chromium efficiently are high enough to cause sintering between the powder

TABLE II.—*Relation of Powder Production Method to Typical Applications of Some Resulting Powders*

Production method	Typical powders	Typical applications
Atomization	Stainless Steel	Filters, mechanical parts, atomic reactor fuel elements
	Brass	Mechanical parts, flaking stock, infiltration of iron
	Iron	Mechanical parts (medium to high density), welding rods, cutting and scarfing, general
	Aluminum	Flaking stock for pigment, solid fuels, mechanical parts
Gaseous reduction of oxides	Iron	Mechanical parts, welding rods, friction materials, general
	Copper	Bearings, motor brushes, contacts, iron-copper parts, friction materials, brazing, catalysts
Gaseous reduction of solutions (hydrometallurgy)	Nickel	Iron-nickel sinterings, fuel cells, catalysts, nickel strip for coinage
	Copper	Friction materials, bearings, iron-copper parts, catalysts
Reduction with carbon	Iron	Mechanical parts, welding rods, cutting and scarfing, chemical, general
Electrolytic	Iron	Mechanical parts (high density), food enrichment, electronic core powders
	Copper	Bearings, motor brushes, iron-copper parts, friction materials, contacts, flaking stock
Carbonyl decomposition	Iron	Electronic core powders, additive to other metal powders for sintering
	Nickel	Storage batteries, additive to other metal powders for sintering
Grinding	Iron	Waterproofing concrete, iron from electrolytic cathodes—see Electrolytic above
	Manganese	Welding rod coatings, pyrotechnics
	Nickel	Filters, welding rods, sintered nickel parts

particles; under milder conditions, incomplete reduction is often the result. Weeton and Quatinetz overcame these problems by compacting the uncleaned powders into wafers and then simulta-

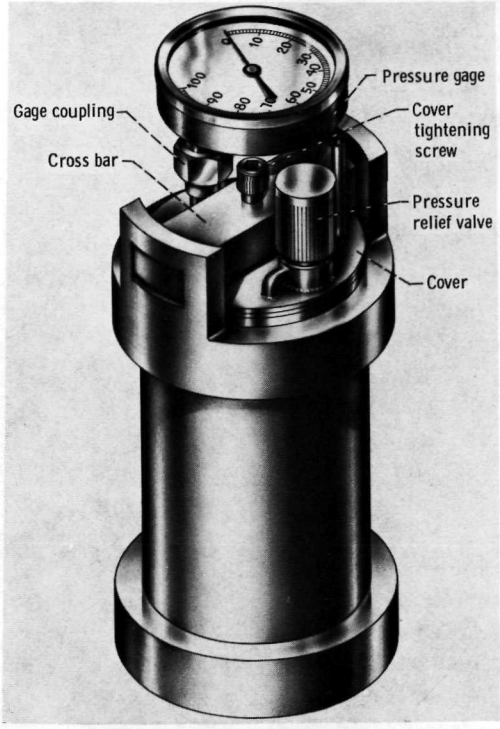

FIGURE 2.—Gas-tight ball mill with pressure gage (ref. 3).

neously cleaning and sintering them (ref. 10). The fine particle size in this dispersion-strengthening work is required to create an initial dispersion. Sintering after the dispersion has been established in the compact does not harm the final product if it is adequately cleaned. One NASA contractor took a different approach (ref. 11), by suspending ultrafine nickel powder in a stream of hydrogen and passing it through a heated tube at 335° C. The flow was adjusted to give the powder a 22 sec residency time in the hot zone, which lowered the oxygen content to a level of 0.05% by weight. Even in this arrangement, however, the average particle size increased to some extent. One advantage of this technique is the ability to feed the cleaned powder directly into storage containers and to seal it under the same hydrogen.

Arias, at Lewis, used reactive metal vapors to reduce these oxides (ref. 6). He reduced Cr_2O_3 powders that had been ground to a true colloidal size (as small as 0.0068 micron) with magnesium vapor in a vacuum furnace. Lithium and sodium vapors also

worked in this procedure. Nickel powder (1.25 microns) was made from NiO reduced with lithium vapor.

Other reactive techniques can be utilized to reduce particle size in ball-milling. Hydrogen halide gases, for example, form metal halides, which are far more easily reduced than the oxides. Research at Lewis took this approach also, and 0.04-micron chromium powders were produced by ball-milling under hydrogen chloride gas (ref. 12). The product contained chromium chloride, which was reduced in flowing hydrogen gas at 680° C. Milling nickel in hydrogen bromide produced 0.023-micron powder containing 23% nickel bromide, which was easily reduced at 350° C in hydrogen.

Alloy powder was developed for NASA by spray-drying an aqueous mixture of salts (ref. 7). Cobalt and nickel oxalates, chromium acetate, molybdenum trioxide, and thorium nitrate are all soluble in an aqueous solution in proportions equivalent to those found in L–605 cobalt-base superalloy. Spray drying is a technique developed by the chemical industry for drying solutions with low content of solids by contacting a spray with a blast of hot air. The powders so produced were calcined to convert all the metal compounds to the oxides at 800° C in air and then reduced in hydrogen. As expected, all elements in the alloy except thorium were reduced, and the final product was a superalloy powder with dispersed thoria.

Ultrafine particles of iron, nickel, and beryllium have been produced by electrolysis using a mercury cathode. This process is most suitable for high-melting-point metals which do not react or dissolve in mercury to an appreciable degree. Beryllium, for example, has a solubility of 0.001% by weight in mercury. One procedure was developed for NASA to produce ultrafine beryllium for eventual evaluation as a rocket fuel (ref. 5). Its potential value in powder metallurgy was also recognized, since such a powder will yield a high-density, fine-grained compact at low compaction pressures and low sintering temperatures.

A fused salt composed of approximately equal parts of $BeCl_2$ and NaCl is used as the electrolyte. Water has to be excluded because beryllium hydrates so readily that water prevents the formation of the free metal. Sublimed $BeCl_2$ is fed into the electrolysis cell which is at a temperature of 270° to 300° C. It is then reduced and collected in the mercury cathode as sort of a quasi-amalgam which is drawn off and filtered. The paste is pressed to squeeze out all possible mercury and the rest stripped by vacuum distillation. A powder with a particle size of 0.1 to 0.2 micron results.

POWDER BLENDING

The mixing or blending of powders is an important step in the powder metallurgy process that is often overlooked. It is required in the preparation of alloys from elemental powders, in the production of dispersion-strengthened metals, and even in the preparation of effective sintering mixtures through control of particle size. Many disappointing results in materials prepared from powders result from incomplete understanding of the mixing process. Some problems which can occur during mixing are: Changes in particle size distribution through grinding or agglomeration, oxidation of particle surfaces, segregation of particle sizes during removal from the mixer, or difficulties in obtaining a representative sample. Fundamental investigations of mixing and blending require a careful analysis of the frictional conditions in the powder mass which affect the relative movement of the particles during mixing.

The properties of compacted and sintered composite materials are dependent upon the thoroughness of the blending process. Norris et al. compared a high-speed blender, a twin-shell V-blender, a plastic mill with glass balls, and a stainless-steel blender with nickel balls (ref. 13). Both dry mixing and wet mixing with oleic acid dissolved in heptane as a dispersant were evaluated. The powders used were 0.054-micron nickel powder with 0.025-micron alumina powder proportioned to yield a dispersion-strengthened nickel containing 5% alumina. Electron micrographs show the resulting dispersions clearly. For example, comparison of a good dispersion and a poor one is shown in figure 3. The good one was obtained under wet conditions and the poor one under dry conditions. This was a typical result of this program, pointing up the value of wet blending. The oleic acid used as a dispersant in the wet-blending technique tended to be absorbed by the surfaces of the particles, preventing effective sintering until it was removed. This could be done to some extent by a vacuum treatment at 950° F, but it was found best to clean the powder with hydrogen.

Agglomeration of fine, dispersed particles often occurs during sintering, making evaluation of the dispersion obtained through mixing and compaction difficult. Also, the sintering temperature may cause chemical reactions with some of the impurities that are usually present in ultrafine powders. Three alternative techniques were tried at Lewis to avoid these problems (ref. 14). Two involved the immobilization of the dispersed powder in a plastic matrix for metallographic examination. While these techniques

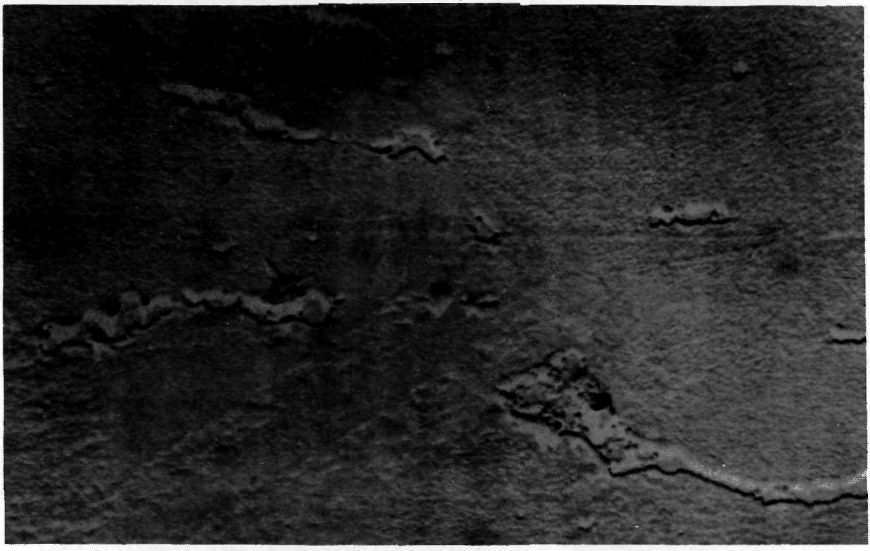

Dry blended in plastic mill.

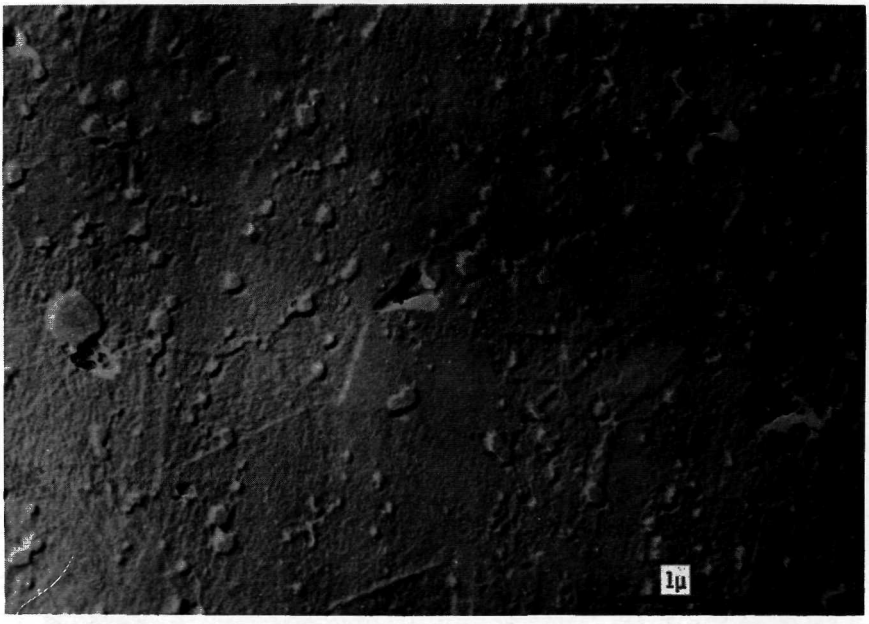

Wet blended in plastic mill.

FIGURE 3.—A comparison of blending techniques (X46 000) (ref. 13).

were successful, the application to compacted samples was difficult. The third technique was to compact the mixture by high energy without heat. The results, in general, were high-density samples that could be prepared for examination, and which clearly indicated the degree of dispersion that had been achieved without agglomeration. The compaction techniques tried included a cartridge caliber .45-actuated compaction press, a Dynapac high-velocity press, and an explosive compaction in which sheet explosive was used at a shock velocity of 15 000 fps.

POWDER COMPACTION

The cartridge-actuated press (fig. 4) and the Dynapac (fig. 5) operate on a similar principle, i.e., the instantaneous application of a tremendous amount of energy to the sample through the use of a projectile. The Dynapac fires a 9000-lb ram at a speed of 210 fps at a 0.81-in. sample. The total energy is about 70 000 ft-lb, but part of this appears to be dissipated through the deformation of the plunger and die. Samples compacted in this way tended to delaminate easily, although pieces were suitable for examination.

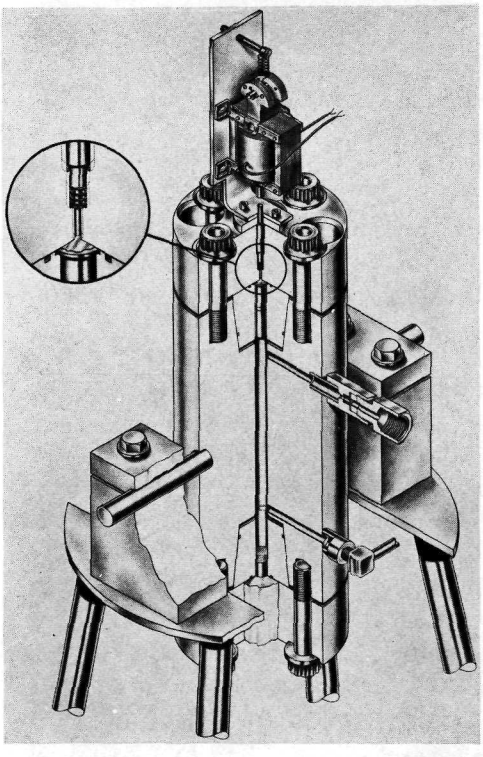

FIGURE 4.—Cartridge-actuated compaction press (ref. 14).

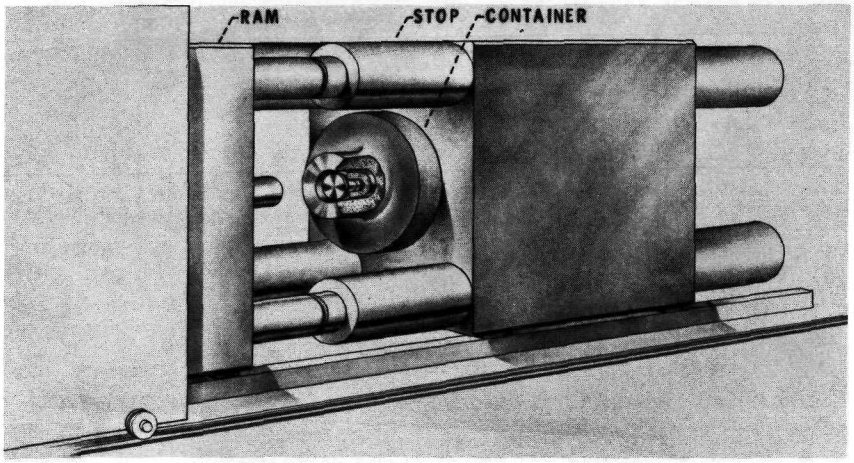

FIGURE 5.—High-velocity impact compaction in Dynapak (ref. 14).

The cartridge-actuated press imparts only about 220 ft-lb of energy to the sample by firing a 22.5-g slug at velocities up to 600 fps. The small size (0.45-in diameter by $^1/_{16}$-in. thick) of the sample allowed loading and firing in a dry box with an inert atmosphere. A sample of this size was also convenient for metallographic work. Heating the compact to 1700° F considerably improved the contrast between the dispersed particles and the matrix in electron micrographs without causing any appreciable agglomeration.

The sample that was explosively bonded in this program was not successful, probably because the detonation velocity was too high. Reece reports that a detonation velocity of 8000 to 12 000 fps is the right range for the compaction of powders (ref. 15). Cyclonite-based explosives have velocities in excess of 20 000 fps, and Prima Sheet, about 15 000 fps. Dynamite and nitroguanidine are in the 8000- to 12 000-fps range, but the latter is much safer (less sensitive), cleaner (a white fluffy material), and cheaper (about 35¢/lb.). Reece's initial work with explosive compaction centered around the production of fiber reinforced sheet materials, but more recently he has begun powder-compaction experiments (ref. 16). He tested a variety of dissimilar materials. For example, titanium, magnesium, aluminum, molybdenum, and niobium powders were compacted around thin stainless steel wires. Other materials include superconductive intermetallic compounds and self-lubricated electrical brush materials. An almost limitless variety of metals can be bonded without regard to melting point

or solubility. Extrusion billets can also be prepared with mixtures of metals not obtainable by other means, such as titanium with magnesium. Similarly, the production of bimetallic joints used to join different metals is possible. Also, explosive compaction can be used to make specially shaped articles by compacting powders around a rigid form. For example, a porous filter with precise external dimensions could be made by placing a powder mixture of the desired metal and a leachable metal inside a rigid cylindrical die with the explosive charge at the center. The resulting cylinder would be solvent-treated to produce the filter.

The technique for experimental explosive compaction of metal powders is rather simple (fig. 6). The powder mixture is placed in a ¼-in.-diameter copper or aluminum tube. The ends of the tube are crimped without precaution against atmospheric contamination, and it is placed upright in the center of a cardboard cylinder 5-in. in diameter by 15-in. The remaining volume of the cylinder is filled with nitroguanidine explosive, packed to a density which will yield the desired detonation velocity. A blasting cap and a tetryl booster are positioned about an inch above the sample and the whole apparatus placed on a steel anvil. Too high a detonation velocity results in the initial appearance of a pinhole running longitudinally down the center of the sample. Higher ve-

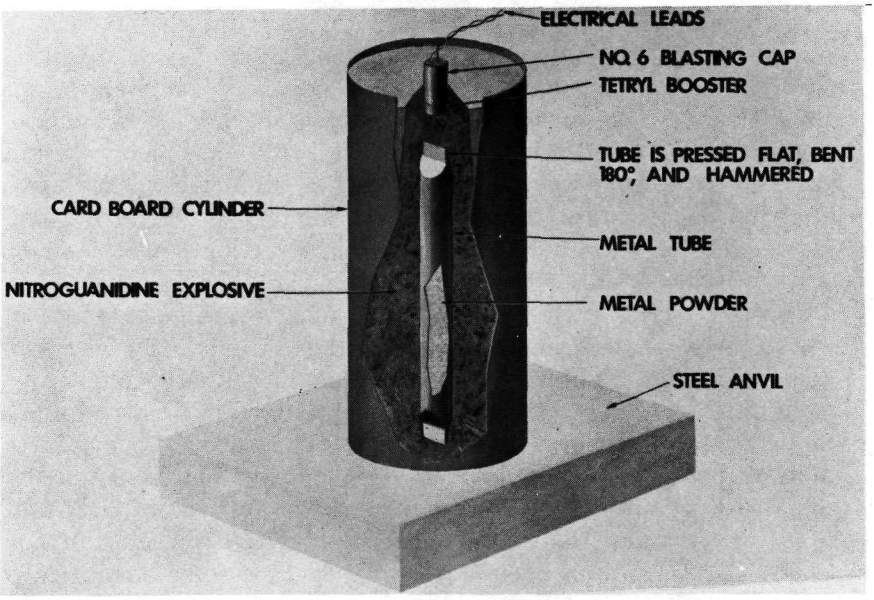

FIGURE 6.—Setup for explosive compaction of metal powders (ref. 15).

locities cause larger holes, finally rupturing the sides of the sample. This occurred in the Lewis work mentioned previously (ref. 14).

The high-energy-rate compaction techniques are not common in industrial powder metallurgy, and even in NASA work, they constitute experimental shortcuts. There are isolated examples where it is a useful technique, such as in the high-velocity manufacture of printing characters, and these can be expected to become more common (ref. 17). More common methods of compaction include hydraulic pressing with metallic dies, hydrostatic pressing, isostatic pressing, extrusion, rolling, and forging. There are also techniques of powder consolidation which do not involve any pressure, such as slip casting, vibrational compaction, and loose powder sintering in molds. Hydraulic and isostatic compaction can be done either hot or cold. When done cold, the mechanical interlocking and deformation of the powder particles as well as cold-welding determine the green strength which holds the compact together until it can be sintered. Hot-pressing involves a certain amount of sintering during compaction and a resulting fused matrix which can be used as is or further worked by forging, extrusion, or rolling. Also, loose powders are often sealed in metal cans to protect them from oxidation while being forged, rolled, or extruded. These processes impart great amounts of energy and deformation to the powder and the result is a fully dense part. Cold-compaction requires powders with irregular shapes to build enough green strength before sintering. The newer spherical powders have low green strength when cold compacted and so are either hot-pressed or are canned before working. Pressureless techniques are used where special shapes or specific properties are required. For example, loose-powder sintering is a way to form porous filter material. Slip casting green strength comes from adhesively bonding a powder matrix. The organic binder burns off during sintering.

Several of these pressureless and pressure technqiues were involved in a project undertaken for the Marshall Space Flight Center (ref. 18). The purpose was to manufacture a complex beryllium machining blank that would consist of an 8-in. irregularly shaped block with several 3 in.-holes entering from various directions and to various depths. The initial fabrication technique was cold isostatic pressing. The cavities were formed by leachable solid copper mandrels. Since these samples failed because of nonuniform deformation around the mandrels, porous mandrels of approximately the same volume density as the beryllium powder to be compacted around them were used. The mandrels were first

produced by pressure compaction. The green-pressed density of −200-mesh copper powder as a function of hydropressing pressure is shown in figure 7. The density of vibrationally compacted beryllium powder is about 57%, indicating 15 000 psi pressure should be used to form the mandrel. Even at 20 000 psi, however, the samples were too friable, risking the contamination of the beryllium during compacting. Pressureless sintering was the alternative means of forming these mandrels. The desired density could be achieved by sintering −20-mesh copper powder in a graphite mold for 2 hr at 1600° F in hydrogen. Different lots of powder were found to sinter to different densities, so it was necessary to check each lot for sinterability before use.

In forming the beryllium compact, a welded-steel mold lined with a rubber bag was constructed (fig. 8). Vacuum lines attached to the sides insured proper alignment of the bag during filling. The porous copper mandrels were attached to the walls of the bag with rubber cement and the bag was filled with powdered beryllium. This was vibrationally compacted to its limit of 57% of theoretical density, and a rubber top was stretched across the open end and cemented in place. Its shape was determined by a steel cap which fit over it. The mold was placed in an autoclave to be isostatically hot compacted. The final compact with the man-

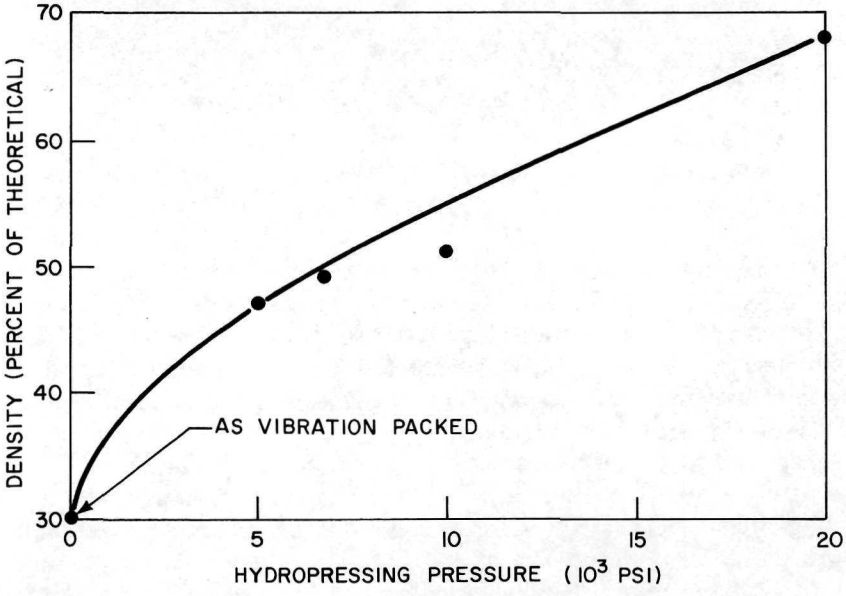

FIGURE 7.—Hydropressing density of −200-mesh copper as a function of pressure (ref. 18).

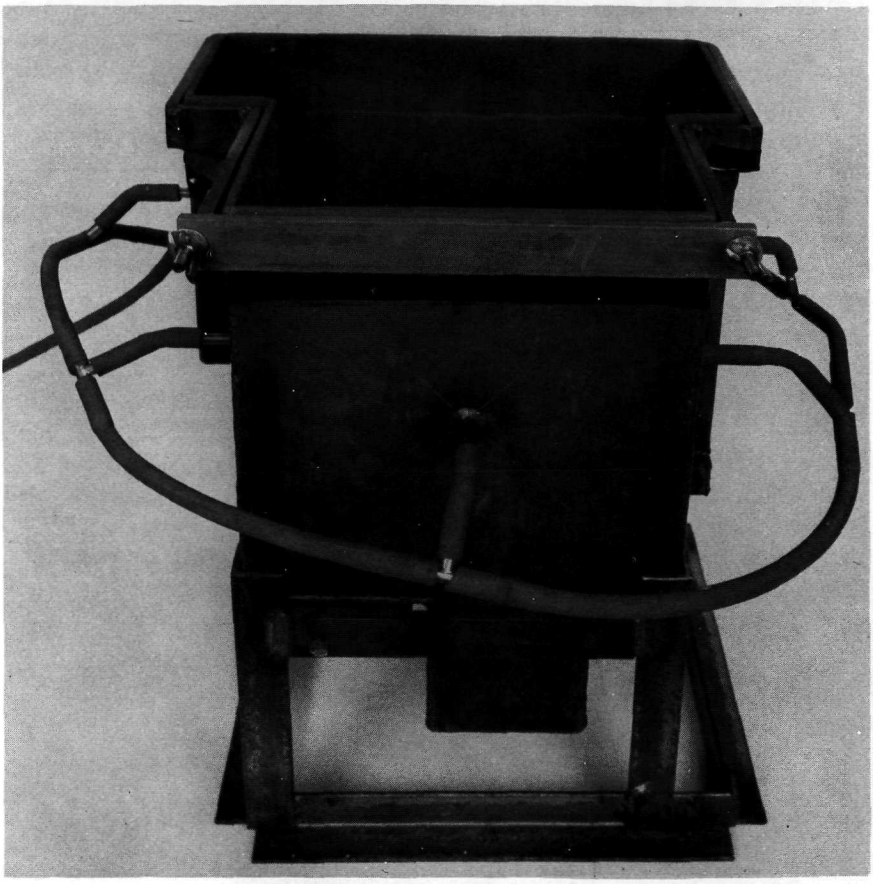

FIGURE 8.—Mold for isostatic compaction of beryllium powder (ref. 18).

drels in place is shown in figure 9; with mandrels removed, in figure 10, and the final machined compact, in figure 11.

Hot-isostatic compaction combines pressing and sintering. The compacting pressure is usually considerably less than that applied in cold pressing, and the temperature is usually considerably less than in the sintering of cold-pressed powders. It is done in a high-pressure autoclave such as is diagrammed in figure 12. The hot-pressed powder compacts have practically full density and fine-grain structure. A basic study of hot-pressing copper and nickel powders for use in rocket engine components containing complex flow channels was recently completed for NASA (ref. 19). The effect of hot-pressing time on the density of copper powder of −270 to +325 mesh at 1000° F is given in figure 13. Com-

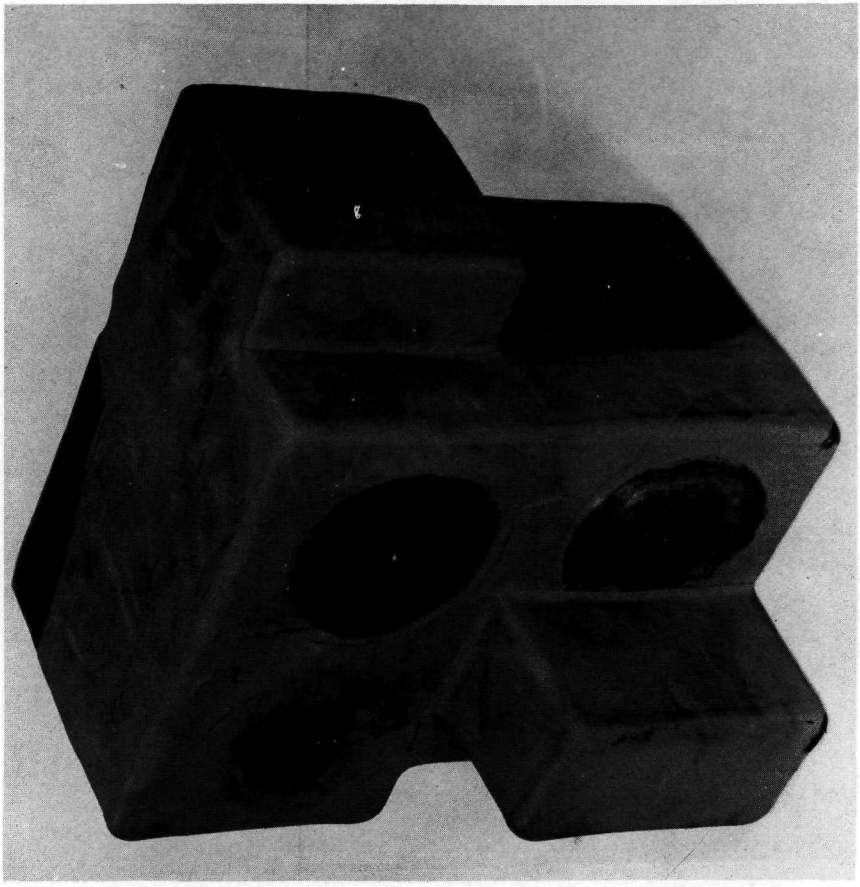

FIGURE 9.—Compacted beryllium block with inserts in place (ref. 18).

paring this to figure 14, which shows the effect of the same variables for nickel, indicates the difference in densification during hot-pressing for these two metals and reflects their differing plastic deformability. The most suitable powder for the fabrication of rocket engine components by hot isostatic compaction had (1) high specific-surface area, (2) fine particle size, (3) small scatter in the particle size distribution, and (4) low-interparticle porosity.

The fabrication techniques developed in this project were based on the compaction of these powders around leachable inserts. Borosilicate glass was found to be compatable with copper and could be selectively removed with a hydrofluoric acid solution. The copper was hydraulically pressed at 20 000 psi and isostatically

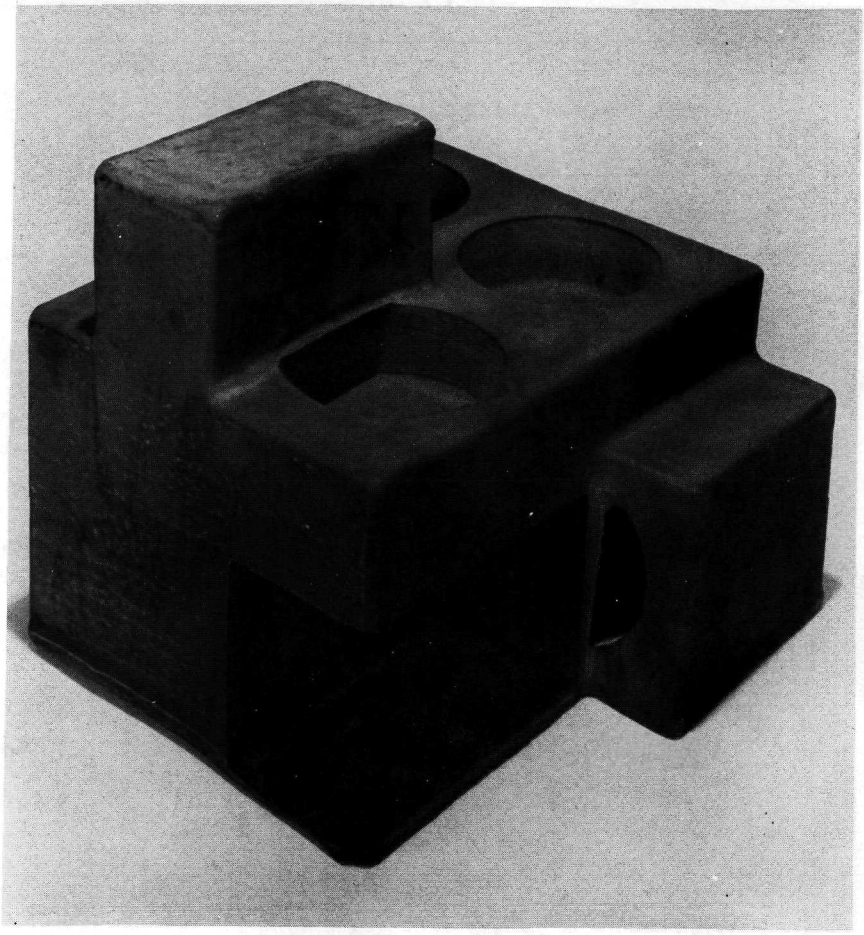

FIGURE 10.—Compacted beryllium block with inserts removed (ref. 18).

hot pressed at 1000° F and 10 000 psi for 3 hr without altering the geometry of the inserts. Nickel powder was similarly compacted around steel or aluminum inserts achieving 98% density. The steel inserts were removed with a sulfuric acid solution and the aluminum with sodium hydroxide or hydrochloric acid solution. The final parts were successfully pressure-checked and alignments of the channels formed by the removal of the inserts were within 0.01 in. The surface finishes were smooth and the mechanical properties comparable to or better than wrought and annealed commercial products.

Jet Propulsion Laboratory (ref. 20) has hot pressed magnesium oxide ceramics. Ceramic compacts were fabricated of high

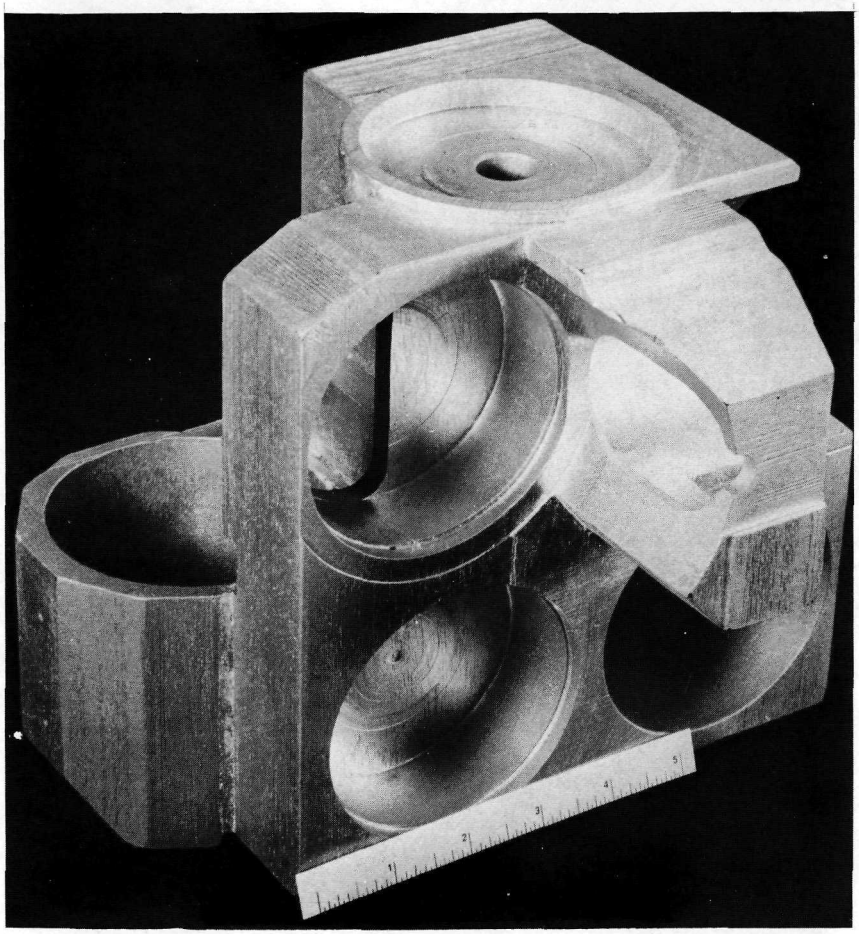

FIGURE 11.—Final machined beryllium compact (ref. 18).

purity MgO at room temperature by isostatic compaction at 90 000 psi in rubber bags and then sealed in metallic containers for hot isostatic compaction at 15 000 psi and 800° C for 30 min. The resulting fine-grained compacts were 95% to 98% of theoretical density and were highly translucent.

Slip casting is common in the ceramic industry. It is a process of pressureless powder consolidation. A fluid suspension of solid particles is cast into a mold. The particles harden into a solid which can be removed from the mold, dried, and then sintered. The value of this technique for powder metallurgy has long been known (ref. 21), but it still is largely overlooked. The process as illustrated in figure 15 first requires the preparation of a metal

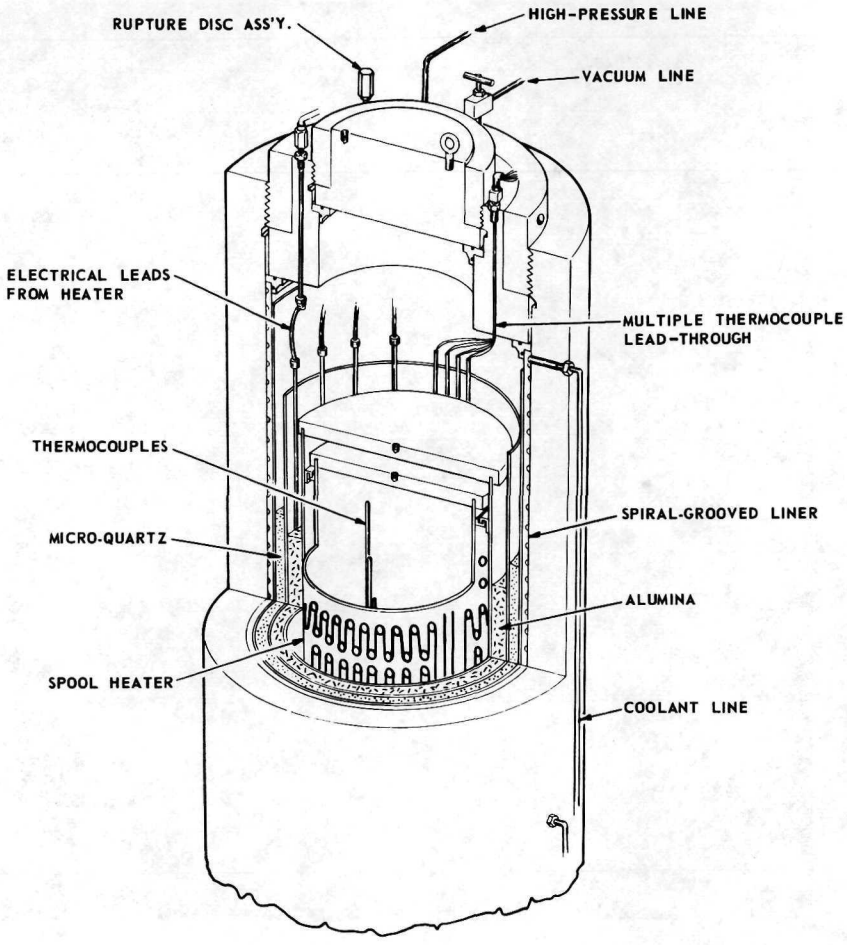

FIGURE 12.—Cold-wall hot-isostatic compaction autoclave (ref. 19).

"slip", that is, a suspension of metal powder in a fluid (ref. 22). Several commercial suspension agents are available: typically salts of alginic acid, or acrylic acid polymers. Acidic or basic additions must be made to the suspension to adjust the pH to a point where the viscosity of the slip is at a minimum for each metal. As shown in figure 16, this minimum is a function of the type of metal, the liquid-to-metal ratio, the surface oxide on the powder, and the speed and duration of agitation in the slip preparation (ref. 23). The slip is poured into a plaster-of-paris mold which absorbs the liquid, leaving agglomerated powder. Inserts can be placed in the molds for hollow objects, or sometimes the

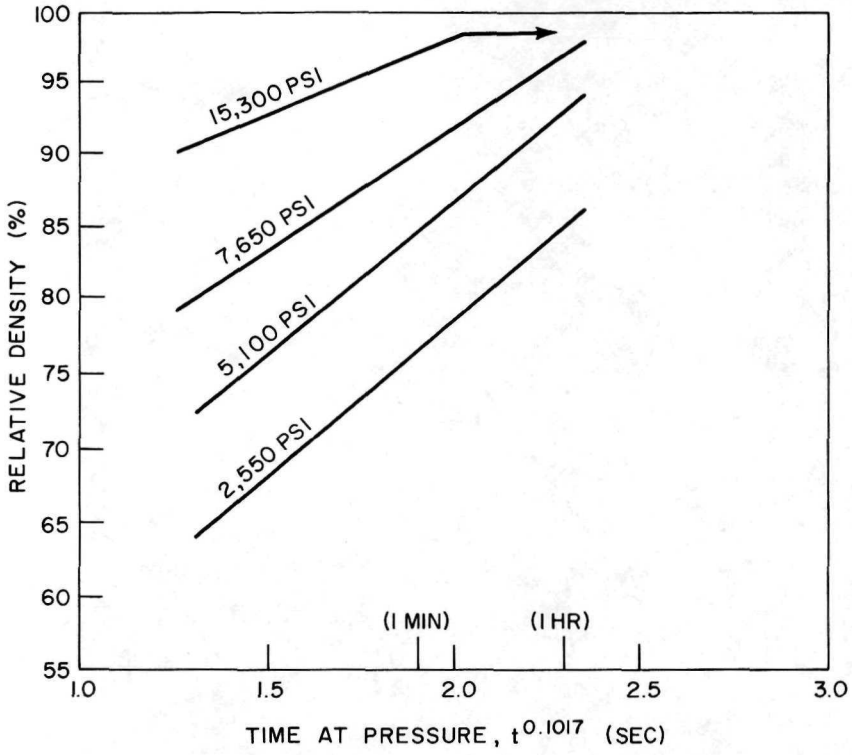

FIGURE 13.—Relative density-time-at-pressure curves for −270 to 325-mesh copper powder hot-pressed at 1000° F (ref. 19).

mold is inverted immediately after filling to drain out part of the slip, leaving a thin coating on the walls of the mold. When the binder has hardened sufficiently, the part is removed from the mold and dried in an oven. It is then sintered in the normal manner, depending on what metal is being used. As the compact heats up in the sintering oven, the binder carbonizes at about 400° F, and the residual carbon burns off at 1250° F, leaving a compact with some finite level of porosity. Slip casting is used for the refractory metals and compounds, but it can also be successfully applied to copper (ref. 24), nickel (ref. 25), and stainless steel (ref. 26).

Edgar Kastelberg, Langley Research Center, has applied slip casting to the production of rocket guidance fins. These are mounted directly in the nozzle to guide the rocket during its first few seconds of flight before it gains enough speed for the aerodynamic fins to work. Graphite is currently used, but it is difficult to machine and replacement by a slip refractory metal would be

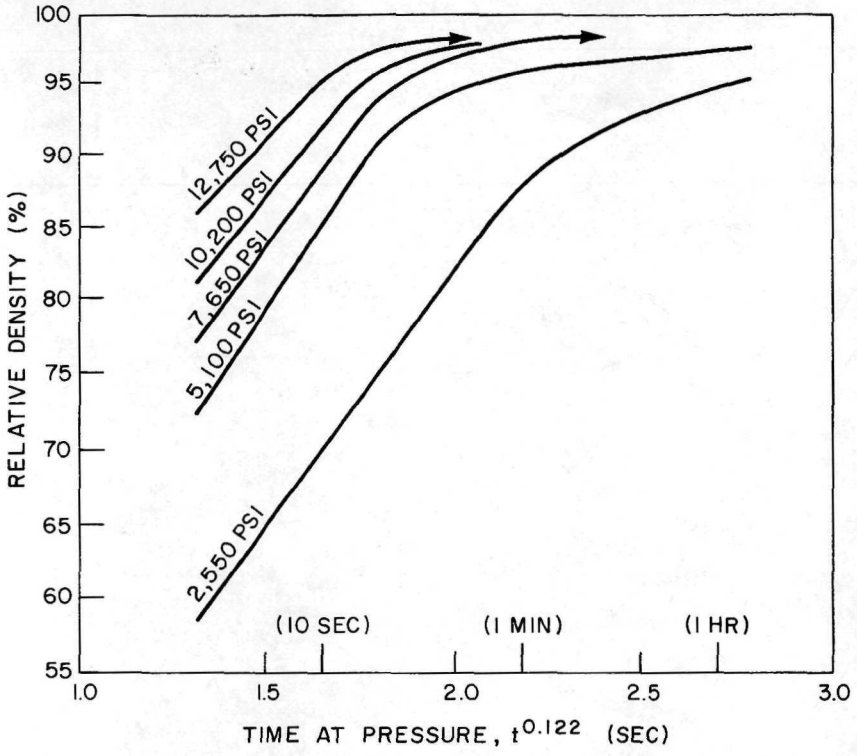

FIGURE 14.—Relative density-time-at-pressure curves for −270 to 325-mesh nickel powder hot-pressed at 1000° F (ref. 19).

desirable. Current work is being done on a ⅓-scale model with stainless-steel powders. A slip composed of ten parts of -100-mesh stainless-steel powder to one part of an aqueous solution containing 3% of a binder mixture and 2% of a wetting agent is poured into the plaster molds. Ammonium hydroxide is used to adjust the pH prior to degassing the suspension in a vacuum chamber. While this is being poured into the mold, continuous vibration is applied to insure settling, and after 40 min, more is added. The resulting slip casting is approximately 65% dense after oven drying at 100° C. Some shrinkage occurs during sintering, and the resulting parts have properties comparable to cast metals (ref. 27).

Slip-casting was used to fabricate samples in a Lewis refractory-fiber-reinforcement program (ref. 28). Nickel-base matrix alloys were vacuum-cast and then atomized into a powder having a particle size of −325 to +500 mesh. This was mixed into a 2.5% aqueous solution of ammonium alginate and diluted to give a

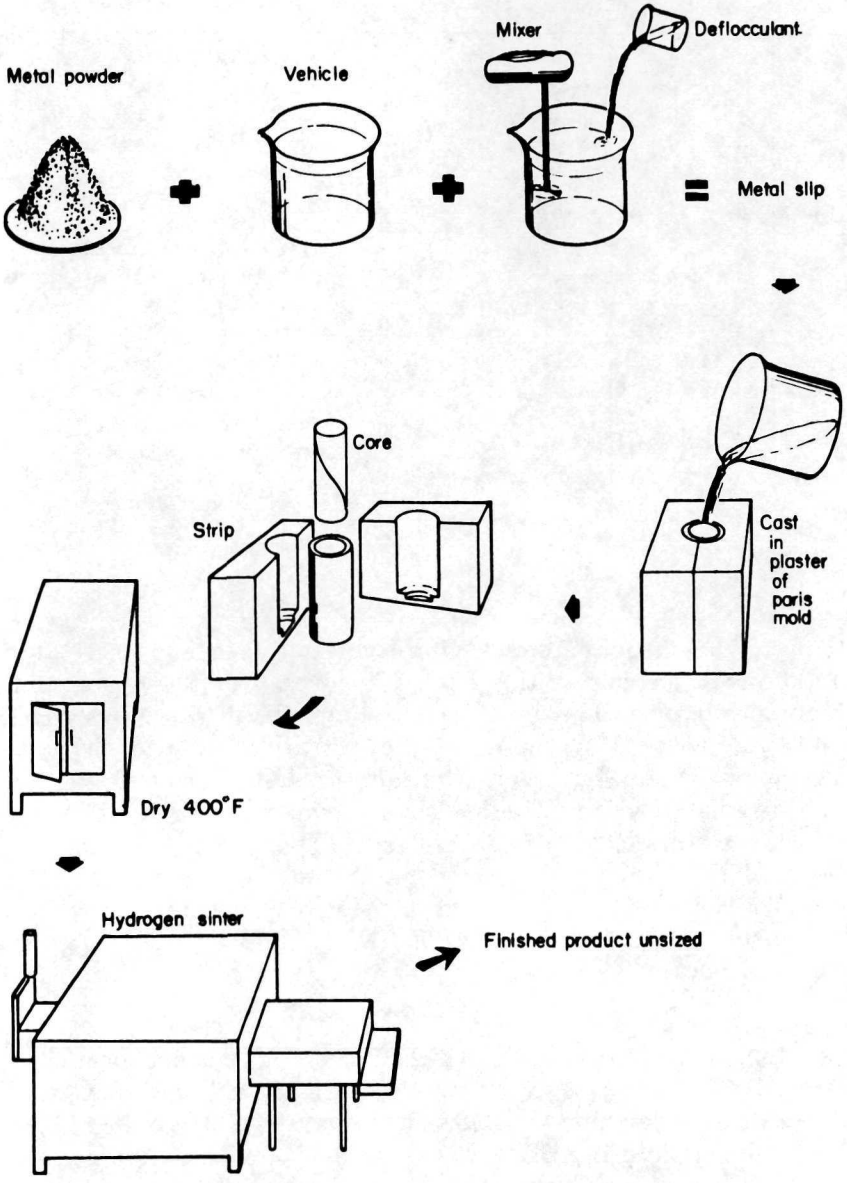

FIGURE 15.—Slip casting (ref. 22).

pourable slip at a pH of 7.4. Previous work (ref. 27) had shown that this formulation gave densities as high as 95% with no noticeable contaminants after sintering. Refractory fibers were arranged into bundles in sufficient number to give the final compos-

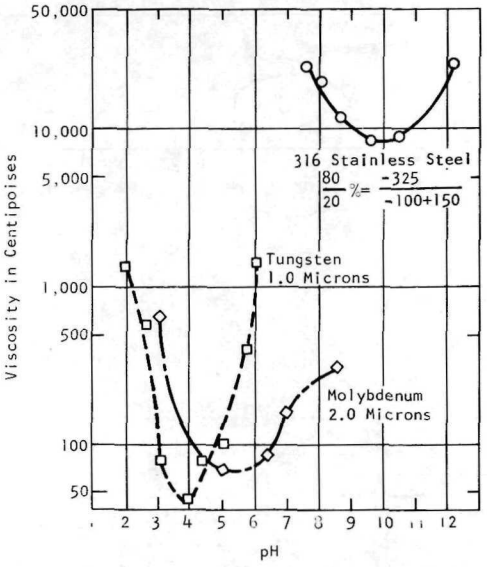

FIGURE 16.—The pH vs vicosity curves for three different metal powder slips (ref. 23).

ite up to 70% fiber content. A vibrating table assisted the settling of the metal powder as the slip was poured over the fibers, and the excess liquid was siphoned off the top. When the wires were completely covered by the metal, the vibration was stopped and vacuum was applied to the bottom of the apparatus (fig. 17) to take off the remaining liquid. The specimen was then removed and allowed to air-dry. A 1-hr sinter in dry hydrogen at 2000° F drove off the binder and reduced any nickel or chromium oxides present. The specimen was then canned in nickel under vacuum and isostatically hot-pressed at 2000° F for 2 hr under 20 000 psi helium pressure.

SINTERING

Sintering is a process by which a mass of powder particles, compacted under pressure or simply confined in a container, are physically bonded into a coherent body under the influence of heat. During sintering the mass of powders increases in strength and may densify and also recrystallize. Sintering of a single component powder takes place below the melting point of the powder material and occurs in a solid-state reaction. In a two or more component system of powders, sintering may sometimes take place above the melting point of the lower-melting component in a solid-liquid phase reaction.

The porosity in a mass of powder particles undergoes substantial changes during sintering. The pores change in shape, size,

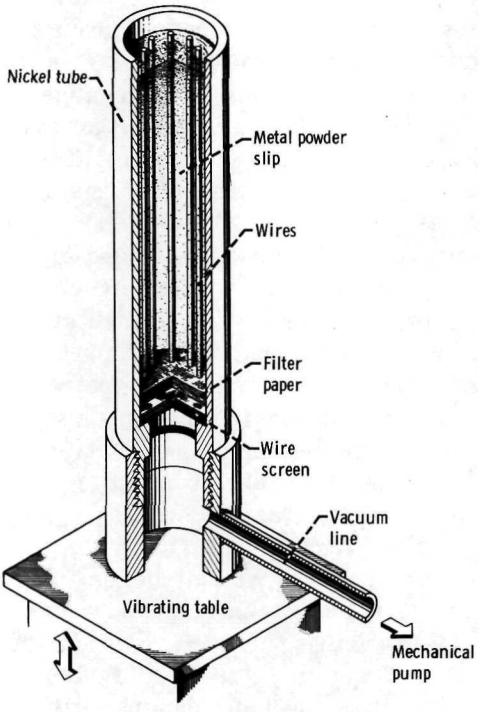

FIGURE 17.—Slip-casting apparatus (ref. 28).

and number, sometimes causing considerable shrinkage and densification of the powder mass. During sintering, the bonding starts at the contact points between the particles where necks are formed by a variety of mechanisms for material transport such as diffusion (surface, volume, and grain-boundary diffusion), plastic flow, and sometimes by evaporation and condensation. Some or all of these mechanisms of material transportation can act simultaneously, and the dominant mechanism depends on the powder material, its characteristics, and the sintering conditions (temperature and atmosphere). The migration of the atoms during sintering depends to a large extent on the occurrence of defects (vacancies) in the crystal lattices. The properties of a sintered mass of powders depend on the sintering conditions, i.e., sintering temperature, sintering time, time to build up the sintering temperature and cooling time, and the atmosphere of sintering.

When it was recognized that the surface of the Moon could be covered with a powder of rather small particle size, investigations were made to determine the effects of radiation on a mass of powder. The idea that bonding of particles may occur under irradiation was recognized as early as 1957 by Dienes (ref. 29),

and sintering of a powder mass under irradiation was discussed by Hausner (ref. 30). Irradiation at low temperature may cause defects in the structure and, therefore, some kind of exchange of atoms between powder particles. The result is a diffusion process, which, without radiation, will occur only at elevated temperatures.

Upon NASA's request, investigations of sputtering effects on a simulated Moon surface have been made (ref. 31). In laboratory experiments, steel powders showed indications of strong cementation when dc-sputtered by Hg ions. Other powders, when rf-sputtered by Hg ions or H_2 ions, exhibited lesser cementation. There is no doubt that some bonding between powder particles occurs under these conditions, which may be of great importance to investigations of the Moon's surface. These findings are also of great significance in determining the fundamentals of material movement during the sintering process and are stimulating further research on sintering of metallic and ceramic powders.

Sintering conditions are usually selected empirically on the basis of what works best for the specific material being fabricated, coupled with the equipment available. Sintering in vacuum or in a reducing atmosphere may remove surface oxides on the particles or prevent oxidation. Hydrogen or dissociated ammonia, sometimes diluted with inert gases, are the most common reducing atmospheres. The temperature range used varies betwen 0.5 and 0.8 of the metal's melting point on the absolute temperature scale. The time at temperature, as well as the sintering temperature itself, determines the final density obtained, but the length of time taken to reach this temperature and the cooling-off period are also determining factors. Of course, whether the compact is to be further worked or used "as is," determines the sintered-strength requirements.

When alloys are prepared from elemental powders, it is sometimes necessary or advantageous to sinter them at a temperature where one metal is in the liquid state. This temperature may be very low with respect to the other elements' melting points, and sintering takes place by the dissolution of the higher-melting-point metal into the liquid phase. A dentist's amalgam is actually sintered at the temperature of the patient's mouth. Another form of liquid-phase sintering is exemplified in work by Clarkin et al. (ref. 32). In this case, a cobalt-based prealloyed powder was hydrostatically compressed and sintered in a vacuum induction furnace by slowly raising the temperature. The sample was viewed continuously, and when incipient melting was detected, the temperature was held constant for 5 sec and then lowered. By sintering in this way, melting occurred only at the surfaces of the individual par-

ticles in the compact, whereas the interior of the particles remained solid. This quasi-liquid-phase sintering resulted in dense specimens that retained their initial pressed shapes. Elemental segregation that occurs in fused samples of the same alloy and might occur during a slower sintering process was prevented.

POST-SINTERING PROCESSES

In order to obtain desired properties in a metal part prepared by powder metallurgy, it is necessary to select carefully the powder with the right characteristics, compacting pressure, and sintering cycle. Many smaller parts are produced by these steps alone. It is sometimes necessary, however, to add a subsequent treatment after sintering to meet special property specifications. Coining or sizing, the simplest treatment which might be required, is a light forging operation to improve the surface properties and dimensional tolerance of the part. High-energy processes of forging, extrusion, and rolling cause major changes in the compact, bringing it up to full density, changing its shape radically, and strengthening it through lattice deformations. These changes can be seen to some extent in the results of the previously mentioned project at Lewis, in which the influence of fabrication variables on the stress-rupture properties of a powder metallurgy cobalt-base alloy was investigated (ref. 32). For this investigation, a S–816 alloy powder which has the nominal composition of Co–20Cr–20Ni–4Cb–4Mo–4W–3Fe in a particle size range of -100 mesh was mixed with a paraffin binder and a predetermined amount of graphite. The mixture was sealed in a rubber tube, hydrostatically pressed at 50 000 psi, and then sintered in a vacuum induction furnace. Test specimens were machined from the alloy compact, and tested under various conditions of subsequent working. The effect of carbon content, the subsequent treatments on stress-rupture life (25 000 psi at 1500° F), and on elongation as expressed in percent reduction of area are given in table III. The high-carbon sample that was hot-swaged and heat-treated had the best stress-rupture life.

Extrusion and forging are important post-sintering processes used to develop fully the strength potentials of powder metallurgy materials. They involve the heating of a sintered billet to an elevated temperature and then suddenly forcing it either into a shaped die or through an orifice. In both cases, the equipment is basically the same and consists of a high-pressure accumulator, a fast-action piston press, a heater for the sample, and a die. The type of lubricant for the die depends mostly on the extrusion tem-

TABLE III.—*Effect of Subsequent Working on the Stress-Rupture Properties of Sintered S–816 Steel*

Carbon %	Subsequent treatment	Stress-rupture life, hr	Reduction in area %
0.1–0.2	(a)	51.4	19.7
	(b)	34.6	21.2
	(c)	22.3	16.1
	(d)	101.4	15.3
0.5–0.6	(a)	226.9	15.2
	(b)	58.4	12.5
	(c)	176.9	19.0
	(d)	211.0	33.9
0.65–1.0	(a)	264.3	7.43
	(b)	657.0	5.66
	(c)	523.3	3.91
	(d)	620.0	13.9

[a] As sintered.

[b] Heat-treated (solution treated 24 hr at 2150° F, water-quenched; aged 16 hr at 1400° F, air-cooled).

[c] Hot-swaged at 2150° F (50% reduction in area).

[d] Hot-swaged from 2150° F (reduction in area of about 50%) and heat-treated (solution-treated 24 hr at 2150° F, water-quenched; aged 16 hr at 1400° F, air-cooled).

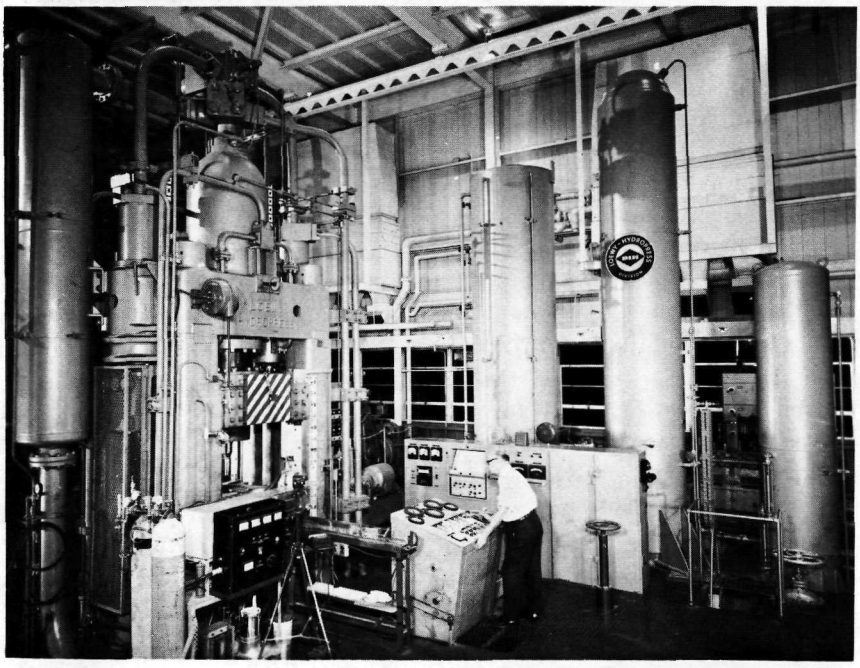

FIGURE 18.—1020-ton water hydraulic extrusion-forging press (ref. 33).

perature. The modern refractory alloys particularly benefit from the hot-extrusion process; however, their temperature requirements impose severe difficulties on the equipment. They require working temperatures as high as 4000° to 5000° F, but are prone to oxidize. In addition, these temperatures are almost twice as high as the melting point of the common tooling. To solve these problems and better define some of the extrusion variables, the Lewis Research Center developed a 1020-ton, three-stage vertical-forging extrusion press for work at temperatures up to 5000° F (ref. 33). This press along with its hydraulic power supply is illustrated in figure 18, and figure 19 is a diagram of the hydraulic system. The press is a three-stage unit with three different extrusion-force levels available without changing the accumulator pressure. The maximum pressure available from the accumulator is 3600 psi. Through valving at the top of the press, the operator can select either the two side cylinders, giving a 340-ton force, the main cylinder for 680 tons, or all three for 1020 tons. While the maximum speed of the press is 18 in./sec, generally speeds of 0.5 to 6.0 in./sec are used to assure good sur-

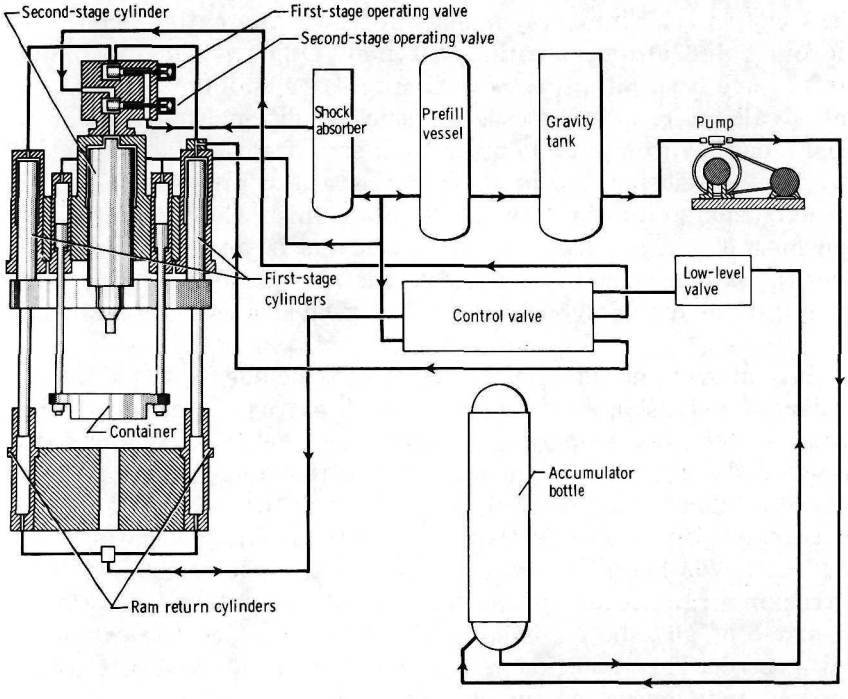

FIGURE 19.—Hydraulic diagram for 1020-ton extrusion press (ref. 33).

face finishes on the extruded product. Experience has shown that the slowest speed possible to complete the extrusion produces the best surface.

The extrusion stem which forces the billet down, the container through which it passes, and the die which effects the reduction in size are all made from wrought AISI H–12 tool steel heat-treated to a Rockwell C hardness of 48 to 54. These can be maintained at temperatures up to 1000° F without appreciable deterioration, but the best procedure is to hold them around 600° F. The stems are often stressed up to 200 000 psi during extrusion, and newer alloys under development will raise this to as high as 250 000 psi. Dies employed for materials extruded below 2500° F are oxidized and then coated with a colloidal graphite in mineral oil. For materials extruded in the 2500° to 3000° F range, flame-sprayed alumina is coated on the die, and for temperatures above 3000° F, a plasma- or flame-sprayed zirconia is necessary.

Lubrication for extrusion ranges from mineral oil, either plain or mixed with colloidal graphite swabbed on the inside of the container and the extrusion die for room-temperature extrusions, to glass cloth impregnated with tungsten disulfide in a cured epoxy or similar carrier for extrusions from 3000° to 5000° F. The glass cloth is cut into proper sizes to cover the entire length of the billet and also to lap the container. Other lubricants found useful have been oil-dispersed graphite for aluminum and copper and a calcium-graphite grease for steel. Additional lubricant in a plastic bag is often placed on the back end of steel billets immediately before closing the press to decrease the pressure required for extrusion and to improve the surface finish. Contamination of powder-metallurgy billets by the lubricants is prevented by canning the billets, which also protects the billet from oxidation and galling in the die. Molybdenum is often used as a canning material for tungsten.

The innovations of the Lewis press include a rapid billet loader, an extrusion straightener, and an extrusion retriever. The billet loader was employed to minimize the time required to transfer the hot billet from the oven to the press. The heat-loss rate of a billet heated to 4000° F has been measured at 42° F/sec, so transfer times of less than 5 sec are desirable. The system used at Lewis has achieved transfers in as little as 2.5 sec. The extrusion straightener was placed beneath the extrusion press. It consisted of an asbestos-lined steel tube into which the extruded rod passed. This addition eliminated the usual post extrusion straightening operation, which required an additional warm-up cycle. In this device, 8-ft rods were straight to within ¼-in.

Lastly, the extrusion retriever consisted of a pit 16-ft deep below the press into which had been built an apparatus capable of holding and quenching, if necessary, eight extruded rods made in quick succession.

The furnace for heating the billets (fig. 20) includes an induction coil and a hydrogen supply. The temperature is measured through a quartz viewing port and a black-body hole by means of an optical pyrometer. At 4000° F, the temperature can be maintained to within ±5° F. The power supply for the oven is a 75 kw-10 kHz motor generator. Billets are inserted into and removed from the oven through the bottom in a fashion to allow rapid access to the billet loader. Some typical results obtained through the use of this press with both cast and powder-metallurgy samples are summarized in table IV.

SAFETY IN HANDLING POWDERS

In 1966 Lewis Research Center sponsored a comprehensive survey of the health hazards resulting from ultrafine metal and metal oxide powders (ref. 34). It included a review of the literature, the analytical procedures including urine analysis, contamination possibilities inside and outside of plants, monitors for air contaminants, and special engineering recommendations. The literature survey was conducted for information on the toxicological properties and toxic potential of the metals and metal oxides of concern at Lewis, with special emphasis on the influence that extremely small particle sizes, 0.002 to 0.03 microns (20 to 300 Å), may have on the toxic hazard of these materials.

Very few studies on man or animals have included the effects of ultrafine dusts of less than 0.1-micron size. It appears that an estimate of the safe limits of exposure to the ultrafine metal dusts must be based on the known toxic potential of the various materials as determined in more conventional particle-size ranges and a theoretical consideration of how particle size may effect (1) the transport and penetration of the materials to reactive tissue sites, (2) the capacity of physiological protective mechanisms to rid the organisms of this material, and (3) the inherent reactivity of the material with constituents of living tissue.

Exposure of the skin to the ultrafine metals must be considered. In cases where significant dermal reactions from the specific materials (e.g., nickel) have been previously reported or suspected, care should be taken to minimize skin exposure, especially by the individuals who may have dermal hypersensitivity to such materials. The ultrafine state of the material may enhance pene-

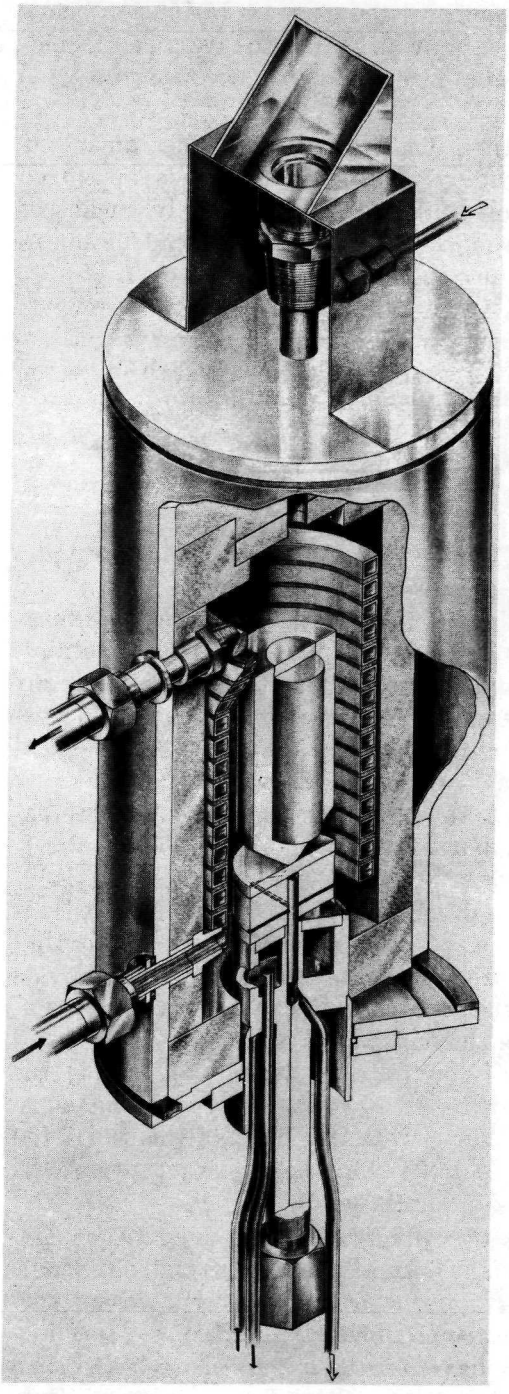

FIGURE 20.—High-temperature extrusion preheat furnace (ref. 33).

TABLE IV.—*Extrusion Characteristics of Refractory Tungsten Alloys Extruded at Elevated Temperatures in 1020-Ton Press (ref. 33)*

Alloy composition	Nominal billet diameter, in.	Overall reduction ratio	Extrusion temperature, °F	Stress on external stem, psi	Material recovery, %
Tungsten—0.5 weight % zirconium—15 weight % tantalum [a]	2.0	12:1	4400	199 600	60
Tungsten [b]—4 weight % hafnium	3.0	8:1	4200	177 000	90
Tungsten—8 volume % hafnium carbide [a]	2.0	8:1	4200	197 000	50
Ultrafine tungsten [a]	2.0	8:1	4200	200 000	40
Tungsten—4 volume % thoria [a]	2.0	12:1	4000	185 000	60

[a] Powder-metallurgy sintered.
[b] Arc-melted.

tration into and obstruction of the ducts of sebaceous and sweat glands, and thus contribute to dermatological effects. Penetration of ultrafine particles into the human body may occur also by inhalation and this is probably of greatest concern in the processes involved. The current limit values recommended by the American Conference of Governmental Industrial Hygienists (ACGIH) and the more strict threshold limit values (TLV) suggested for ultrafine dusts of ten rather common materials are shown in table V.

The toxicological data available in the literature was reviewed, and tentative TLV for occupational exposures have been proposed. These values reflect the potential increase in toxicity of the materials in the ultrafine particle state.

The materials involved were studied to ascertain how they would behave if made airborne. It was determined that these substances, when airborne, are highly agglomerated, and that 95% or more of the weight of such materials are agglomerate in particle sizes more than 0.1 micron in diameter.

Many powders can be handled in air; however, in all cases, a ventilation system should be provided in the room. Some powders should be handled in dry boxes (glove boxes). Planning of an installation for powder handling must be done with the greatest care, preferably with the help of an expert.

TABLE V.—*Threshold Levels of Contamination (ref. 34)*

Metal	Current ACGIH limit	Special caution	Suggested [a] TLV for ultrafine dusts
Aluminum	15 mb/m³ or 50 million particles per cubic foot of air, whichever is the smaller		2.0 mg/m³
Chromium [b]	0.1 mb/m³ and CrO_3	Carcinogenic potential sensitization	0.002 mg/m³
Cobalt [b]	0.5 mg/m³ [c]	Sensitization	0.002 mg/m³
Magnesium oxide	15 mg/m³		2.0 mg/m³
Molybdenum	5 mg/m³ (soluble) 15 mg/m³ (insoluble)		0.5 mg/m³
Niobium			1.0 mg/m³
Nickel [b]	(0.007 mg/m³ for carbonyl) 1.0 mg/m³—tentative value for metal and soluble compounds	Carcinogenic potential sensitization	0.002 mg/m³
Thorium oxide		Carcinogenic potential (radiotoxicity)	0.002 mb/m³
Tungsten			0.5 mb/m³
Zirconium oxide [b]	5 mg/m³	Sensitization potential	0.1 mg/m³

[a] Concentration of metal element.

[b] Avoid skin contact.

[c] Has been proposed (AIHA Newsletter, Jan. 1966) that TLV be reduced to 0.002 mg/m³.

CHAPTER 3

Powder Metallurgy of Specific Metals

LIGHT METALS

The light, high-strength-to-weight-ratio metals that are used extensively as structural materials in aerospace and aircraft applications are aluminum, titanium, beryllium, and magnesium, usually in alloy form. These metals and their alloys, when processed by powder metallurgy, often exhibit superior mechanical properties. Despite this, fusion techniques dominate virtually all of the structural-parts production that is based on the use of magnesium, aluminum, and titanium. Powder metallurgy, however, is playing an increasing role in the fabrication of small precision parts from both aluminum and titanium. Beryllium is still in the experimental stage as far as structural applications are concerned with powder metallurgy also important in this development. It is used in nonstructural areas where its high-heat conductivity or its desirable nuclear properties are useful. NASA is concerned primarily with titanium and beryllium because of potential applications of these metals in the space program. The properties of typical alloys in this group of metals are compared in table VI (ref. 35).

Aluminum

With the exception of the cermet, sintered aluminum powder (SAP), aluminum failed to interest powder metallurgists until very recently. SAP, a dispersion-strengthened aluminum-aluminum oxide composite made by powder-metallurgy techniques, appears to have academic interest only in this country. Even after 20 yr of development work with this alloy, few American companies manufacture it. The reason for this probably can be attributed to (1) the difficulties of fabricating SAP without destroying its properties, and (2) the development of other alloys with better strength-to-weight ratios at high temperatures, particularly titanium alloys.

Until recently, many technical difficulties prevented the use of pure aluminum powder for the production of compacts by indus-

TABLE VI.—*Comparative Properties of Be and Alloys of Ti, Al, and Mg (All Properties at Room Temperature) (ref. 35)*

	Cross rolled Be sheet [a]	Cross rolled Be sheet [b]	Hot pressed Be block [c]	62 Be–38 Al sheet	Mg alloy HM21A–T8	Al alloy 7075T6	Ti alloy sheet T1–6V–4 Al
Tensile yield strength, psi	55 400	40 300	40 700	36 600	30 000	63 200	137 000
Tensile ultimate strength, psi	75 000	53 800	48 400	50 400	37 000	72 200	147 000
Tensile modulus $\times 10^6$, psi	43.1		42.4	29.2	6.50	10.3	16.0
Tensile elongation, %	8	3.2	1	8.1	4	7	10
Compressive yield strength, psi	58 300		27 000	34 200	22 000	68 000	126 000
Compressive modulus $\times 10^6$, psi	42.6		42.6	29.1	6.5	10.0	16.4
Density, lb/in^3	0.066	0.066	0.066	0.0756	0.064	0.101	0.160
Coefficient of thermal expansion $\times 10^{-6}$ in./in./°F (77 to 212° F)	6.4			9.0	21.8	12.9	4.8
Thermal conductivity, Btu/hr ft °F	104		104	123	80 (est.)	76	3.8

[a] Powder-derived; all values in longitudinal direction.
[b] Ingot-derived; all values in longitudinal direction.
[c] SR–200 powder.

try, including: (1) galling of die walls during compaction, (2) cold-welding of aluminum to the tooling, (3) inadequate sintering procedures, (4) poor flow properties of the powder, and (5) lack of proper lubricants (ref. 36).

These and other problems have been finally overcome, resulting in production of a pure aluminum powder (99.5%) and two alloy blends equivalent in composition to the wrought alloys 2014 and 6061. The pure powder is designated 1202, and the alloys, 201AB and 601AB respectively. The newly developed powder is made by inert-gas atomization and has 55% of the particles in a 200- to 325-mesh range and the rest between 50 and 200 mesh. They are nodular in shape. Iron and silicon impurities have been controlled to provide a very soft, ductile powder with a low oxide content. Special lubricants improve the flow characteristics. The optimum performance was achieved with organic fatty acids or waxes low in moisture and ash content. Current practice by one firm involves blending the lubricant and a wax with the powder, then removing the wax after compaction by vacuum, and finally sintering the compact in a controllable atmosphere (ref. 37).

Fabrication parameters for aluminum powder include compaction at 25 000 psi for 95% density and sintering temperatures ranging between 1000° and 1175° F. These values are about 50% of those required for iron and copper alloys. Sintering furnaces for aluminum powder require close temperature control and the capacity to hold the dew point between −40° and −60° F.

While the powder alloys compare closely to their corresponding wrought alloys in composition, they differ in mechanical properties. The ultimate tensile strength of alloy 201AB measures 48 000 psi vs 60 000 psi for the wrought alloy, and the elongation is only 2% compared to 13% for the wrought alloy. For certain applications, aluminum powder metallurgy offers the advantages of powder metallurgy combined with those of aluminum over other metals, and, at the present time, cams, gears, housings, and self-lubricated bearings are being made this way.

Titanium

The aerospace industry is responsible for the development and growth of titanium as a structural material, and consumes about 80% of the total titanium produced. Titanium's strength-to-weight ratio, particularly in alloy form, and resistance to high temperatures are indispensable in this application. In this respect, titanium alloys are superior to aluminum and high-strength steels in the temperature range up to about 1000° F. Applications

occur in the compressor sections of jet engines, airframes of high-performance aircraft, structural and skin components of space vehicles, rocket motor cases, and fuel tanks for liquid hydrogen. It has been estimated that supersonic commercial airliners will contain 90 000 to 100 000 lb of titanium. Also, titanium has excellent resistance to attack from most organic acids, mineral salts, and gases, and has good resistance to alkaline solutions and some mineral acids (ref. 38). It is particularly resistant to fresh and salt water, which makes it an ideal candidate for use in desalinization. A small percentage of titanium used in the above listed applications is presently being fabricated by powder-metallurgy methods, but this can be expected to increase as the price of powders becomes more competitive.

Powder metallurgy is a natural consideration for the fabrication of titanium for two reasons. First, the initial refining process (the Kroll process) produces titanium sponge which must be crushed into a powder for a final leaching process to remove magnesium impurities. Second, titanium is highly reactive, becoming easily embrittled in the presence of oxygen or nitrogen. Even melting in an inert atmosphere will result in embrittlement if a refractory crucible is used. Consequently, the early work in titanium was done by powder metallurgy. In 1946, for example, Dean and co-workers at the Bureau of Mines achieved tensile strengths as high as 82 000 psi and elongations of 28% in 2-in. specimens by these techniques (ref. 39).

Shortly after this work was completed, the technique of arc-melting titanium in a water-cooled copper hearth was developed. This technique was adopted by industry and now provides the high tonnages of titanium that are used today. Powder metallurgy has other advantages for parts production from both handling and materials standpoints. There are obvious economic benefits in producing parts that require little or no machining and, consequently, produce no scrap. Also, the powder metallurgical process produces parts with a finer grain structure, and hence better mechanical properties than are otherwise available. These parts also have improved chemical homogeneity. For the best properties, an additional step of hot-working is required.

The common techniques of powder production, such as water atomization, pyrometallurgical reduction, or chemical precipitation, are not applicable to titanium, since most of these methods would produce an oxide film on the powder particles which could not be reduced in subsequent operations. Thus, titanium powder-making processes are limited to those which cause little or no oxidation of the powder particles. They include the hydride-dehy-

dride process, mechanical attrition, and the rotating electrode process. These three processes are also applicable to the production of alloyed powders. The extra step necessary to produce the alloyed feed material for them introduces an additional expense, however, so one company has experimented with mixed elemental powders (ref. 40). Low alloys of aluminum and titanium and a Ti–6Al–4V alloy were successfully produced in this way. Sintering time, temperature and pressure influenced the amount of homogeneity that occurred.

Because of its inherent simplicity, the rotating electrode process produces alloy powders at reasonable cost. An electrode made from the desired alloy is atomized inside an 8-ft diameter drum. The electrode is mounted in a spinning chuck and brought into contact with a stationary tungsten electrode placed opposite it on the axis of the drum. When an arc is struck, fine metal droplets are thrown about the inside. They harden while suspended in the helium atmosphere of the drum, so a minimum of impurities is picked up (ref. 41).

The hydride-dehydride process depends on the increased solubilities that many metals have for hydrogen at elevated temperatures. Titanium or one of its alloys is placed in an atmosphere of hydrogen and heated to 600° F where a hydride is formed, and then cooled. The brittle hydride phase can be easily crushed to a powder of the desired fineness and the hydrogen removed by vacuum decomposition.

Titanium exists in two crystal forms. The low-temperature form is the alpha structure, which converts to the beta form with an expanded lattice at 882° C and above. Research in alloying elements for titanium has been concerned mainly with the variation of the properties of these two forms. Iron, chromium, manganese, and vanadium are known as beta stabilizers since they lower the transformation temperature between the two forms. Aluminum, oxygen, nitrogen, and carbon, on the other hand, raise it. If sufficient beta stabilizer is present, some beta phase can be retained at room temperature. High-temperature alloys contain mixtures of the two phases through the use of both alpha and beta stabilizers. A common example is the alloy containing 6% aluminum and 4% vanadium. It has tensile strengths in the 130 000- to 160 000-psi range, which can be raised as high as 225 000 psi and still retain ductility by proper heat treatment.

Most of the common powder metallurgy processes can be used for the compaction of titanium powder, including cold-pressing, hot pressing, extrusion, slip casting, and spark sintering. The press and sinter techniques are generally used with irregularly

shaped powders such as hydride and attrited powders. Compacts are made with pressures as low as 30 000 psi without lubricants and sintered at 1950° to 2730° F under a vacuum of 10^{-4} torr. High-pressure helium and argon have also been used as sintering atmospheres. Some typical parts pressed from titanium powder are shown in figure 21. Parts produced in this way vary from 5% to 15% in porosity and are not as strong as their wrought counterparts. When elemental powders are mixed to produce alloys, liquid phase sintering occurs, which produces materials of somewhat higher densities and strengths. A Ti–6Al–4V alloy produced this way had a tensile strength of 119 000 psi with 6% elongation (ref. 40). In general, however, a hot-working step after sintering, such as forging, is necessary to develop full strength. Cargo hold-down rings produced for the U.S. Air Force are shown in figures 22 and 23. These are produced from hydride Ti–6Al–4V powder and forged to final shape. The forged ring is shown in figure 22 and the preform is shown in figure 23.

A comparison of the properties of hot-pressed powders of Ti–6A1–4V and Ti–5A1–2.5Sn prepared by mechanical attrition, hydride-dehydride, and rotating-electrode processes is given in table VII. This is the result of a NASA project to evaluate these

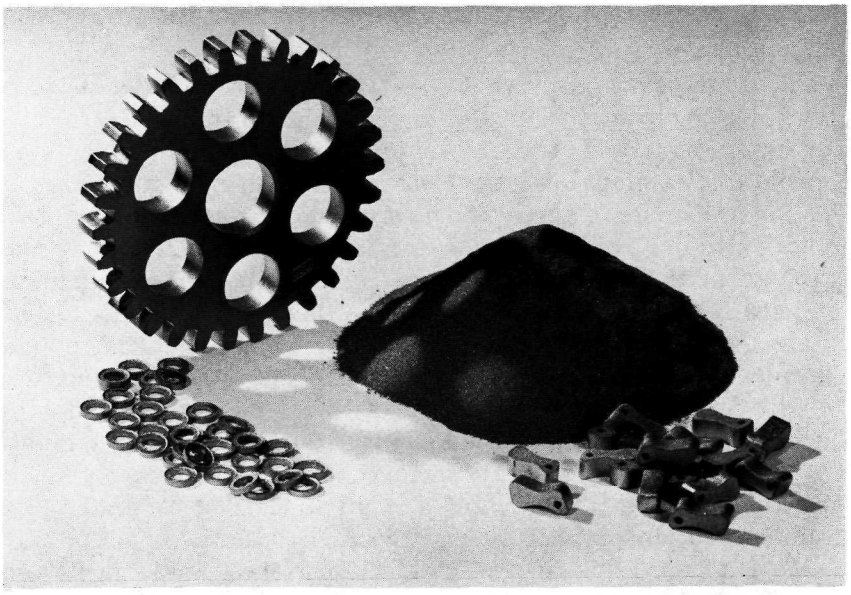

FIGURE 21.—Parts pressed from pure titanium powder. (Courtesy Dynamet Corp.)

FIGURE 22.—Ti–6Al–4V powder forging performs (pressed and sintered). Part is cargo tie-down ring for Lockheed C5A. (Courtesy Nuclear Materials and Equipment Corp.)

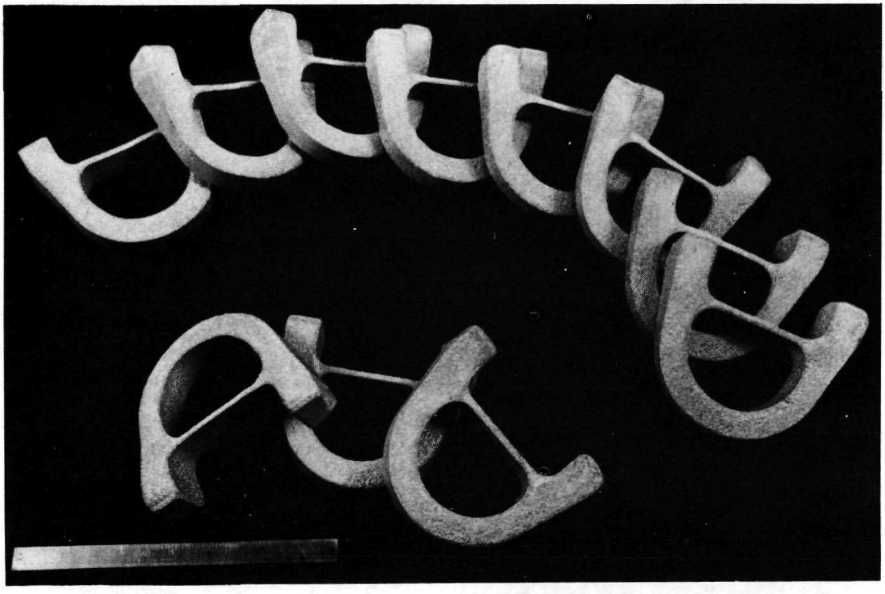

FIGURE 23.—Several Ti–6Al–4V powder preforms, as in figure 22, showing reproducibility of process. (Courtesy Nuclear Materials and Equipment Corp.)

TABLE VII.—*Properties of Hot-Pressed Titanium Alloys (ref. 42)*

Sample	Tensile ultimate strength, ksi	Tensile yield strength, ksi	Elongation, %
Ti–6Al–4V			
Mechanically attrited	144.8	135.9	1.5
Rotating electrode	145.1	134.1	7.5
Hydride-dehydride	149.3	141.3	2.0
Ti–5Al–2.5Sn			
Mechanically attrited	92.8		0
Rotating electrode	130.7	130.7	4.0
Hydride-dehydride	126.3	120.3	5.5

different powders under identical conditions. The rotating-electrode process produced powders with the lowest impurity levels and generally with the best physical properties (ref. 42).

The rotating-electrode process produces spherical particles which are difficult to cold-press because of the lack of green strength in the compact. Several means can be used to overcome this difficulty, including hot pressing as in the above work, canning and extrusion, or simply extrusion from powder. The latter process is normally done at 1600° to 1700° F and produces fully dense compacts. A typical procedure for the production of titanium tubing would include the following steps (ref. 43):

1. Hot-press at 1650° F to a tube-preform billet
2. Extrude at 1650° F to redraw size
3. Draw to size
4. Anneal
5. Straighten
6. Stress-relieve.

Beryllium

Beryllium has a remarkable combination of properties which has prompted extensive research on it for the last 20 yr. For example, its elastic modules of 44×10^6 psi is considerably higher than that of iron at 30×10^6 psi, but its density of 1.8 g/cc is less than one quarter that of iron, which provides a high strength-to-weight ratio and a Young's modulus in the neighborhood of the carbides and nitrides. If it were used in aircraft as load-carrying struts, beryllium would reduce the structural weight to less than half of that required by present day materials. At the same time, beryllium has good corrosion resistance and a high melting point (1284° C). An additional property of this metal is its extremely

low nuclear cross section which makes it desirable for use in nuclear reactors.

Despite these advantages, beryllium is not used to any great extent in the aerospace industry except in some isolated places where its high heat conductivity is valuable. This is due to its brittleness, which is an inherent property of beryllium at temperatures below about 200° C. Between 200° and 600° C, there exists another form of brittleness caused by impurities, which can be decreased by purification procedures involving the reduction of iron contaminants. Heat treatment also helps. Nothing has been effective in lowering brittleness under 200° C, however; a result, perhaps, of a property of the crystal structure in this temperature range. Most designs for beryllium components are limited to compressive loading, but it can also be used in tension if the directions of the weak crystal planes are taken into account. Another common means of raising the low-temperature ductility is to maintain a polycrystalline matrix. This can be done only by powder-metallurgy processes.

Powder metallurgy is traditionally used for beryllium fabrication in practically all the present commercial production. The reason for this has been the poor quality (large grains and orientation) of beryllium ingot castings. Vacuum castings have improved the situation by controlling the oxide content to less than 0.3%, giving a finer-grain material that is ductile enough to be worked easily. It is much higher in cost, however, and has a lower modulus than the powder-metallurgy product. Another advantage of the powder-metallurgy process is the uniform dispersion of an oxide phase into the matrix of the compact. This has the ability to harden the matrix, stabilizing the grain structure against grain growth to within 20° C of the melting point. The oxygen level in commercial powders is normally specified around 1% maximum to accomplish this.

The major source of beryllium is the semiprecious mineral beryl. Two refining processes are common: the reduction of beryllium fluoride with magnesium at 1300° C and the electrolysis of beryllium chloride. The metal is then vacuum-cast to reduce the volatile contaminants. Powder is produced by mechanical attrition of the ingots, and a final ball-milling operation produces a fine powder (19 microns average). This is highly toxic and requires enclosed processing areas because workers should not be exposed to concentrations of airborne particles above the level of 2 micrograms /m^3/day. In addition, inert atmospheres are necessary for these operations to prevent the oxidation of the powder. Finer powders (less than 10 microns average) are produced by

ball-milling in methyl alcohol under argon for very high-modulus applications such as gyroscopes. Another process which has been successful in producing extremely fine beryllium powder is the amalgam process. Powder was produced in this way for NASA in particle sizes down to 0.1 to 0.2 micron in diameter (ref. 5). This work is described in more detail in chapter 2.

Hot pressing in vacuum is the most common method for consolidating beryllium powder. This is normally done at 800° to 1100° C in graphite dies or steel cans using pressures from 100 to 2000 psi. Even with the vacuum, the surface of the resulting sintered block must be machined to remove contamination. Billets as large as 6 ft in diameter with weights up to a ton, have been produced in this method. Further working of these billets rapidly orients the crystal structure and reduces the polycrystallinity. Above the optimum temperature of 1100° C, the residual porosity becomes disconnected by the migration of the grain boundaries. At 1200° C, loose beryllium powder will achieve high densities under vacuum without pressure, and a wide range of shapes can be made through the use of shaped graphite dies. For instance, hollow objects can be formed around graphite cores. Slip casting and plasma spraying have also recently received attention.

Mechanical working at elevated temperatures is done by many of the conventional metalworking techniques. Among these are rolling, extrusion, drawing, forging, deep drawing, roll forming, and spinning. The temperature of these operations greatly affects the final ductility. Sheet produced by rolling hot-pressed blocks or ingots will have directional strength properties, so a technique known as cross rolling is used to give good bidirectional strengths. The highest mechanical properties are obtained by lowering the temperature of final rolling to the range of 760° to 800° C. This is the lowest temperature normally used without causing the formation of cracks, but it is dependent on the oxide content of the material since increased oxide increases the resistance to deformation.

Both open and closed die forging are successful and economical forming techniques for beryllium. The billet is generally jacketed in steel first to allow more complex structures to be made. Some aircraft components have been forged without jacketing, but these are special procedures (ref. 44). The previous history of the input stock is important in the final properties of the forged component.

Beryllium and beryllium alloys can also be extruded, but the operation is subject to problems of seizing, galling, and oxidation, and to the danger of toxic contamination of the environment. The

best results are obtained with jacketed billets. Mild steel is the most common jacket material because it has extrusion properties similar to those of beryllium, it is inexpensive, and it can be readily removed with hot 50% nitric acid. When cracking occurs because of different thermal expansion coefficients, alloy steels may be required. Slow ram speeds (0.5 in./sec) are used for large reduction ratios or thin-wall tubes; otherwise normal procedures are used. During extrusion, the crystal structure tends to become aligned in the direction of the applied force, a phenomenon more affected by the reduction ratio than by the temperature. A recent project at Langley Research Center has produced good quality Be–38Al tubing, 0.25 to 0.69 in. in diameter, with 0.020-in. wall thickness (ref. 45). These tubes can be produced to close dimensional tolerances and have the as-extruded and annealed properties given in table VIII.

TABLE VIII.—*Summary of Room-Temperature Mechanical Properties of Extruded Be–38 Al Alloy Tubing (ref. 45)*

Outside diameter, in.	0.2% Offset tensile yield strength, ksi	Ultimate tensile strength, ksi	0.2% Offset compressive yield strength, ksi	Modulus of elasticity, 10^6 psi	Elongation in 2 in., %
		As-extruded			
0.2500	----	66.2	71.2	28.9	<1
0.4375	----	65.0	74.7	28.7	<1
0.5625	78.8	81.3	76.9	28.6	<1
0.6875	81.3	85.6	78.0	29.0	<1
		Annealed			
0.2500	50.1	56.8	55.7	28.7	2
0.4375	50.3	53.4	48.6	29.1	2
0.5625	48.8	60.3	43.8	30.4	5
0.6875	48.6	54.5	43.4	29.3	3

The main factors that affect the physical properties of beryllium are the grain size, grain orientation, and its relative purity with respect to contents of oxygen, silicon, iron, and aluminum (ref. 35). Maximum strengths, ductility, and crack resistance occur when the grains are less than 10 microns in size and equiaxed. Copper as an alloying element has the effect of improving the ductility by preventing microcracks, but the most important factor is the previous history of the compact.

Beryllium is generally available in sheets up to 3 by 8 ft that are made by hot-pressing −200-mesh powder which is then en-

cased in a steel jacket and cross-rolled. After rolling, the jacket is removed and the sheet surface grounded and etched to remove cracks and imperfections. Other available beryllium forms are unworked hot-pressed blocks and ingot sheets. Such material is normally of higher purity than its powder-metallurgy counterpart, but has a poorer surface finish and mechanical properties. Some producers are making 0.001- to 0.005-in. foils which are expensive and usually of nonuniform thickness. Rolling below 0.020 in. often causes excessive grain orientation, which can be avoided by etching heavier-gage materials.

Fabrication is done in a relatively normal fashion with ordinary shop tools, but tool wear is abnormally high. A final 2-mil etch is necessary to remove microcracks that occur during the machining (ref. 46). The difference between success and failure of the final product is dependent upon the amount of care taken in fabrication, to avoid scratches, cracks, and other damage. That machining operations contribute to the brittleness of the final product has been known since 1949, but this knowledge is largely neglected. Even special efforts to minimize the extent of deformation damage does not eliminate the hazard, since even slight damage can cause a significant reduction in strength. It can only be eliminated by either the etching process or annealing.

Marshall Space Flight Center has devoted considerable effort to determining the parameters involved in the fabrication of beryllium (refs. 46, 47, and 48). The temperature relationships were developed for straight and compound curve bends of channels and hemispherical segments. This required the determination of the flow characteristics of beryllium. The feasibility of extreme forming of cross-rolled sheet was also demonstrated (ref. 46). The parameters were reviewed for various metal-removal techniques such as drilling, routing, abrasive wheel cutting, chemical milling, and electrical discharge machining on hot-pressed blocks and extruded rods. In addition, the precautions necessary for plating and brazing were established as well as the effects of various thermal treatments such as high-temperature environments and rapid cooling (ref. 47). Test panels were prepared in anticipation of future structural applications utilizing the criteria set forth in this program (ref. 48).

Pressure-forming of beryllium above 940° F is dependent upon the increased ductility in this temperature range. Sheets are normally placed in heated dies and the pressure slowly applied to obtain the desired shape (ref. 46). Channel sections up to 8 ft long have been produced this way using stainless steel dies and punches.

When beryllium is drawn into fine wires, exceptional strengths develop. A 0.002 in.-experimental wire, for example, was reported to have an ultimate tensile strength of over 200 000 psi (ref. 49). Drawing is done around 400° C in a similar manner to the drawing of mild steel. Extruded rod or machined bars are reduced in area 12% at each pass until a total of 85% total reduction has been accomplished. Wires of from 0.75-in. diam down to 0.005-in. diameter have been made in continuous lengths up to 5000 ft.

Considerable efforts have been made recently by NASA to fabricate beryllium structural members for aerospace uses, and it has been stated that beryllium is now considered competitive with other materials (ref. 50). Marshall Space Flight Center has worked with several manufacturers developing beryllium components with considerable success (ref. 51). Box beam sections made from sheet and fastened with blind rivets have been made. Several different fastening methods have been developed utilizing beryllium to reduce the weight of the Saturn V thrust structure (ref. 52). Blind fasteners were made for effective use in environments up to 800° F, but high-reliability bolts did not seem to be feasible. Langley Research Center has fabricated lightly loaded, truss-type beryllium structures for unmanned spacecraft from thin-wall beryllium tubing 0.25 to 0.75 in. in diameter (ref. 53). Fastening was done by adhesives combined with aluminum joint reinforcement as shown in figure 24. The structure was test-loaded in a similar manner to check methods used to qualify unmanned spacecraft to which powerful acceleration forces are applied. The results showed that beryllium structures could be 53% lighter and 50% more rigid than aluminum structures of the same strength. Similar trusses have been developed for the gimbal support used in the Saturn guidance engine (ref. 35). This program used 5-in.-diameter tubes, 11 ft long, and joined by machined beryllium caps.

The high-heat capacity and light weight of beryllium make it an attractive material for absorbing the frictional heat generated by the atmosphere on the reentry surfaces of aerospace vehicles (fig. 25). Some of the largest beryllium forgings that have ever been made have gone into these structures. The heat shield for the Mercury capsule, for example, was forged from a 58-in.-diameter and 8-in.-thick billet. Subsequent work produced billets up to 75 in. in diameter, weighing 11 000 pounds. These were 99% dense in their hot-pressed state and were machined directly without forging (ref. 54). Typical beryllium billets for the inertial guidance system of the Minuteman missile are shown in figure 26.

Other applications for beryllium's high-heat capacity in aero-

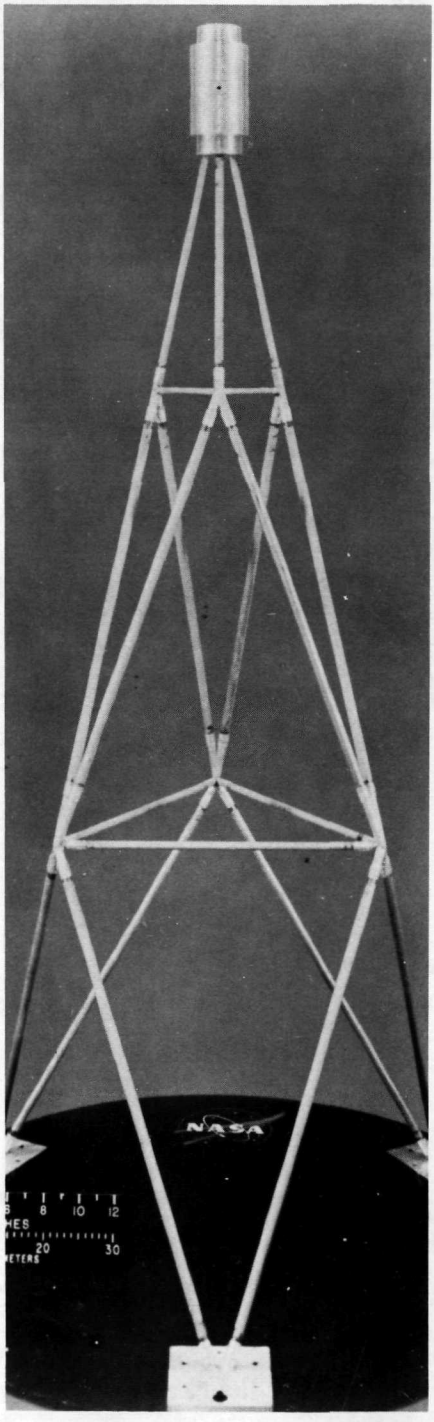
NASA
8 10 12
20 30

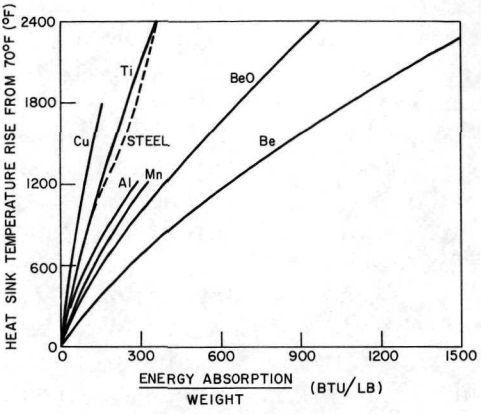

FIGURE 25.—Heat capacity of beryllium compared to other metals.

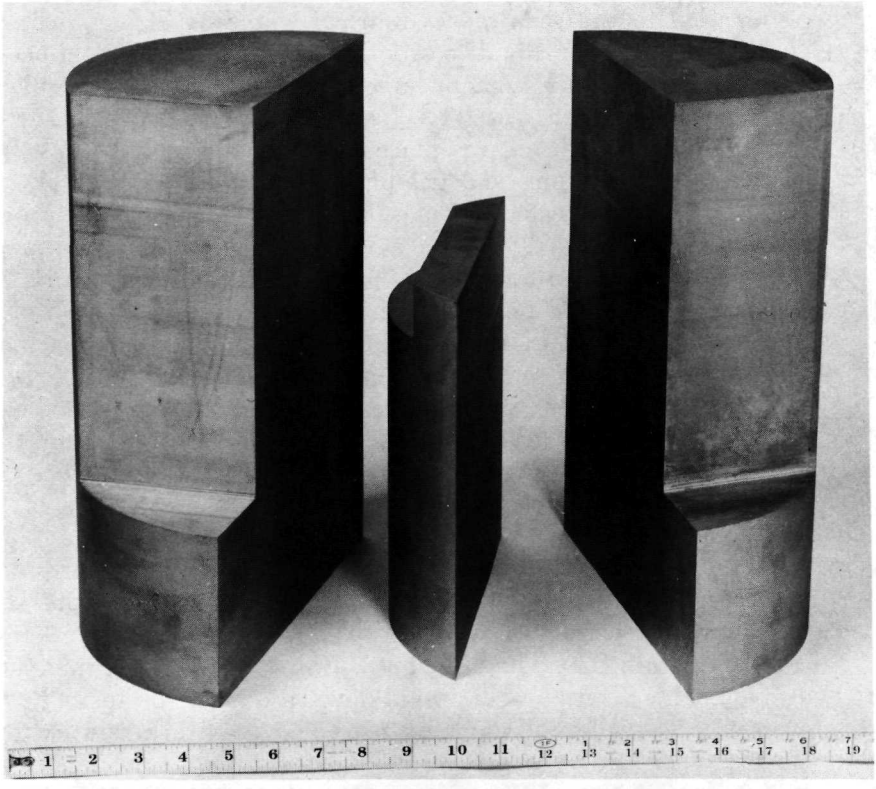

FIGURE 26.—Typical hot-pressed beryllium billet. (Courtesy General Astrometals Corp.)

FIGURE 24.—Bonded beryllium truss (ref. 53).

space technology are for micrometeoroid protection of spacecraft and in aircraft brake shoes. The effects of a high-velocity projectile on a metallic surface have been studied by NASA (refs. 55 and 56), and one mechanism that has been postulated is that impact energy is consumed locally by the sublimation of a small quantity of metal. In this case, the heat capacity and the heats of fusion and vaporization of the metal would define its ability to resist impact. Beryllium's high values in all these properties make it an outstanding candidate for this application.

Extensive studies have been made on the fabrication of beryllium-shielding systems for NASA (refs. 57 and 58). A system of gas-pressure bonding of beryllium around a stainless-steel supporting tube was one result (ref. 57). The composite combines beryllium's high-velocity-impact resistance with steel's tensile strength. The beryllium was fabricated by either cold hydrostatic compaction to the required cylindrical shape or by hot pressing and extrusion. Beryllium powder was vibrationally compacted into a steel mold for cold pressing. A rubber sleeve was placed over the mold which was then pressurized to 60 000 psi. The resulting tubular compact was placed over a stainless-steel test bar, canned under vacuum, and gas-pressure bonded at 1400° F and 10 000 psi. Under test conditions, impact by high-velocity projectiles on the surface of these targets caused brittle-crack propagation which diverged from the impact area. Previous work has shown that a ductile phase within a brittle one will absorb much of the energy spent in cracking the brittle matrix, thereby limiting the extent of the cracking. Applying this to the target preparation, stainless-steel wires were embedded into the cold-compacted beryllium structure and bonded to the steel backing (ref. 58). Both woven and randomly placed wires were successfully incorporated into these structures without stress cracking in the final composite.

The use of beryllium in aircraft brake shoes has recently been perfected resulting in a weight saving of 50% over the commonly used steel brakes (ref. 59). This potential has been known since the late fifties, but problems with brittleness have hampered development. Stress cracks would develop during the testing cycle even when beryllium was being used only as a heat sink with a backup steel structure absorbing the structural loads. The development of a new grade of beryllium specifically for aircraft brakes made the difference. This alloy contains a reduced amount of aluminum, which is known to cause embrittlement through grain-boundary segregation. In addition, the remaining aluminum is tied up in the form of a high-melting-point intermetallic com-

pound through heat treatments and controlled additions of iron. The new brakes show no cracking and can be reused by means of replaceable linings, unlike steel discs which are discarded after wear. The manufacturing technique for brakes for the C–5A starts with an 18-in. diameter by 40-in. long compact which is trepanned to form a cylinder. Discs are then sliced off, and thermal slots cut out with an electronically controlled milling machine. An etching process completes the fabrication. In use, these brakes on all 24 wheels of the C–5A reduced the plane's weight by 1500 lb and showed a reduced temperature rise (ref. 60).

COMMON METALS

Iron, nickel, and cobalt can be considered basic to the needs of industry because of their economic and technological importance. When alloyed with each other, they provide through a synergistic effect improved physical and magnetic properties, which can be applied in every segment of industry. Alloys of this type are particularly useful for operation at the higher temperatures or in corrosive atmospheres, while still retaining their physical properties. The addition of dispersants enhances these properties substantially, and ultimate tensile strengths of 40 000 psi at 2000° F and 250 000 psi at 70° F have been achieved. Permanent magnets of Fe, Ni, Co, Al, and Cu alloyed by powder metallurgy provide some of the highest energy products and remanences of any magnetic materials developed to date. Nickel, with varying percentages of Fe, Nb, Cr, and Co, is the basis for ferromagnetic alloys with permeabilities up to 800 000, a value far above iron or steel alone.

These three metals and their alloys are often formed by powder-metal processing; in some cases, this is the only practical method of obtaining certain alloys. If particle shape and size, composition, compaction pressure, and sintering conditions are controlled, the alloys can often be tailored to specifications far better than those conventionally processed. The higher purity of powder metal is largely responsible. Commercially refined and cast metals or alloys often contain undesirable inclusions which affect their properties. A further advantage of the powder metallurgy product is the close control of grain size.

Iron

Iron is the fourth most abundant element by weight in the Earth's crust, and the cheapest, most useful, and most important

of all the metals. Alloys in which iron is the principal component dominate the metallurgical field and account for the major volume of products made by industry. In proportion, one of the fastest growing sectors of this field is powder metallurgy. Iron-powder parts are displacing cast, forged, and machined parts because dimensions can be held closely and a good surface finish is possible. Improved equipment combined with a predicted drop in iron-powder costs could accelerate this trend markedly. Articles fabricated by powder metallurgy may not require surface finishing, except where sales appeal or corrosion resistance are involved, and their physical properties are comparable or better than their conventionally processed counterparts. Iron powder is currently being used at a rate of about 150 000 tons per year (ref. 61), and this is increasing rapidly.

NASA's interest in iron powder has been very slight, consisting to a large extent of Dr. Nicholas J. Grant's work at the Massachusetts Institute of Technology (MIT) on dispersion-strengthened iron powders (chapter 4). The reason for this apparent lack of interest is the current high degree of development of ferrous-based alloys. With the exception of the dispersion-strengthened materials, most ferrous alloy systems have been improved to high-strength levels. The requirement for light weight in aerospace vehicles almost categorically excludes iron alloys, except where truly superior high-temperature properties are apparent. The stainless steels are an example. Their superior corrosion resistance and high-temperature stability make them useful in certain aircraft and space vehicles. These ferrous-based alloys are indispensable in handling corrosive liquids or gases at room temperature, and will resist oxidation at temperatures up to 2050° F. They are classed as austenitic, ferritic, or martensitic, depending on their microstructures.

The martensitic grades of stainless steel are the only ones that can be hardened by heat treatment and, when alloyed with carbon (up to 1.0%), can be hardened to Rockwell C 63. The austenitic grades are the most corrosion resistant, while the ferritic grades are used where cost is the overiding factor.

The powder metallurgy of stainless steel is becoming increasingly popular as the price and quality of the powders improve. The most commonly used powders are the austenitic types, such as 316L and 304L, which are made by an atomization process that produces spherical powders. They are more difficult to press and sinter than the more common iron powders because of low green strength and extrusion; forging and hot-pressing are the preferred techniques for fabrication. Two excellent and compre-

hensive reviews of stainless-steel powder metallurgy have been sponsored by NASA (refs. 26 and 62). These surveys present a complete picture of the powder metallurgy process of producing stainless-steel shapes, as well as the resulting properties.

Nickel

Nickel is a hard, ductile, corrosion-resistant metal widely used for high strength at high temperatures without oxidation. In combination with other alloying elements it can provide materials with such unusual properties as zero coefficient of expansion and near zero coefficient of resistance. Ferromagnetic materials with very high permeability, and strong permanent magnets are typical nickel-alloy products. Modern technology would be badly handicapped if such alloys were not available. Jet engine parts made of superalloys incorporating nickel can operate at temperatures close to the melting point of iron. At the other extreme, nickel steels are usable down to cryogenic temperatures with minimum loss of ductility or tensile strength. While roughly ten times the cost of iron, nickel can be justified where its magnetic, anticorrosive, or high-temperature properties are necessary.

The development of nickel powder metallurgy by industry is not as extensive as that of iron or copper principally because of the high cost of nickel powder. Nickel strip is made from powder for electronic applications, and is reported to have greater purity and better properties for electronic components than conventional strip. Canada is using these strips in coin production. Nickel-iron, nickel-cobalt, and nickel-copper alloys are readily produced by rolling mixed elemental powders. Where property requirements overide the economic factors, structural parts can be made from nickel powder by virtually the same procedures employed for making iron parts, i.e., cold-die pressing in steel or carbide dies followed by sintering. The sintering atmosphere is less critical for nickel than it is for iron, so either dissociated ammonia or hydrogen is adequate. Sintering temperatures would be in the range of 2150° to 2350° F. Slip casting, hydrostatic compaction, or hot-gas-pressure pressing have all been successfully applied to nickel-alloy powders.

NASA's participation in the development of nickel powder metallurgy has been more extensive than in that of iron. A review of the current technology was completed for NASA in 1965 (ref. 23). Experimental work has consisted of an extensive project at Lewis in the development of dispersion-strengthened nickel (chapter 4), and in certain nickel-base super-alloys (ref. 63).

Cast and wrought nickel-base alloys are presently the most important high-temperature materials used in gas-turbine engines, for turbine buckets, stator vanes, and compressor disks. The temperatures at which these materials must operate are steadily being increased to meet requirements of greater performance from the engines. As a result, alloying requirements are becoming more complex. Casting these new alloys often results in macro- and micro-segregation of some components, thus reducing the strength of the alloy. In addition, highly alloyed compositions with high as-cast properties cannot be worked by normal procedures.

These problems can be largely overcome through the use of prealloyed powders in a powder metallurgy process. Freche and Waters selected two nickel-base alloys for evaluation (ref. 63). One was a commercial cast alloy, Alloy 713C, and the other, an experimental cast alloy, TAZ–8A (ref. 64). The composition of these alloys, both as specified and as found in the final materials, is shown in table IX.

The alloys were melted under argon in an induction furnace and atomized by an argon stream to spherical powder. The rapid solidification of the melted droplets produced a homogeneous powder with a low oxygen content. A −60-mesh cut from each sample was sealed in evacuated mild-steel cans and extruded into 9/16-in. bars at 2200° F. Tensile properties were determined for each alloy both as-extruded and after various heat treatments. The as-extruded samples had very high elongations in elevated-temperature tensile and stress-rupture tests, suggesting super plastic behavior. For example, Alloy 713C had a rupture elongation of 230 percent after testing at 2000° F and 2000 psi for 7.6 hr. TAZ–8A had an elongation of more than 600 percent at 1900° F, 1000 psi for 4.1 hr (fig. 27). This plastic behavior makes possible the hot pressing of finished products directly from extruded prealloyed powder. A 5/8-in. piece of TAZ–8A before and after upsetting at 2000° F with a low-strain rate of 0.03 to 0.07 in./in./min and a low load (initially 155 lb) is shown in figure 28. No cracks were present in the forged sample and its excellent properties at 1200° F indicate a great potential for this material in high-temperature engine parts.

The superplasticity of these alloys is caused by a very fine-grain structure. This can be coarsened by a programmed heat treatment consisting of a series of heat cycles starting at 2000° F, then 1500° F, and finally 1400° F. After heat-treating, the samples are no longer superplastic because of grain growth, and they exhibit substantially improved stress-rupture lives. At 1200°

TABLE IX.—*Chemical Analyses of Alloys (ref. 63)*

Element	Alloy 713C			TAZ–8A		
	Specified composition	Powder	Extrusion	Specified composition	Powder	Extrusion
	Element, wt. %					
Tantalum	-----	-----	------	8	8.17	7.72
Tungsten	-----	-----	------	4	4.00	3.93
Molybdenum	4.5	4.49	4.57	4	3.99	4.02
Niobium	-----	-----	------	2.5	2.67	2.49
Niobium and tantalum	2	2.42	2.30	-----	-----	------
Chromium	14	13.55	13.33	6	6.10	6.17
Aluminum	6	5.78	5.26	6	6.08	5.68
Titanium	1	0.66	0.64	-----	-----	------
Zirconium	0.10	0.08	0.14	0.75	0.62	0.77
Boron	0.01	0.012	0.015	-----	0.006	0.005
Carbon	[a]0.2	0.14	0.14	0.125	0.15	0.17
Iron	[a]3.0	0.80	0.70	-----	0.13	------
Cobalt	[a]1.0	0.42	0.67	-----	0.36	------
Manganese	[a]1.0	0.05	0.05	-----	0.03	------
Phosphorus	-----	0.002	0.002	-----	0.002	0.002
Sulfur	[a]0.015	0.003	0.004	-----	0.004	0.006
Silicon	[a]1.0	0.15	0.18	-----	0.04	[b]0.10
Nitrogen	-----	0.008	[b]0.0079	-----	0.018	[b]0.0087
	-----	0.016	[b]0.0170	-----	0.013	[b]0.013
Oxygen	-----	-----	[b]0.0113	-----	-----	[b]0.0150
Nickel	Balance	Balance	Balance	Balance	Balance	Balance

[a] Maximum.
[b] By independent laboratory.

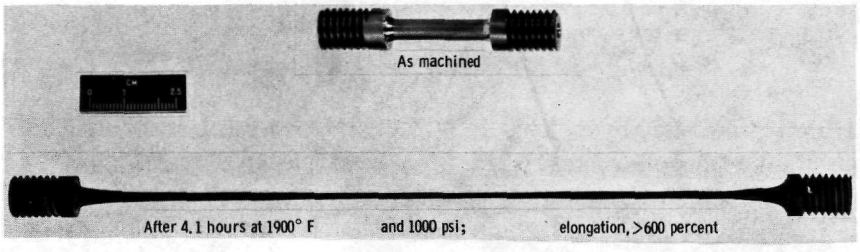

FIGURE 27.—Stress-rupture specimen of as-extruded TAZ–8A powder product before and after testing at 1900° F (ref. 63).

F and 105 000 psi, TAZ–8A had a rupture life of 975 hr. This compares to 100 hr for Inconel 718, one of the stronger conventionally wrought nickel-base alloys available. Grain growth in TAZ–8A can also be effected by heating it under a pressure of

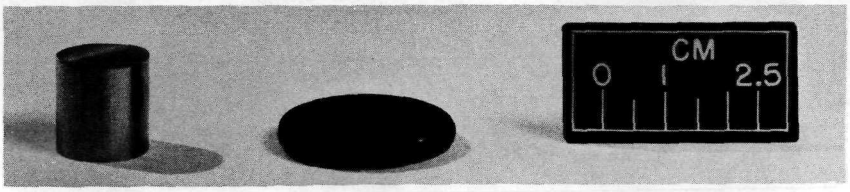

FIGURE 28.—Sample of TAZ–8A extruded powder product after upsetting at 2000° F (ref. 64).

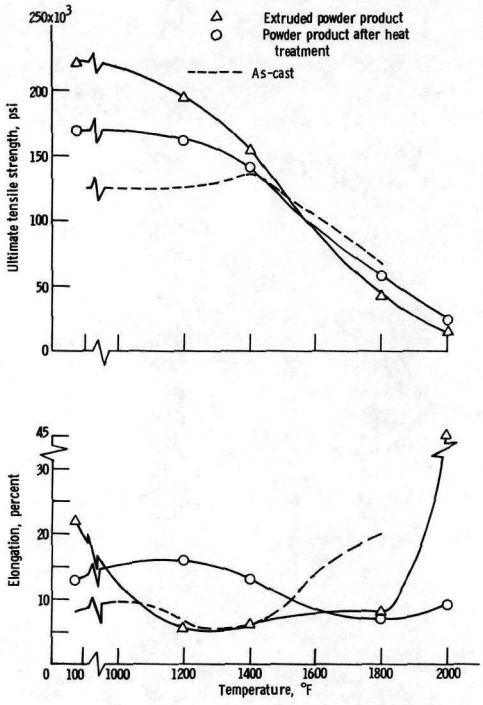

FIGURE 29.—Comparison of tensile properties of Alloy 713C powder products and as-cast Alloy 713C (ref. 63).

10 000 psi to 2400° F. This is 50° F above the incipient melting point at atmospheric pressure. It is possible to forge a piece of as-extruded TAZ–8A alloy in a die made from the same alloy, but heat-treated. The properties of both alloys in cast, as-extruded, and heat-treated conditions are shown in figures 29 and 30.

Cobalt

Cobalt is a tough, hard, and wear- and corrosion-resistant metal similar to nickel and iron in its properties. It is also ferromagnetic and constitutes an important alloying element in per-

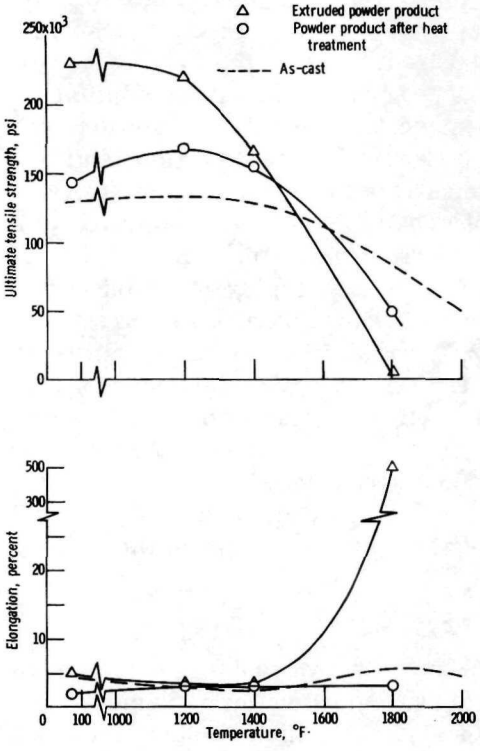

FIGURE 30.—Comparison of tensile properties of TAZ–8A powder products and as-cast TAZ–8A (ref. 63).

manent magnets and superalloys intended for high tensile strength, high-temperature use. Cobalt is particularly valuable as the matrix or binder for the alloys containing tungsten carbide where toughness, shock resistance, hardness, and high rupture strength are the dominant properties. An alloy consisting of 65% Co, 30% Cr, and 5% Mo has proved invaluable in surgical applications because of its compatibility with body tissues. Powder metallurgy is used extensively in the formulation and fabrication of the super-alloys containing cobalt permanent magnets, and the tungsten carbides, as it permits higher purities of the constituent metals and better control of the composition.

NASA's work in powder metallurgy cobalt has been concerned with cobalt-base superalloys (ref. 65) and dispersion-strengthened alloys (refs. 7 and 66). The powder metallurgy of cobalt-based superalloys was studied because cast highly alloyed materials tend to lose strength through segregation. The cobalt-base superalloy S–816 is one in which carbides form during ingot formation, tying up alloying elements and making them unavailable for age hardening. This alloy is a heat-resistant, forging

alloy, and has been used for many years in jet engines for turbine buckets. It has a nominal composition of 18–22Ni, 18–22Cr, 3.5–5.0 Mo, 3.5–8.0 W, 2.5–4 Cb, 4 Fe, and the balance cobalt. The wrought alloy contains 0.4% carbon. The effect of different amounts of carbon on S–816 made from prealloyed powder was investigated at Lewis Research Center. The preparations and test results are described in chapter 2 (see table III). The majority of the powder-metallurgy samples had larger stress-rupture lives than standard wrought S–816 tested under the same conditions (25 000 psi at 1500° F). They were also highly workable. Even specimens containing as much as 1.0% carbon were successfully hot-swaged with a reduction in area of 50 percent. Ductilities of 20% to 30% reduction in area were recorded for samples containing from 0.2% to 0.5% carbon, while the wrought alloy was much lower.

Projects to develop dispersion-strengthened cobalt alloys for NASA are described in chapter 2 (ref. 7) and chapter 4 (refs. 7 and 65). The results of both of these projects indicate the infancy of this research.

REFRACTORY METALS

Until very recently, powder metallurgy was the only way to consolidate the refractory metals. Tungsten-lamp filaments are still produced by a press and sinter technique followed by hot working, a process that was perfected a half century ago. The other refractories, molybdenum, tantalum, and niobium, were also processed primarily in this manner until five years ago. At that time, consumable-electrode arc and electron-beam furnaces reached a stage in their development where they could reach temperatures over 3000° C. These furnaces are now playing a dominant role in the production of new high-strength refractory alloys. For most commercial production of these metals, however, the powder-metallurgy route is still the most economical and efficient. Although NASA and other aerospace organizations have almost exclusively employed fusion processes to form the refractory metals, their considerable work devoted to the powder metallurgy of these metals should not go unnoticed.

The outstanding characteristic of the refractory metals is their high melting point. Usually, only metals with melting points above 2000° C are considered refractory, but often the noble metals, rhenium, rhodium, iridium, ruthenium, platinum, palladium, and osmium, are also included. These too are most often prepared by powder metallurgy, but at this time, they do not enter into aerospace technology to any great extent. All these metals are

listed in table X by their melting points, and it is immediately apparent that those of structural importance are very dense when compared to iron (7.97 g/cc) or titanium (4.5 g/cc). Their high melting points, however, offset this factor in applications such as rocket nozzles, electrode supports, furnace linings, filaments, heat exchangers, and heat shields. The main problems in these applications are:

1. Low oxidation resistance at high temperatures. (Rapid-strength losses in just the temperature region where the metals would be of the most use because of reduced cross sectional area as the metal is oxidized.)

2. Very low ductility above the recrystallization temperature for powder metallurgy materials.

3. High ductile-brittle transition temperature (DBTT) of tungsten and molybdenum, which increases after high-temperature exposure. Various means of coating, alloying, and dispersion-strengthening as well as the traditional method of hot working to increase ductility have been used with varying degrees of success to overcome these problems.

The powder metallurgy process starts with a high-purity powder which is isostatically compacted into a bar at pressures up to 60 000 psi. Self-resistance sintering is most often used because high temperatures are required to achieve reasonable densities in these metals, but a presintering step in a hydrogen furnace may be required to provide enough strength to undergo this step. Wa-

TABLE X.—*Properties of Refractory Metals*

Metal	Melting point		Density, g/cc
	°C	°F	
Palladium	1552	2826	12.02
Platinum	1769	3217	21.45
Zirconium	1852	3366	6.53
Thorium	1750	3182	11.66
Vanadium	1890	3434	6.11
Rhodium	1960	3560	12.41
Hafnium	2150	3901	13.29
Ruthenium	2250	4082	12.41
Niobium	2468	4474	8.57
Iridium	2410	4370	22.42
Molybdenum	2610	4730	10.22
Osmium	3000	5432	22.57
Tantalum	2996	5425	16.6
Rhenium	3180	5756	21.02
Tungsten	3410	6170	19.3

ter-cooled electrodes are clamped to each end of the bar and temperatures are raised to 2560° to 3100° C for tungsten, 2000° to 2400° C for molybdenum, 2400° to 2600° C for tantalum, and 1800° to 2300° C for niobium by adjusting the current. Tungsten and molybdenum are sintered in vacuum. Indirect resistance (using separate resistance heaters) and induction heating have also been successful for sintering. For wire or rod production, the sintered bar is swaged down to the required diameter at 1200° and 1500° C respectively for molybdenum and tungsten, and fine wires are hot-drawn at lower temperatures. Tantalum and niobium can be cold-worked by drawing, swaging, or rolling, with occasional annealing steps under vacuum. Sheet production is accomplished by similar procedures in which forging replaces swaging and hot rolling replaces drawing. Extrusion is often used to produce wrought tungsten shapes from the sintered compact. It is done at temperatures close to or above the recrystallization temperature and results in a fine, equiaxed grain structure. The ultimate tensile strengths obtainable in the 3000 to 4000° F range by extruding tungsten are given in table XI (ref. 67).

The 3000° C sintering temperature of tungsten is a major problem in its fabrication. The equipment required to reach this temperature is highly specialized, and the temperature itself causes problems in dispersion strengthening or fiber reinforcement. Several metallic additives have been proposed in the past to lower the sintering temperature, but these have generally resulted in materials with poor mechanical properties above 2000° F. McIntyre has successfully developed an alloy that matches or

TABLE XI.—*Elevated-Temperature Tensile Strength of Powder Metallurgy, Extruded Tungsten* [a] *(ref. 67)*

Specimen	Extrusion temperature		Test temperature		Ultimate tensile strength, ksi
	°F	°C	°F	°C	
1	3000	1650	2900	1590	17.2
2	3540	1950	2920	1600	16.5
3	4000	2200	2980	1640	15.6
4	3000	1650	3420	1880	10.5
5	4000	2200	3420	1880	9.9
6	3540	1950	3430	1890	10.2
7	3000	1650	3930	2170	4.8
8	3540	1950	3950	2180	5.1
9	4000	2200	3950	2180	5.2

[a] Extruded at a 12 to 1 reduction ratio and tested at a strain rate of 0.05 in/in/min (0.05 mm/mm/min).

improves on tungsten's properties in the 3000° to 4000° F range, and can be sintered as low as 2200° F (ref. 68). The alloy was prepared by blending micron-sized powders in a proportion to form a W–0.3 Ni–0.2 Co alloy with a 1% paraffin in benzene binder. A sheet was pressed out of this blend and sintered in vacuum for a half hour, and then rolled to 50% reduction at 3000° F. The density of the sintered compact was 18.4 g/cc, which increased to 18.9 g/cc after rolling. The properties of this alloy can be seen in table XII. The strength and ductility are comparable to wrought tungsten in the 3000° to 4000° F range.

Hall and Sikora examined the high-temperature properties of tungsten and molybdenum at temperatures from 2200° to 4400° F, and found that the ductility decreased at these temperatures in the case of commercially pure, sintered, and swaged tungsten (refs. 69, 70, and 71). This material was also found to be unusually sensitive to strain under these conditions, and an intensive study of this phenomenon was initiated. An increase in strain rate at a constant temperature was found to increase the ultimate tensile strength significantly (ref. 71). The magnitude of this strain hardening, which is greatest at approximately 3000° F, is shown in figure 31. At this temperature, a strain rate of 0.002 in./in./min produces an ultimate tensile strength of 5200 psi for a 1-in. specimen, but increasing the rate to 20 in/in/min increases the strength to 25 700 psi.

The change in ductility between 3000° and 5000° F of tungsten samples processed in various ways was studied at the Jet Propulsion Laboratory of the University of California (ref. 72). The differences found in the ductility of arc-melted, flame-sprayed, and powder metallurgy tungsten are shown in figure 32. The high

TABLE XII.—*Alloy Tensile Data (ref. 68)*

Composition, weight %	Condition	Test temperature, °F	Ultimate tensile strength, psi	Elongation, %
Tungsten-0.3 nickel-0.2 copper	Heat-treated	77	23 000	9.0
	Rolled	77	77 300	12.0
	Sintered	2000	24 200	3.0
	Sintered	2500	14 000	4.0
	Sintered	3000	10 000	4.0
	Heat-treated	3000	9 000	20.0
	Sintered	3500	8 000	52.0
	Sintered	4000	4 500	75.0

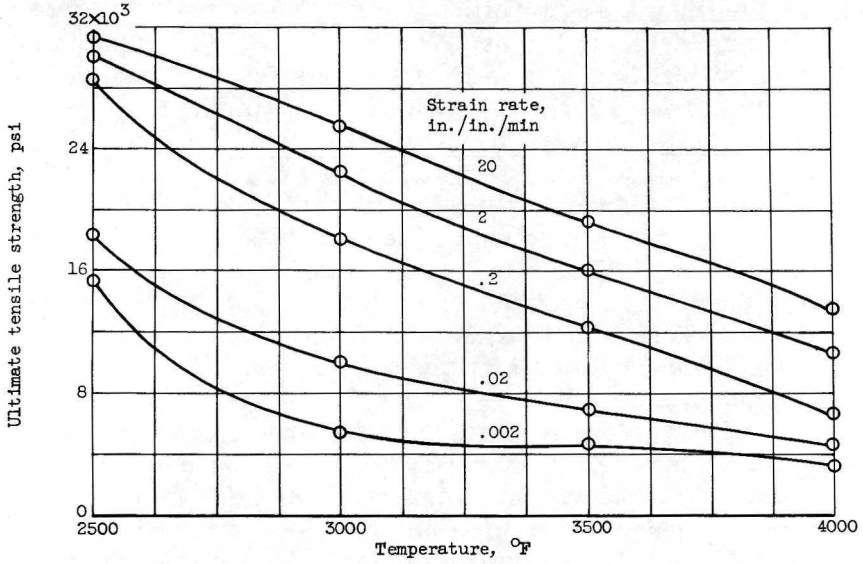

FIGURE 31.—Effect of temperature on ultimate tensile strength of tungsten at various strain rates (ref. 71).

ductility and lower strength of the melt-formed tungsten are attributed to the ease with which stress-induced grain growth occurs. A ductility minimum can be seen in the curve of the powder-metallurgy sample at about 3500° F. This phenomenon has been observed in other metals at about 50% of their melting points and is caused by the sliding of the grain boundaries, which causes the formation of voids at that temperature.

Plasma spraying of tungsten has been researched for many years as a way to form structural tungsten shapes. Burnett and Jansen reported in 1962 that the variations in spraying techniques, powder characteristics, and sintering conditions must be standardized before any real progress can be made (ref. 73). Chemical vapor deposition by the decomposition of either WCl_6 or WF_6 has been evaluated more recently as a means of coating structural shapes and producing tubing. Vapor-deposited tubing from several manufacturers was evaluated for NASA and compared with extruded tubing (ref. 74). Vapor deposition produced a very pure tungsten except for halogen impurities which affected the DBTT. It resisted grain growth better than wrought tubing, and when growth did occur, it started at the surface where small, randomly-formed grains were left from the deposition process. A similar, more recent comparison of tubes made by vapor-deposi-

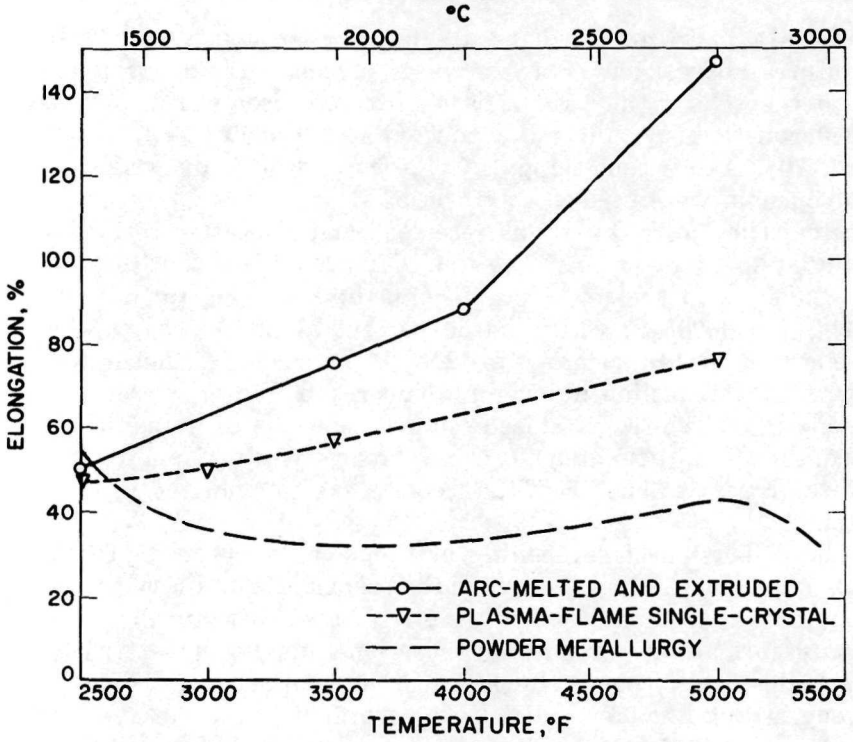

FIGURE 32.—Elongation as a function of temperature for arc-melted and extruded tungsten and plasma-flame single-crystal tungsten (ref. 72).

tion, extrusion, and electroforming techniques also indicated the favorable potential of the vapor-deposition process (ref. 67). The evaluation was done by burst-testing thin-wall tubing ⅜- and ½-in. thick in inert atmospheres at 3000° to 4500° F. Interestingly, the burst strengths were all equal to or higher than the ultimate tensile strength of extruded or swaged-extruded tungsten powder metallurgy rod at all test temperatures. In the wrought samples, recrystallization and grain growth occurred at 3400° F or higher, but did not occur in the vapor deposited samples below 3960° F. There was, however, evidence of voids in the walls of the vapor-deposited samples.

Alloying tungsten with other refractory metals has produced significant improvements in both the high-temperature strength and the strength-to-weight ratio. Tungsten, with small additions of tantalum or niobium, with or without carbon, has a much higher strength in the high-temperature range (ref. 75). This also is true when molybdenum is alloyed with tungsten, together with an added advantage of lower density of the final material

(ref. 76). Sikora reported the ultimate tensile strengths at temperatures above 2500° F for a series of commercially prepared powder-metallurgy alloys. The basis for comparison was a study of powder-metallurgy tungsten conducted at Lewis Research Center (ref. 70). Alloys containing 10%, 25%, and 50% by weight of molybdenum were used in the form of swaged bars 0.5 in. in diameter. They were tested "as received" and also after recrystallizing at 3550° F for 1 hr. The results indicated that the 10% and 25% alloys had greater strength than the unalloyed tungsten at 2500° and 3000° F, while the 50 percent alloy had comparable strength to pure tungsten up to 3200° F. Because of its lower density, a 25% reduction in weight would result by the substitution of this alloy. The recrystallized samples showed a drop in Vickers hardness of approximately 70% in comparison with the unrecrystallized types at 3000° F. These reports are summarized in table XIII.

The dispersion strengthening of tungsten to lower its DBTT and improve its high-temperature properties is discussed in Chapter 4. An offshoot of this effort is the work aimed at the *in situ* formation of refractory fibers in tungsten by extrusion. While this is also covered in chapter 5, its similarity to dispersion strengthening should be noted. The main difference in the two products is the size of the dispersant particles that make up their formulations. Dispersion-strengthened tungsten has extremely fine, well dispersed particles, while the *in situ* fiberizing method produces relatively large particles which are grossly deformed

TABLE XIII.—*Tensile Properties of Tungsten-Molybdenum Alloys (ref. 76)*

% tungsten	Temperature (°F)	Ultimate tensile strength, psi	Elongation, %	Reduction in area, %
100	2500	37 800	25	87
	3500	9 180	35	42
	4400	4 080	23	30
90	2500	44 600	21	98
	3500	10 200	27	39
	4400	2 660	35	56
75	2500	46 350	20	63
	3500	8 200	11	18
	4000	4 500	15	25
50	2500	36 200	22	68
	3500	6 500	11	16
	4400	1 900	14	29

longitudinally during extrusion. The chemical makeup of the second phase and the extrusion process are very similar for both final products.

Most of the experimental work involving tungsten is done via the extrusion process because of the low ductility of the pressed and sintered product. The extrusion of tungsten at low-reduction yields bars with fine-grain structures that can be forged, swaged, or rolled. Extrusion is particularly necessary for dispersion-strengthened and alloy-strengthened materials. In the dispersion-strengthened alloy, however, the high temperature of extrusion can cause undesirable reactions between the dispersant and the matrix. Other problems also arise with these high temperatures, such as difficulties of furnace control, die erosion, and container abrasion. NASA, however, has successfully avoided these problems by the use of molybdenum cans. Foyle, et al first suggested the cladding approach in 1960 (ref. 77) and reported the following advantages:

1. Protection from the atmosphere during preheating and extrusion
2. Improved lubrication during extrusion
3. Decreased temperature loss during transfer from furnace to extrusion press
4. The possibility of applying isostatic pressure to the billet, which may aid in producing plastic flow.

Another advantage found in a later study (ref. 78) was that the extrusion temperature could be lowered from a 2800° F minimum to as low as 2400° F, with no change in the as-extruded hardness, grain size, or tensile strength up to 3500° F.

Arc- and electron-beam-melted refractory metals start with a powder metallurgy process. Pure powders of the desired alloy constituents are mixed together, pressed, and sintered into 10- to 15-lb electrodes. These are then consolidated by one of the two processes under vacuum. Large-grained, high-purity ingots are produced, which are initially broken down by hot extrusion. In this and subsequent swaging or rolling, in the case of tungsten alloys, the ingot is encased in a molybdenum can.

The increased ductility of arc-melted tungsten (fig. 32) is common to all samples made by these methods. Low ductility at temperatures above the recrystallization temperature is characteristic only of powder metallurgy tungsten. A study reported in 1964 at Lewis Research Center showed that the DBTT, tensile strength, and creep behavior of arc-melted tungsten were similar to powder metallurgy tungsten when the grain sizes and internal structures

were comparable (ref. 79). The rate of grain-growth was found to be related to impurity content, with the purest materials exhibiting the higher overall rates.

Alloying tungsten with tantalum, hafnium, niobium, rhenium and carbon had yielded significant strength improvements with the highest observed in the W–Hf–C system. Lewis Research Center has pursued this for several years (refs. 80, 81, and 82) culminating with the development of W–4Re–0.35Hf–0.35C. This alloy, acknowledged by Industrial Research magazine with one of the IR–100 awards for 1967, has shown a ninefold strength advantage over unalloyed tungsten in a swaged condition at 3500° F (ref. 82). The high-temperature strength of this alloy is attributed to the precipitation of hafnium carbide particles at the grain boundaries, stabilizing the structure at high temperatures. In addition, low-temperature ductility is achieved by the solution-strengthening effects of rhenium. Above 3500° F, the carbide particles tend to agglomerate fairly rapidly, thus limiting the alloy's usefulness in this temperature range, but, between 3000° and 3500° F, it is superior to any other known refractory material with lifetimes in thousands of hours.

The same strengthening principles were applied to arc-melted molybdenum with favorable results (refs. 83 and 84). Attractive mechanical properties were obtained in strain-aged alloys such as Mo–0.6Hf–0.5C, extruded at 4000° F prior to swaging. These alloys had ultimate tensile strengths greater than 100 000 psi over the temperature range of 1500° to 2700° F.

Welding of refractory metal alloys is of major importance to the aerospace industry because of the resulting increase in their usefulness. One example is in the construction of a space power plant that converts thermal energy to electrical energy by the Rankine cycle. To meet the objective of maximum efficiency at minimum weight, the highest operating temperature possible is desirable. Refractory-metal construction would be logical if welding were possible. Lessman studied the weldability of a large number of refractory alloys (ref. 85). These could be grouped as niobium-based, tantalum-based, and tungsten-based alloys. Initial efforts in the program were directed to the evaluation of several grades of powder-metallurgy tungsten, but it was found that the resulting welds had high porosity. Further work was done with vacuum-arc and electron-beam melted alloys. Manual and automatic tungsten-arc welding and automatic electron-beam welding in a vacuum purged chamber were evaluated in the study. The niobium- and tantalum-base alloys gave the best results. In particular, FS–85 (Nb–27Ta–10W–1Zr) and T–111 (Ta–8W–2Hf)

demonstrated superior combinations of strength and fabricability. Tungsten, on the other hand, was not easily welded because of brittleness at room temperature, and a W–25Re proved to be hot-tear sensitive as well as brittle.

Uranium dioxide-containing nuclear fuel elements are frequently made from composites containing tungsten as the strengthening element (see Chapter 6), and since these composites might form part of the structure of a nuclear reactor designed for use in space, flexibility in joining and forming the materials is highly desirable. Direct fusion welding is not possible since UO_2 vaporizes at a temperature lower than the melting point of tungsten, so considerable interest has been expressed in brazing techniques (refs. 86, 87, and 88). In the latest work (ref. 88), cylinders were formed from a cermet sheet made by rolling a mixture of 80% tungsten and 20% UO_2 powder, and bonding the resultant sheet between 0.0015-in. tungsten sheets. Cylinders with a 1-in. diameter were formed which had 1.5 in. longitudinal seams. Gas tungsten-arc brazing of the seams left excess brazing metal, so a furnace-brazing technique was developed. Successful welds were achieved by covering the joint with a mixture of tungsten-25% osmium powder and then heating to 3000° C for one minute in a helium atmosphere. A 15-min post-brazing treatment at 2865° C was required to convert the crack-sensitive sigma phase of the braze alloy to the more stable alpha phase. A 20% loss in strength of the parent cermet at 2500° C resulted from this treatment. This loss could probably be avoided by the use of a lower-melting brazing alloy such as molybdenum-5% osmium.

The vulnerability of the refractory metals to oxidation at high temperatures has stimulated interest in developing coatings for them. An example of this work is the use of iridium as a coating in a NASA project (refs. 89 and 90). The initial program showed iridium to have promising oxidation-resistant characteristics when tested on hot-pressed tungsten in an oxygen-methane flame (ref. 90). The iridium could be pressure-bonded to the substrate or applied by electroplating with a fused-salt electrolyte. The best results were obtained with tungsten. A 5-mil-thick coating of iridium was estimated to last indefinitely at 1700° C. Niobium and molybdenum also were effective, lasting 700 and 600 hr respectively at that temperature. Tantalum gave good results only when a diffusion barrier was placed between the coating and the base.

Silicide coatings have been used widely for the protection of the refractories up to 3100° F. The low-temperature brittleness that causes crazing and chipping of these coatings has been a

source of problems, however. Frequently rapid "pest" oxidation occurs at intermediate temperatures. Modifications, such as the addition of other metals to the coating, have helped reduce these problems, and have extended the elevated-temperature lifetimes. The following methods have been used to apply these coatings:

1. Pack-cementation of silicon
2. Chemical-vapor deposition of silicon
3. Electrophoretic deposition of disilicides followed by isostatic pressing and sintering
4. Fused-salt deposition of silicon
5. Slurry application of silicon and modifying elements followed by fusion
6. Slurry application of a modified alloy followed by (a) sintering in vacuum and (b) application of silicon by pack cementation.

An example of the last of these methods was developed for NASA for use on tantalum and niobium (refs. 91 and 92). Elemental powders in the ratio 35Mo–35W–15Ti–15V were ball-milled in an organic solvent. The tantalum substrate was either sprayed or dipped into this mixture and then heated in vacuum. Silicon was then applied by the pack-cementation process in argon at 2400° F to produce a coating consisting of disilicides of tantalum and the modifying elements. This coating has a lifetime of over 1000 hours at 2400° F and good crack resistance.

CHAPTER 4

Powder Reinforced Compacts

Almost every material known to man is a composite. One reviewer of the field (ref. 93) devoted nearly 2000 words to defining the term between the limits of one microscopic substance containing different kinds of atoms and another macroscopic one built out of different materials. For the purposes of this survey, the definition used by the Bureau of Mines (ref. 94) can be adapted.

> A metal powder composite is a metal or an alloy with built-in strengthening agents which may be in the form of filaments or powders of a strong material.

Many powder metallurgical materials that contain two distinct phases are now eliminated from this discussion because their second phase is not included for strengthening purposes. Thus, for example, nuclear fuel elements and powder metal bearings will be discussed elsewhere.

Very early in the space age, the critical requirements of aerospace vehicles quickly outran the properties of the ordinary metals. The development of the more exotic metals and the superalloys provided only a temporary lead, and now, composites have become the high-temperature and high-strength materials of the near future.

Two very different types of composites have been researched by NASA. The first of these has extremely fine refractory particles that stabilize the matrix of certain metals and allow their use at temperatures far above those previously thought possible. The widely publicized sintered aluminum powder (SAP) is an example of such a material. The other type of composite has the high strength of fibers or whiskers dispersed in structural matrices, which bond the materials into rigid networks. The ubiquitous fiber glass is a nonmetallic example.

Powder metallurgy has entered into the development of both of these types of composite. It is the most successful method of producing a fine dispersion of one material within another, and it provides a method of placing a high-melting matrix around fibers

without the deleterious effects of fusion infiltration. Fiber-related technology will be described in the following chapter.

Dispersion strengthening is a remarkable new concept in materials science that was discovered quite by accident. In ordinary powder metallurgy, the existence of an oxide film during sintering of compacted powders would impair the processes of adhesion, surface diffusion, and volume diffusion. To prevent this, it is usually necessary to work in a reducing atmosphere. The oxides of some metals such as aluminum or beryllium, however, cannot be reduced by any gas, and since aluminum forms an oxide covering immediately on contact with air, it was not suitable for sintering. In 1950, the laboratories of Aluminum-Industrie-A.G. in Switzerland announced the discovery of SAP (refs. 95 and 96). Not only did this material represent an exception to the idea that the oxide layer always was detrimental, but more importantly, for the first time, a powder metallurgy product had better properties than the cast or wrought metal. It appeared that an entirely new material had been created. Containing up to 13 percent oxide, SAP was made from ordinary pigment-grade aluminum flake. It had a tensile strength of around 14 000 psi at 500° C and maintained it for over 700 hours. Compared to a maximum of 3000 psi at 500° C for conventional aluminum alloys, the new material was superior to any other aluminum material including even the precipitation-hardened alloys at temperatures above 200° C. It even retained some strength up to the melting point of aluminum.

Production of SAP involves a critical milling step during which the aluminum flakes are further oxidized and agglomerated to a coarse (100 micron) powder containing an internal dispersion of oxide (6–14% Al_2O_3). The powder is then cold-compacted, wrapped in aluminum sheet, and sintered at 500° C in air. Billets are hot-pressed and extruded into bars. The final working is necessary to develop the strength of the material because, up to that point, the adhesion between the particles is largely due to the bonding between Al and Al_2O_3, and extensive shear is needed to develop sufficient Al/Al bonding (ref. 97). This, however, explains only how the sintered material could have strengths comparable to those of the cast metal. The increased high-temperature properties must be explained by an entirely new theory.

A photomicrograph of SAP (fig. 33) shows the fine Al_2O_3 particles dispersed in a matrix of aluminum. The superior properties result from the characteristics of this dispersion. Most metals and alloys undergo recrystallization at some characteristic temerature, which greatly affects their properties. This phenomenon

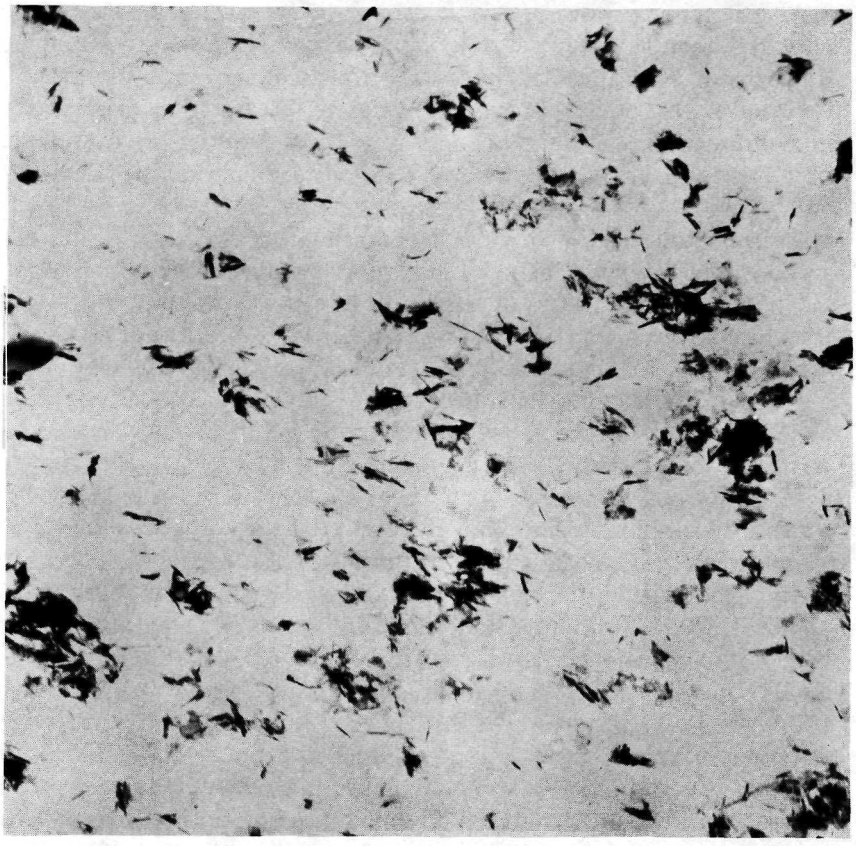

FIGURE 33.—Electron micrograph (20 000X) of 6% dispersed oxide alloy prepared by milling. (Courtesy Aluminum Co. of America.)

occurs when the energy that is built up through various deformations of the original crystal structure (work hardening) is released. Above the recrystallization temperature, when this energy is dissipated, a weak strain-free grain structure remains. SAP materials of more than 7% oxide do not recrystallize until very near the melting point, and, consequently, the cold-worked strength is retained to a higher temperature. Dispersion-strengthened materials have a "high stored energy of cold work" (ref. 98).

Recrystallization, as well as any form of plastic deformation of a metal, requires the movement of vacancies (voids in the crystal lattice) through the atomic lattice to positions of less strain. The dispersoid particles in SAP seem to block this movement, thereby raising the recrystallization temperature and increasing the yield

strength. The number of particles and their spacing in the matrix should affect these properties more than the volume percent of dispersoid. This has been proved experimentally many times. In fact, an expression has been derived (ref. 99), which predicts the minimum interparticle spacing for a given particle size and volume percent. When agglomeration of the dispersed particles occurs, the spaces between the agglomerates must be large. Thus, one important criterion for dispersion strengthening is: the smaller the interparticle spacing, the more useful the dispersion.

The many advantages of the SAP system became apparent only when metallurgists tried to apply dispersion strengthening to other metals and alloys. The formation of oxide on aluminum powder in an extremely thin (100 Å) layer as soon as it is exposed to the air is the cause of the almost ideal dispersion in SAP with the interparticle spacing around 0.4 micron. Agglomeration does not occur. The oxide itself is one of the most chemically and thermally inert materials known. Few other structurally desirable metals have usable oxides, therefore, strengthening other metals requires different dispersoids and dispersion methods. The work on SAP brought about a wide field of research based on the postulate that any inert powder well dispersed in any metal matrix should increase its strength and high-temperature properties in proportion to the increase of SAP over aluminum.

It was soon noted that thoria, which for many years had been mixed with tungsten powder to achieve smaller grain structure and better ductility in lamp filaments, was another example of this concept of strengthening. Other systems were slow in coming, however, and it was not until 1955 that an oxide-strengthened molybdenum was announced (ref. 100), followed by copper with alumina in 1956 (ref. 101). The reason for this apparent lack of attention, which lasted into the early sixties, was the difficulty in obtaining high quality, fine (1 to 5 micron) metal powders (ref. 102). Research in reliable structural parameters and strengthening mechanisms had to await the availability of proper materials.

Since 1960, the situation has changed. Industrial corporations have introduced a few metal-metal oxide products despite the increased cost of extra manufacturing steps necessary to produce the dispersion (ref. 102). Of these, the thoria-dispersed nickel alloys are among the best known. These alloys are intended for such high-temperature applications as aircraft turbines, furnaces, and heat exchangers. Lead lead-oxide alloys enable radiation shielding at higher temperatures, and can be employed in the electronic, building, and chemical industries. Also, several dispersion-strengthened alloys of copper and silver have been developed

TABLE XIV.—*Dispersion-Strengthened Materials Developed by Industry and Academic Institutions*

Matrix	Dispersoid
Aluminum	Alumina,* iron aluminide
Beryllium-copper-tin	Beryllium
Chromium	Magnesium oxide
Cobalt	Thoria, various oxides
Cobalt-chromium	Various oxides
Columbium	Various dispersoids
Copper	Silicon dioxide, alumina, beryllium oxide*
Inconel	Various oxides
Iron	Beryllium oxide
Iron-chromium	Thoria
Iron-nickel-chromium	Thoria
Lead	Lead oxide*
Nickel	Alumina, thoria,* various oxides
Nickel-chromium	Alumina, thoria*
Nickel-cobalt	Various oxides
Nickel-molybdenum	Thoria
Silver	Silver oxide
Stainless steel	Various carbides, thoria, beryllium oxide
Tantalum	Various dispersoids
Tungsten	Thoria
Vanadium	Various oxides
Zinc	Various oxides
Zinc-copper	Titanium
Zirconium	Beryllium, various oxides

* Production item.

for use in electronic components. These and other materials in the research or development stages are listed in table XIV.

In the early sixties, NASA became interested in dispersion-strengthened metals to meet the need for materials that could operate from 1000° C, where superalloys began to fail, to 1300° C and above, where the refractory metals could be used (refs. 103 and 104). These materials were needed in air-breathing gas turbines for stator vanes, turbine buckets, nozzle guides, and afterburner liners. They had to be oxidation resistant as well as strong. Since more severe requirements were required by the space program, steps were taken to develop dispersion-strengthened superalloys.

Careful study of previous dispersion-strengthened alloys, and in particular, the "ideal" one, SAP, indicated the characteristics that were required. For example, the dispersoid in SAP is about 0.01 micron in thickness, and the interparticle spacing (IPS) is approximately 0.5 micron (ref. 105). The high-temperature

strength also depends on the stability of the dispersion. It should not react with the matrix, and must have a higher melting point. These characteristics are summed up in table XV. Materials with these properties usually form very readily, but are difficult to decompose. Oxides such as thoria (ThO_2), alumina (Al_2O_3), beryllia (BeO), and magnesia (MgO) are much more stable than carbides, dispersoids often used in precipitation-hardened steels. (These steels do not have good high-temperature properties, since the dispersed phase is not stable and migrates or dissolves at elevated temperatures.) Thoria, on the other hand, strengthens tungsten at temperatures up to 1600° C. Finally, based partially on the degree of improvement of SAP over wrought aluminum, and partially on the needs of the aerospace program, it was established that successful alloy for space applications should have a 3000-hr stress-rupture strength of 15 000 psi at 1100° C. This far exceeds the best superalloys, which lose most of their strength by 1000° C.

Calculations have shown that even to obtain an IPS of 1.5 microns, matrix and dispersoid powders in flakes 0.5 and 0.1 micron in thickness respectively are required (ref. 106). In 1960, however, fine metal powders were not commercially available, so the earliest efforts at Lewis were designed to develop such powders. The metals chosen were primarily nickel, chromium, and cobalt because of their previous roles in high temperature alloys. Particle-surface cleanliness was found to be very important. Nickel, for example, could be cleaned (reduced) easily by the reaction:

$$NiO + H_2 \xrightarrow{300^\circ\ C} Ni + H_2O,$$

but others required more severe treatment. This is particularly true of chromium. A small percentage of Cr_2O_3 can cause thoria in nickel-chromium alloys to agglomerate at high temperatures and destroy the strength of the alloy. It can be removed by hydrogen, but only at high temperatures that also cause thoria agglomeration. Alternative methods of producing pure nickel-chromium powder at lower temperatures have been developed.

In the last five years, the requirement to develop a dispersion-strengthened alloy with the 3000-hr stress rupture of 15 000 psi at 1100° C was established and submitted by NASA to many industrial and academic laboratories. "Here every novel trick of the trade to produce a dispersion-strengthened product has been tried" (ref. 103). In the meantime, Lewis Research Center has perfected several powder-production techniques and powder-cleaning methods, and has established microstructural criteria. These

TABLE XV.—*Variables Affecting the Mechanical Properties of Dispersion-Strengthened Materials*

Material variables	Geometric variables	Particle morphology
Melting temperature of the matrix material and the dispersoid.	Volume fraction of the dispersoid.	Shape of the particles.
Possible reactions between the components at various temperatures and atmospheres.	Particle size of the dispersoid.	Any preferred orientation.
Stresses in the components	Interparticle spacing	Surface characteristic of the particles.
		Distribution in the microstructure.

accomplishments are reviewed in chapter 2. The strength goal has not yet been met, but the research to achieve it has been productive of some interesting and valuable new materials and, more importantly, a deeper understanding of the phenomena of dispersion strengthening. Examples of some dispersion-strengthened base metals are listed in the succeeding paragraphs.

NICKEL

The technique of ball-milling metal powders to extremely fine particle sizes was developed quite early at Lewis (ref. 107). Because NiO can be easily reduced, pure, extremely fine nickel powders were among the first to become available. In 1961, a magnesia-dispersed nickel alloy was reported (ref. 104). In the best samples obtained, nickel powder particles less than 1 micron in size were mechanically mixed with 7%-by-weight MgO powder. This mixture was then hot-pressed and extruded at 1150° C. As was true with SAP, extrusion was found necessary to develop a useful dispersed structure. Additional cold-working increased the strength of the samples, and at 1000° C they were stronger than any of the commercially available dispersion-strengthened alloys. This had not been thought possible for mechanically mixed powders.

The concept of cleaning precompacted "coins" was introduced in 1966 (ref. 10). Nickel and alumina powders were ball-milled together, washed, pressed into 0.25 in.-thick coins, and heated in hydrogen at a programmed rate up to 1100° C. The thin, porous disks enabled the cleaning gas (H_2) to enter and the reaction product (HO_2) to leave easily. The gradual heating caused sinter-

ing to follow cleaning, and the compacted structure prevented gross movements of the oxide particles. The sintered and cleaned disks then were stacked in cans for hot pressing and/or extrusion. No agglomeration occurred. The alumina was dispersed in particles of 0.05 to 0.6 micron even after an eleven-hour anealing at 1425° C. This is an important test, for if impurities are present, they will cause agglomeration of the dispersed phase at high temperatures.

In other particle-preparation studies at Lewis, both lithium vapor (ref. 6) and hydrogen halides (ref. 12) were used to reduce powder containing NiO. The former method produced rather coarse particles (1.25 microns) but with exceptionally low oxygen contents. It also was useful for reducing nickel and chromium powders together since they require identical conditions for this treatment. Another approach to powder cleaning that avoids the problem of particle growth has been developed. The submicron powder is suspended in a hydrogen stream, passed through a hot zone at 335° C, and stored under argon (ref. 11).

Several extensive reviews of thoria-dispersed nickel have emphasized the values of dispersion strengthening (refs. 25 and 108). Some strength properties of pure nickel compared with those of a commercial TD-nickel, both as-received and after recrystallization are shown in figure 34. The TD-nickel is a commercial product with a 3-hr heat-treatment at 1300° C. At this temperature, it loses its cold-worked energy, and becomes a weaker structure.

Several contractors (refs. 109 and 110) have used a variety of techniques to attain the strengths in nickel-base alloys desired by NASA. In one project, a matrix of Ni–15Mo was selected because molybdenum is an excellent solid-solution strengthener for nickel (ref. 109). MoO and NiO powders were coated with thoria by a salt-decomposition technique and then reduced with hydrogen (ref. 110) (fig. 35). After compaction and extrusion, this product had a microstructure of uniformly dispersed particles and maintained some strength for 100 hr at 2000° F. In another process, a high-intensity arc was used to produce powder by vaporization from Ni–20Co–10Mo–10W alloy with 4%-by-volume thoria (ref. 111). The yield of useful powders obtained in this way, however, was only 20%, which is too low for a commercial process. Sample compacts from this powder had good thermal stability with the average particle size 0.077 micron and IPS 0.84 micron.

Another approach to obtaining satisfactory high-temperature properties was based on the theory that a dispersion-strengthened

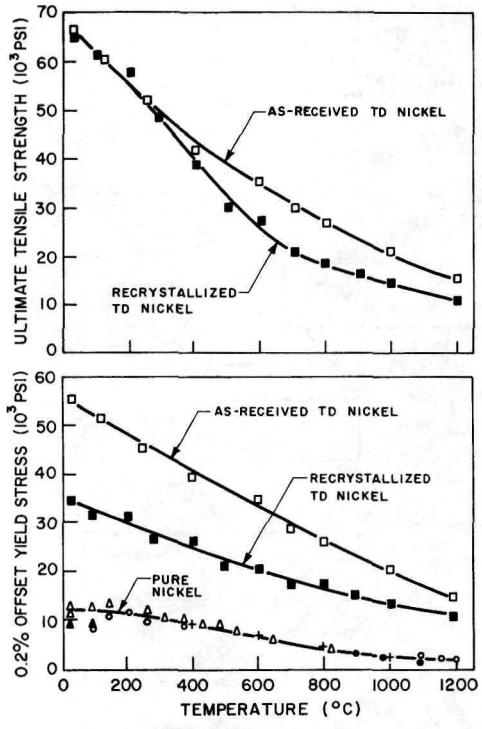

FIGURE 34.—Temperature dependence of the yield and ultimate strengths of as-received and recrystallized TD nickel (ref. 108).

nickel-base alloy containing chromium for oxidation resistance and molybdenum as a solid-solution strengthener should have excellent high-temperature properties (ref. 112). Zirconia particles of 0.1-micron size were suspended in a fluidized bed (fig. 36), and then successively plated with molybdenum, chromium, and nickel by decomposing volatile organic compounds of the metals. Very uniform dispersions were achieved when single elements were deposited on zirconia, but problems of agglomeration arose in the multiple-element experiments.

Oxidation, one of the chief problems of dispersion-strengthened nickel at high temperatures, can be reduced by using oxidation-resistant coatings. Several materials were evaluated to find one which could be made into a 5-mil cladding that would be stable for 800 hr in air at 1250° C (ref. 113). A series of Ni–Cr–Al alloys and one Fe–Cr–Al alloy were produced which lasted for 100 hr at 1250° C. The addition of 0.25% yttrium to Fe–25Cr–4Al increased the survival time of a 10-mil sheet to 800 hr, and Ni–20Cr–5Al with thorium lasted 700 hr at the same temperature. The problem, however, was not solved completely, because, when these sheets were bonded onto TD-nickel and TD-nickel-chro-

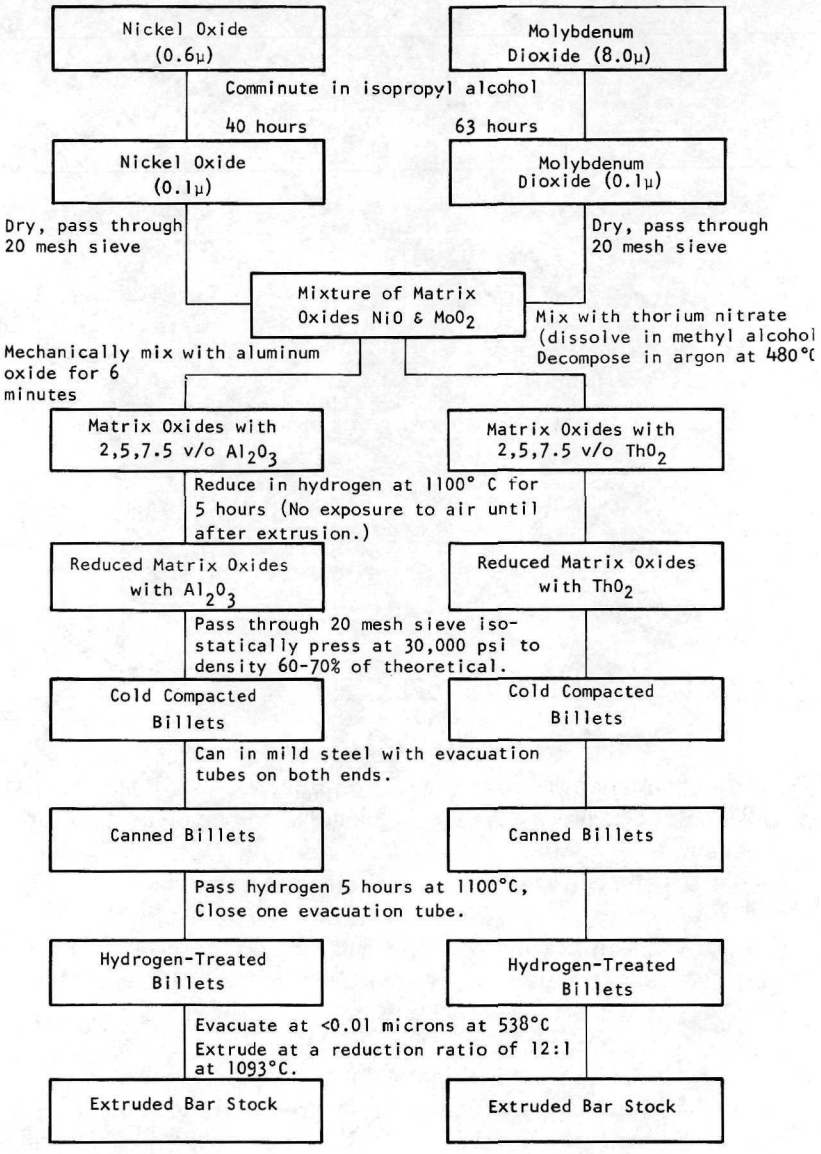

FIGURE 35.—Processing chart for nickel-molybdenum dispersion-strengthened alloys (ref. 109).

mium by hot and cold rolling, interdiffusion occurred before 100 hr had elapsed at 1250° C (fig. 37). After 400 hr at this temperature, diffusion was complete, and the layers were indistinguishable. Another approach was to coat a slurry containing nickel,

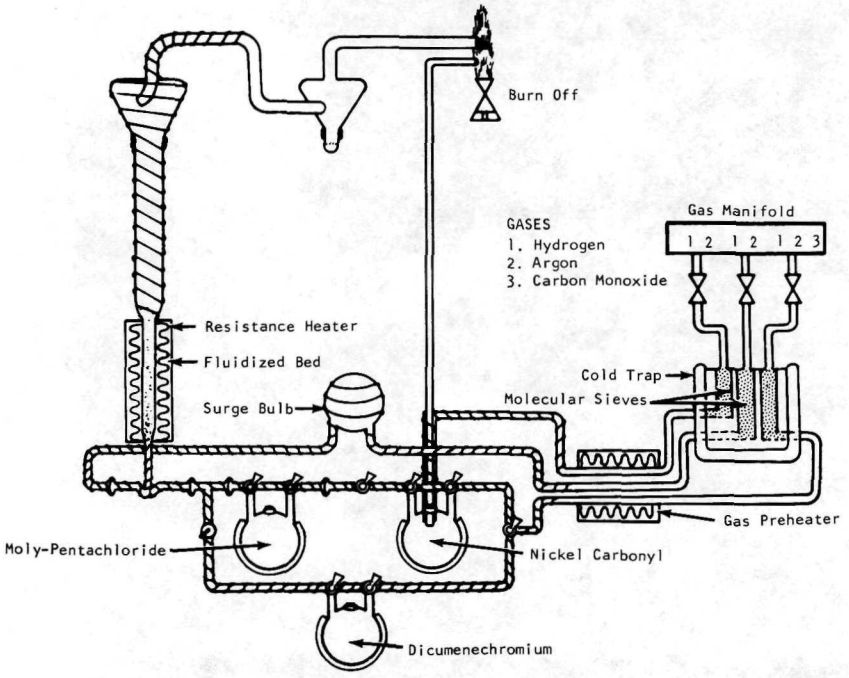

FIGURE 36.—Fluidized-bed reactor for producing dispersion-hardened alloys (ref. 112).

chromium, aluminum, and silicon onto structural parts (ref. 114). The coated layers varied in thickness, especially at the edges, so a two-step process was substituted. A Ni–Cr–Si layer was fused on first, followed by an Al–20Co layer. These coatings protected thoria-dispersed nickel for 200 hr and thoria-dispersed Ni–Cr for more than 350 hr, although they caused some embrittlement.

CHROMIUM

The general lack of success in achieving high-temperature nickel-base alloys has led to the development of other alloys. The refractory-sheet alloys of niobium and molybdenum have load-carrying capacities at 1600° C, but they require oxidation-resistant coatings which restrict their usefulness. Chromium, on the other hand, has good oxidation resistance and excellent high-temperature properties. Because it has a higher melting point, higher elastic modulus, and lower density, it has a significant strength-to-density advantage over nickel. The main reasons that chromium is not used as a structural metal are its high DBTT, and its embrittlement by nitrogen at elevated temperature. The

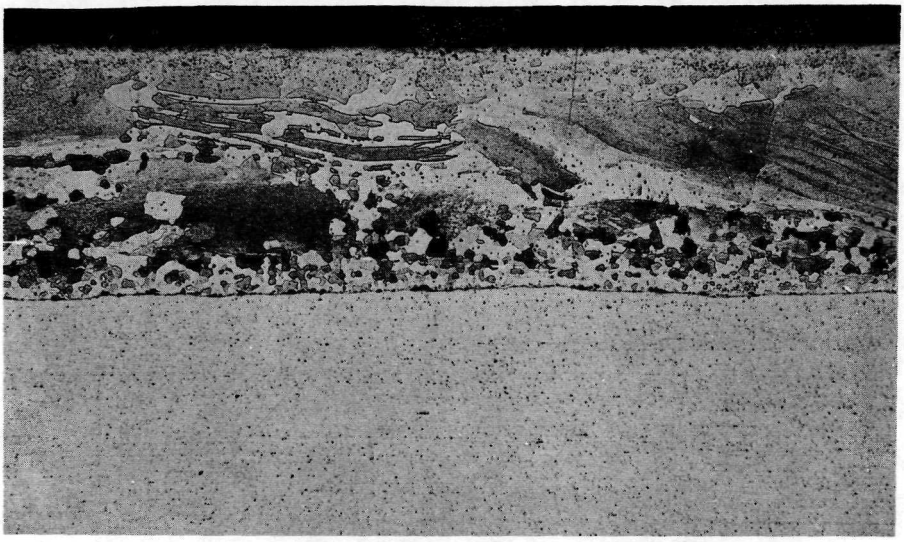

As Hot Rolled (100X)

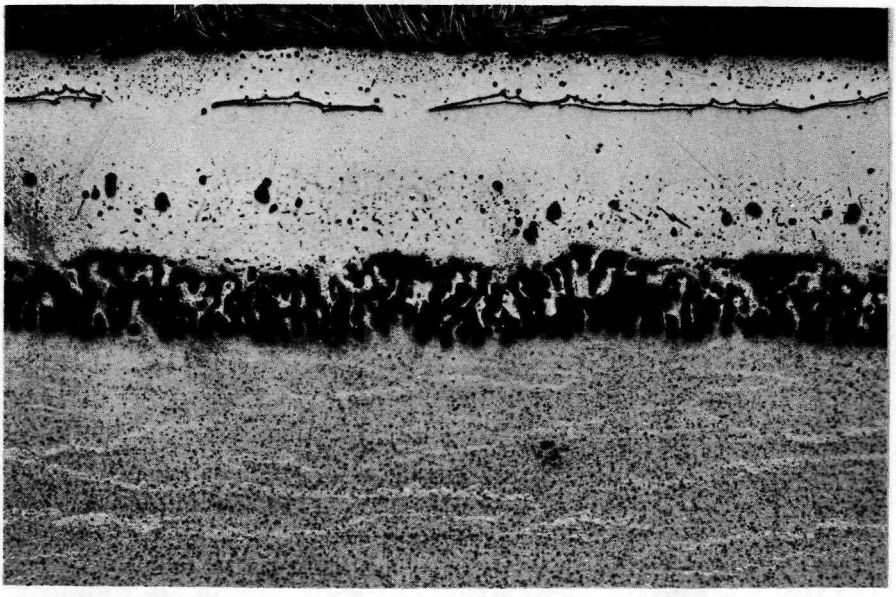

After 100 Hours at 2300°F (100X)

FIGURE 37.—Interdiffusion of TD–Ni–20Cr–4Al and TD-nickel (ref. 113).

DBTT is the temperature below which a metal is brittle and therefore is not applicable to many structural applications. The DBTT of chromium is usually above room temperature and decreasing it has been done in the past only at the expense of its high-temperature properties. However, there is evidence that a thoria dispersion would lower the DBTT by hindering crack propagation (ref. 115), and also would raise the high-temperature mechanical properties. The major problem is the reduction of chromium oxide. Cr_2O_3 must be reduced to less than 0.1% in any dispersion-strengthened alloy to achieve sufficient levels of purity, but this can be done only by hydrogen reduction at 1250° C or higher (ref. 116). Since sintering usually occurs at this temperature, several means of sidestepping this problem have been developed.

The Lewis metallurgists have produced extremely fine chromium powders by ball-milling. Diameters down to the size of cigarette-smoke particles (0.0068 micron) have been measured. When water is used as the grinding medium, the evolution of hydrogen can be used to calculate the amount of Cr_2O_3 formed, and from that, the surface area and particle size (ref. 3). Powders of 0.03-micron particles were obtained in this way, but some welding occurred, trapping oxide between layers of metal. When hydrogen halides like HBr or HCl were used as the grinding media, chromium powders could be milled with or without thoria to a particle size of 0.04 micron (ref. 12). Fifteen percent of the metal is converted to halide in the process, but its reduction occurs at much lower temperatures than those of oxides. This exploratory work did not remove all the impurities, however, and some thermal instability was caused by dispersoid agglomeration. Extremely pure powders have been produced by the reduction of Cr_2O_3 with vapors of reactive metals (ref. 6). Chromium oxide powders down to 0.16 micron in particle size can be reduced this way. The only impurities that have been found are inclusions of MgO that form when magnesium is the reactive vapor. These powders are suitable for immediate consolidation, yielding an MgO-dispersed chromium.

Early in the sixties, a commercially produced magnesia-dispersed chromium was announced (ref. 117) that had structural strength at 1600° C, uncoated. Actual tests, however, showed that only 7% of its room-temperature tensile strength of 80 000 psi remained at 1425° C. In addition, this composite material oxidized rapidly above 1200° C. Micrographs showed that it contained inclusions of MgO up to 5 micron, and it had a 5 to 10 micron IPS.

At present, three dispersion-strengthened, powder-metallurgy

chromium alloys are produced commercially in the United States. They are designated Chrome-30, Chrome-90, and Chrome-90S. The principal dispersant in each is MgO. Chrome-30, developed in 1962, also contains 0.5% titanium, while alloys developed later contain other elements for improved high-temperature strength and oxidation resistance. The main advantage of these alloys is their improved low-temperature ductility and high-temperature oxidation resistance. As seen in figure 38, the Chrome-30 and Chrome-90 alloys exhibit good tensile ductility at room temperature, but low strength at elevated temperatures. The Chrome-90S alloy has better high-temperature strength, but at the expense of a substantial increase in the DBTT.

The decomposition of chromium compounds in the vapor phase or in solution usually results in extremely pure deposits of chromium metal. Because of the low oxide content of chromium plated layers, experiments were conducted to deposit thoria particles simultaneously with chromium by suspending them in the gas stream or the bath. The resulting oxide-dispersed deposit could then be built up into layers to produce structural components. The two projects under which this goal was pursued produced extremely pure metals, but it was not posssible to get sufficient thoria into the deposit (refs. 119 and 120).

Sheets of Cr–4Mo–4ThO_2 have been successfully produced by

Alloy	Composition, wt.%	Ductile-Brittle Transition Temperature, °F	
		Tensile	Impact
Chrome-30	Cr-6MgO-0.5Ti	10	323
Chrome-90	Cr-3MgO-2.5V-0.5Si	0	550
Chrome-90S	Cr-3MgO-2.5V-1Si-0.5Ti-2Ta-0.5C	350	1100

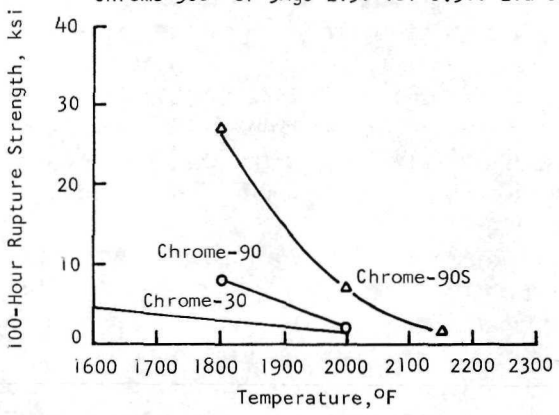

FIGURE 38.—Strength and ductility of commercial dispersion-strengthened chromium alloys (ref. 118).

ball-milling prealloyed chromium powders (ref. 121). The first work was done with powders milled to particle sizes of less than 1 micron, but the usual cleaning developed, so a second run was made by milling for a shorter time. The powder was coarser, but the purity was improved. The size of the dispersoid particles in the final product was around 0.07 micron and the IPS was 1 micron, indicating that prealloyed powders need not be ground exceptionally finely to achieve good microstructures. The alloy had good thermal stability up to 1300° C, but its DBTT was still too high, probably because of a few large inclusions of Cr_2O_3.

The following is quoted from a recent review of chromium (ref. 118).

> Improvements in the intrinsic impact ductility of chromium at low temperature will require modifications in alloying approaches for high-temperature strength. The reliance on solid-solution strengthening should be decreased in favor of precipitate or dispersion strengthening . . . Dispersion strengthening with inert particles has not been effective to date but refinement in particle sizes should be beneficial.

COBALT

The cobalt-base superalloy L–605 has good strength and corrosion resistance. If it could be dispersion-strengthened, a superior material might be achieved. An alloy powder of Co–20Cr–10Ni–8Mo, which is similar to L–605 with Mo substituted for W to lower the density, was produced in an experimental program and strengthened by 2- to 6-volume-percent thoria (ref. 7). An aqueous solution of the metal salts was first spray-dried and the powders then were fired in air first at 350° C, then at 700° C, and finally in hydrogen at 1200° C to reduce all the oxides except thoria. The powder was compacted isostatically at 40 000 psi, followed by sintering at 1200° C in hydrogen. The billets were extruded at 980° C. Analysis indicated a small dispersoid size of 0.02 micron, and the IPS was a very low 0.15 to 0.20 micron. The high-temperature strength was still poor; the best samples failed after only 5 hours at 1000° C under a load of 8000 psi. X-ray diffraction indicated that a cause of the instability might be poor compatability of the various metal matrices.

Cobalt alloys have been dispersion strengthened by means of prealloyed powders (ref. 66). Particle sizes of 0.1 micron have been achieved in Co–20Cr–10Ni–15W with thoria or lanthana dispersoids.

TUNGSTEN

Tungsten's very high melting point (3410° C) makes it particularly desirable for high-temperature structural applications. The

principal difficulty is that the commercially pure metal has a high DBTT, which increases after high-temperature use. The mechanism causing this is not clearly understood, but it may be attributed in part to grain growth and matrix composition. Dispersion strengthening is a method to lower DBTT in chromium; for example, the lamp-filament industry has used inert oxide additives for a long time to inhibit grain growth and control the grain size of the final wire. This technique was also reported by Allen et al to be effective with tungsten sheet (ref. 122), although the relatively high temperatures needed to work tungsten makes interaction between the dispersoid and the matrix more likely. A continuation of this work (ref. 123) confirmed the conclusion that ThO_2 and ZrO_2 do inhibit grain growth in tungsten sheet during sintering and rolling, and also increase the recrystallization temperature of the wrought product. Eight percent of either oxide is the maximum that can be used and still retain acceptable ductility in the fabrication of 0.035-in. sheet. The bend transition temperature (a fatigue test to measure the DBTT) is also decreased in sheet that is both stress-relieved and recrystallized with increasing temperature.

Personnel at Lewis Research Center experimented with both tungsten and tungsten alloyed with zirconium and tantalum with various amounts of oxide additions that were made either by reduction and calcination of mixed oxides or by mechanical comminution of arc-melted alloy (ref. 124). The powders were extruded at 4000° F and evaluated with no further hot-working. The resultant properties, as seen in figure 39, were generally much improved over unalloyed tungsten, even though the dispersions were poor. A W–5HfO alloy, for example, had roughly twice the 100-hr stress rupture strength at 3000° F.

King recently reported a dispersion-hardened W–3.8ThO_2 alloy which had greatly improved yield strengths compared with those of pure recrystallized tungsten at a temperature exceeding 2000° C (ref. 125). The alloy was prepared by blending a thorium-nitrate solution with tungsten oxide followed by hydrogen reduction to metal powder. After reduction, the dispersed second phase was present as ThO_2. Pure tungsten was prepared in the same manner, except that no thorium nitrate was added. The powders were consolidated by cold-pressing and self-resistance sintering in hydrogen. The resulting ingots were about 93% dense before being swaged to fully dense rods.

The yield strengths of the thoria-containing alloy were higher by a factor of about five than pure tungsten over the entire test temperature range from 325° to 2400° C. Even after annealing at

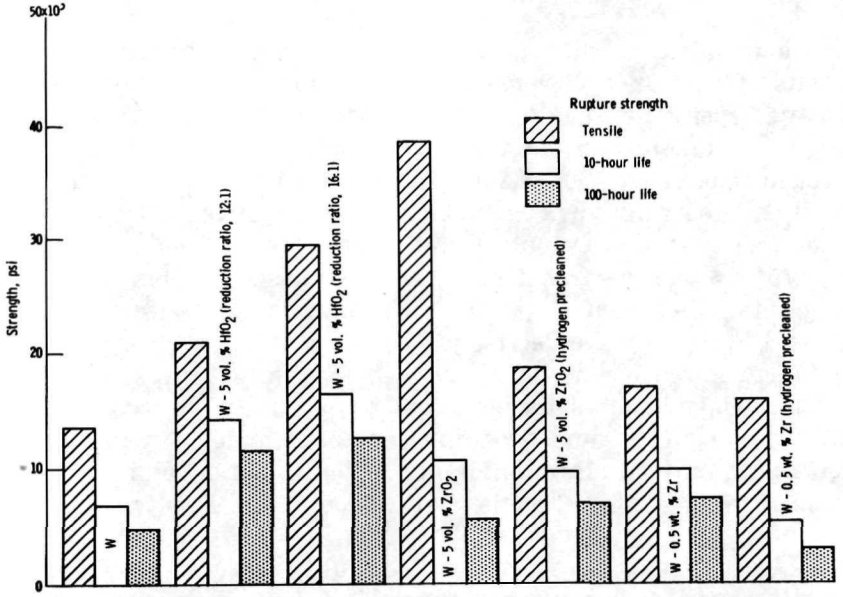

FIGURE 39.—Tensile, 10-, and 100-hr rupture strengths of powder metallurgy tungsten and tungsten-base composites; test temperature, 3000° F (ref. 124).

2850° C, the yield strength of the alloy was still about twice that of annealed pure tungsten. The pure tungsten could be completely recrystallized by annealing at 2400° C for one-half hr. The thoria-containing alloy, however, did not recrystallize at this temperature, and a 6-hr anneal at 2850° C was necessary to cause grain growth. Even at this temperature, an equiaxed grain structure could not be achieved.

IRON AND COPPER

Research studies conducted for NASA at M.I.T. during the period of 1964–1968 on dispersion-strengthened steels has resulted in the development of some promising iron alloys containing from 0.75 to 6.0 volume percent of beryllium oxide (refs. 116, 126, 127, 128, and 129). The alloys were made by atomizing a molten mixture of Fe-Be, screening the powder to 325 mesh, and then internally oxidizing it by exposure to a hydrogen-water vapor (H_2O/H_2) atmosphere in such proportions as to oxidize the beryllium, but not the iron. The particle size of the powder alloy ranged from 44 microns down.

In the oxidation process, the powder was exposed in vertically stacked, spaced layers about 0.25-in. thick and oxidized for 42 hr at 820° C. The H_2O/H_2 ratio was held to below 0.5 to prevent the

formation of FeO. Past experience has shown that even minute amounts of iron oxide adversely affect the high-temperature stability of dispersion-strengthened alloys and, therefore, every precaution was taken to exclude this contaminant. The powder was hydrogen-reduced at 500° C for up to 48 hr and then transferred to a steel tube through a completely closed system and tightly sealed. The tube was evacuated and compacted at 50 000 psi to about 75% of theoretical density and extruded into bar stock. The resultant BeO contents of the three alloy mixtures were 0.75, 3.0, and 6.0 volume %, respectively.

A fourth mixture containing 0.96% beryllium was ground into submicron flakes and surface-oxidized to produce a thin layer of BeO. By using the same procedure as that employed with the other alloys, an iron alloy containing a significant amount of beryllium in solid solution together with about 2.5% BeO was produced.

The four compositions were successfully extruded, yielding 99% dense materials with less than 0.3% FeO. Extrusion was done with a reduction ratio of 17:1 at 1550° to 1570° F. The highest-strength values of these alloys were found to equal those of Al_2O_3 dispersion-strengthened iron alloys derived through mechanical blending of ultrafine powders. In the latter case, the alloy contained 10% aluminum oxide compared to 3.0 to 6.0% beryllium oxide. The lower-oxide content results in a more ductile and workable structure. Tensile tests made at 80° F are shown in table XVI.

Metallographic and chemical analyses indicate that the micro-

TABLE XVI.—*Mechanical Properties of Iron-Beryllium Oxide Alloys (ref. 128)*

Percent BeO in iron matrix alloy	Condition	Upper yield strength X1000 psi	Lower yield strength X1000 psi	Ultimate tensile strength X1000 psi	Elongation, %	Reduction in area
0.75	As extruded	76	62	72	25	75
	1625° F-anneal	57	52	73	27	75
	1725° F-anneal	53	46	61	27	74
3.0	As extruded	82	61	74	19	52
	1725° F-anneal	60	50	68	19	50
6.0	As extruded	84–91	73–80	98–97	9–11	21–32
	1725° F-anneal	71–72	63–67	82–87	9–13	20–33
*2.5	As extruded	130	124	148	10	11

* In Fe–Be matrix.

structures of all the alloy mixtures were similar except for the BeO content. They show an elongated grain structure with some occasional regions of equiaxed grains. A Laué X-ray examination showed a finely recrystallized matrix, and heating to 1725° F did not change the pattern to any substantial degree. Room-temperature hardness measured Rockwell G–60 up to 1625° F for the 0.75% and 3.0% alloys. The 6.0% alloy measured Rockwell G–75 in the extruded condition and maintained that value when annealed at 1625° F. The alloy containing 2.5% BeO in a Fe–Be solid-solution matrix had a Rockwell hardness of G–94 and held that value up to 1725° F.

Cu–7.2Al–0.3Al_2O_3 was produced using the same internal oxidation technique. Cu–7.5Al alloy was atomized to 44 microns, and then ground into flakes 0.1 micron thick (ref. 119). Air oxidation during grinding occurred, but a treatment in hydrogen at 450° C reduced the surface CuO. Extrusion in cans at 740° C produced 99.7% dense billets within ultimate tensile strengths from 50 000 to 90 000 psi. Such strengths are superior to those of any other copper alloys reported, and cold-working increases them by an additional 30%. A cold-swaged sample with a 50% reduction in area showed a jump in the stress-rupture strength at 25 000 psi from 1.35 hr to 103 hr.

In 1966, the NASA Research Advisory Committee on Materials asked why no greater commercial success had been achieved with oxide-dispersion-strengthened alloys. Grant et al, having done considerable research in this field, considered the question, and their findings, together with remarks by other prominent researchers, were published in 1967 (ref. 102). The following quote summarizes their conclusions.

> Oxide dispersed alloys, as serious contenders for use as high temperature materials, were looked at almost casually until about 3 or 4 years ago. They are, therefore, at an early point in their development and considerable additional work must be undertaken to test their potential.
>
> Until recently effort has been concentrated on systems with unalloyed matrices. Work with alloyed matrices is only just beginning. In particular, matrices utilizing oxidation resistant systems will require considerable additional effort. The stability of the refractory oxide in such alloys is largely unknown and must be determined.
>
> The mechanism of strengthening must be clearly established. Deformation and fracture studies must be pursued simultaneously.

Since then, progress has been made in achieving a better understanding of the complex mechanisms which cause strengthening of metals. In addition, the process of internal oxidation has been further developed, and substantial improvements have been

made in the milling and mixing of powders, resulting in the production of more uniform powders with well defined characteristics. This better control of the raw material represents an important step forward in the development and fabrication of dispersion-strengthened materials. The following quote (ref. 102) still holds, however.

> It is not justifiable to compare alloys such as Udimet 700, Inco 713C, or SM–200 with these early oxide dispersion alloys. In the former case, there is a background of 25 years of research and technology, coupled with millions of dollars of research and development; in the latter case we are dealing with a foundling.

The experimental results summarized here indicate considerable potential for these materials. Although they currently may not justify large-scale production, further developmental work is well advised in areas such as the ball-milling of fine powders and internal oxidation where production-line economies are applicable. Problem areas, such as dispersoid agglomeration during cleaning, are avoidable by several means including the use of precompacts. The latter approach should be of considerable interest to those experimenting with preforms for forging. A dispersion-strengthened forging could readily be made if two criteria can be met: (1) it must be possible to make the preform from either internally oxidized prealloyed powder or a metal-metal oxide-powder mixture that is porous enough to be cleaned with hydrogen while sintering and (2) the forging process must impart enough deformation to the compact to give the energy of cold work necessary to develop the strength.

There is good reason to believe that an approach from both sides, the development of compositions as well as the development of forging, will speed up the commercial production of dispersion-strengthened materials for a variety of new applications.

Fiber Reinforced Compacts

One of the oldest structural materials made by man is the strawfilled clay brick. This composite material contains fibers with reasonable tensile strengths that reinforce a matrix having practically no tensile strength but good compressive strength. When stressed, the clay matrix can transfer the load to the stronger straw fibers. The adhesion of the matrix to the fibers, the orientation of the fibers, and the relative percentages of both materials contribute to the performance of the final brick. These same factors also apply in determining the performance of the boron-aluminum composites being used in the latest supersonic aircraft.

Fibers have a special property which makes them highly desirable for use in structural materials. Their tensile strengths go up dramatically as their diameters go down. The reason lies in the higher surface-to-volume ratio of a fine wire compared to that of the same metal in a casting. Molecular ordering occurs at the surface of any material, so fine wires have greater percentages of ordered molecules. Whiskers are actually single crystals of elements and compounds; consequently, all of their molecules are ordered. The relationship between tungsten-fiber diameter and strength is illustrated in figure 40 (ref. 54). Analogous values for other materials are given in table XVII. Even a relatively coarse wire has

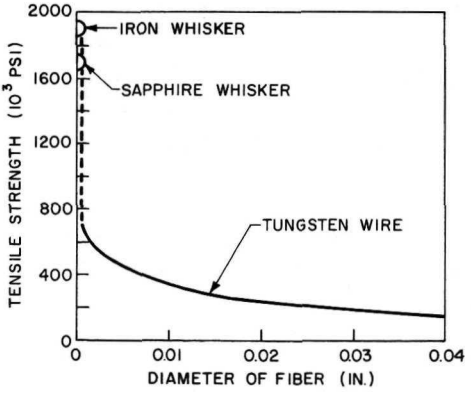

FIGURE 40.—Strength of whiskers and fibers at room temperature (ref. 54).

TABLE XVII.—*Tensile Strength of Various Materials in Fiber Form (ref. 130)*

Material	Fiber form, psi	Bulk form (avg.), psi
Graphite whiskers	3 500 000	2 000
Alumina whiskers	2 200 000	30 000
Iron whiskers	1 900 000	25 000
Ausformed steel	450 000	65 000
Piano wire	350 000	42 000
Fiber glass	200 000	6 000
Nylon	80 000	12 000
Aluminum	60 000	40 000
Wood	15 000	5 000

considerably greater tensile strength than bulk metal, and whiskers can have tremendous strengths. These materials, grown from the vapor phase under closely controlled conditions, have strengths in the millions of psi, although only a small percentage of whiskers in a given sample reaches these values. The values indicate the great potential of fiber reinforced composites for lightweight structural materials (ref. 130).

COPPER-INFILTRATED TUNGSTEN WIRES

The basic parameters for the utilization of fibers were developed at Lewis Research Center by experimentation with tungsten wires infiltrated with copper (refs. 131 to 139). While it would have been desirable to use tungsten whiskers, their excessive strength variation, high cost, and the impossibility of orienting them led to work with fine wires. Cold-drawn 0.001-in. wires have strengths as high as 600 000 psi (almost ten times that of the wrought metal), so the problem was more to maintain this strength in the final composite than to find stronger wires. The initial efforts centered about the copper infiltration of tight bundles of 0.003- to 0.007-in. tungsten filaments (ref. 131). Copper is an excellent infiltrant for this purpose, since it adheres well and does not react or alloy with the tungsten. The strength of these bundles has a linear relationship to the percentage of each component (fig. 41) according to the law of mixtures; that is, the strength of the composite is equal to the sum of the strengths of each component multiplied by its percentage of the total cross sectional area:

$$\sigma_{composite} = \sigma_{fiber} A_{fiber} + \sigma_{matrix} A_{matrix}$$

(where σ = tensile strength and A = cross sectional area)

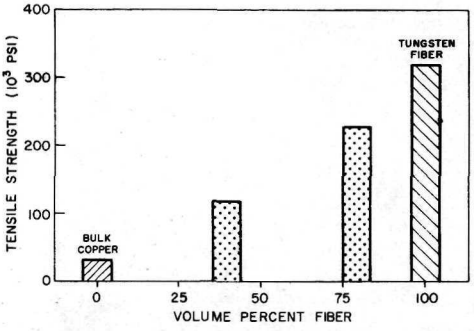

FIGURE 41.—Tensile strength of composites, continuous W fibers in Cu (ref. 54).

The method used to prepare these composites started with tungsten fibers of uniform diameter in the order of 5 mils, which were cleaned with sodium peroxide and ammonium hydroxide and loaded into an Alundum tube, and placed on a piece of copper inside a quartz tube. The system was evacuated and heated to 2200° F for 1 hr during which the copper melted and passed between the fibers by capillary action (fig. 42). A transverse section of the final composite is shown in figure 43 (ref. 132).

The fibers in these composites do not need to be continuous. The effect of short 3/8-in. fibers oriented parallel to the longitudinal axis of the sample is shown in figure 44. The strength is approximately equal to the sample with continuous fibers, so the shorter fibers are apparently able to transmit the load from fiber to fiber. This transmission of stress occurs through the matrix material so that the strength of the matrix enters into the final strength of the composite more than in the case of the continuous filament composite. For this reason, a factor called the critical aspect ratio can be determined for each fiber material. This factor constitutes the limiting ratio between the length and the diameter of the fiber. For example, composites containing tungsten fibers that are at least as long as the length dictated by tungsten's critical aspect ratio (40) will be more than 95% as strong as those made from continuous filaments of the same diameter.

The effects of increasing strain on a composite and on the fibers and matrix separately are shown in figure 45 (ref. 136). Four stages are evident. In the first, all materials exhibit elastic deformation. This condition is maintained through the second stage for the fiber; the composite, however, just starts to exhibit elastic deformation. In stage two, the matrix becomes very plastic. In stage three, the fiber also becomes plastic, and at stage four, it breaks. The composite curve does not fall off rapidly in stage four because the breaking fibers adhere to the matrix which continues to reinforce them as they decrease in length.

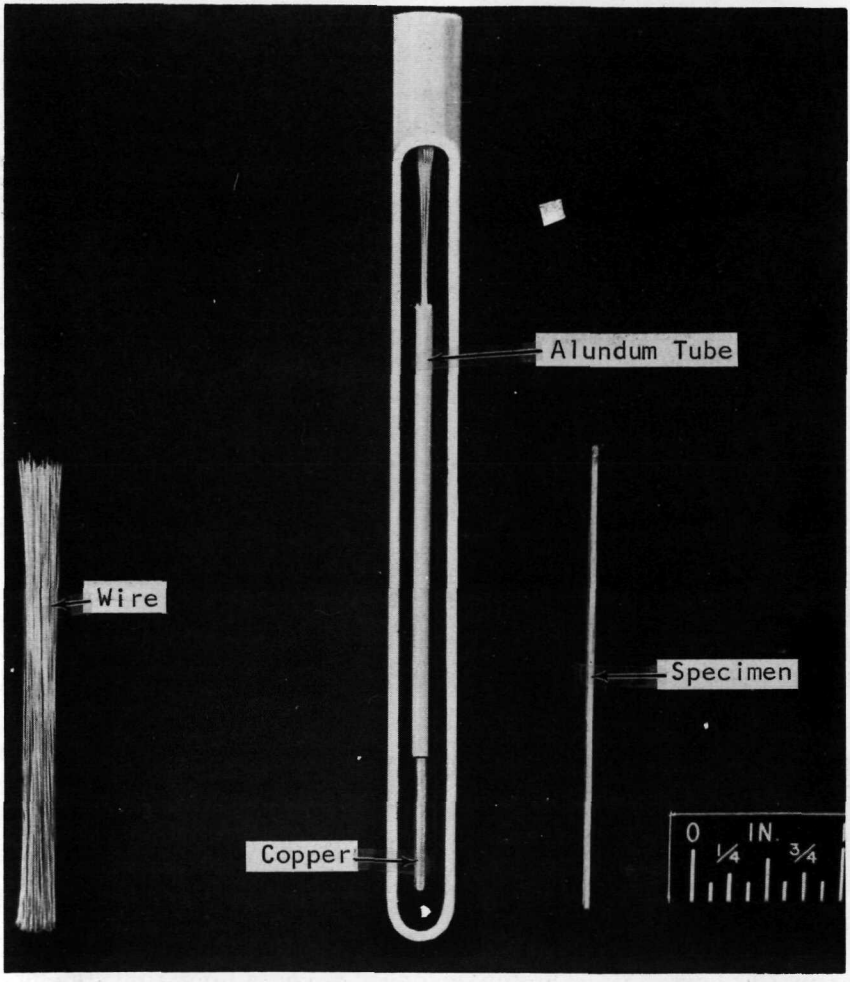

FIGURE 42.—*How tungsten-copper composites are produced (ref. 132).*

As a result of work at Lewis Research Center, it was concluded that:

1. The fibers should be oriented in the direction of the load
2. The fibers should be surrounded and wetted by the matrix material
3. The fibers should not touch each other
4. The fibers should be uniform in size, shape, orientation, and strength.

The critical aspect ratio of discontinuous fibers in a fiber-reinforced composite normally increases as the temperature increases,

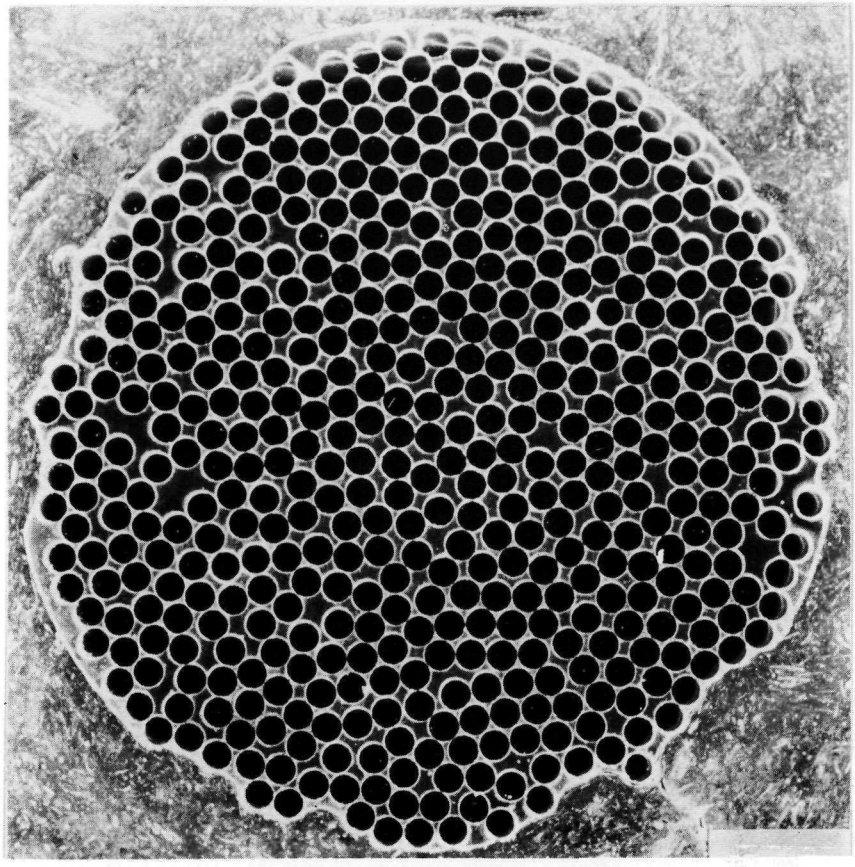

FIGURE 43.—Transverse section of composite containing 483 tungsten wires in a copper matrix (40X) (ref. 132).

since the strength of the matrix material may decrease rapidly. This is particularly true for copper, which has a relatively low melting point. It is obvious that, at some point near the melting point of copper, the fibers will be supporting all the load. Therefore, the critical aspect ratio for tungsten can be expected to increase from 40 at room temperature to infinity as the temperature increases to the melting point of copper. Just how this happens was investigated by Jech and Signorelli at Lewis (ref. 139). A test was designed to simulate and measure the tension placed on a short fiber in a matrix (figs. 46 and 47). The length of the test fiber is calculated to be equivalent to twice the length of a fiber in a composite because the test apparatus exerts all the

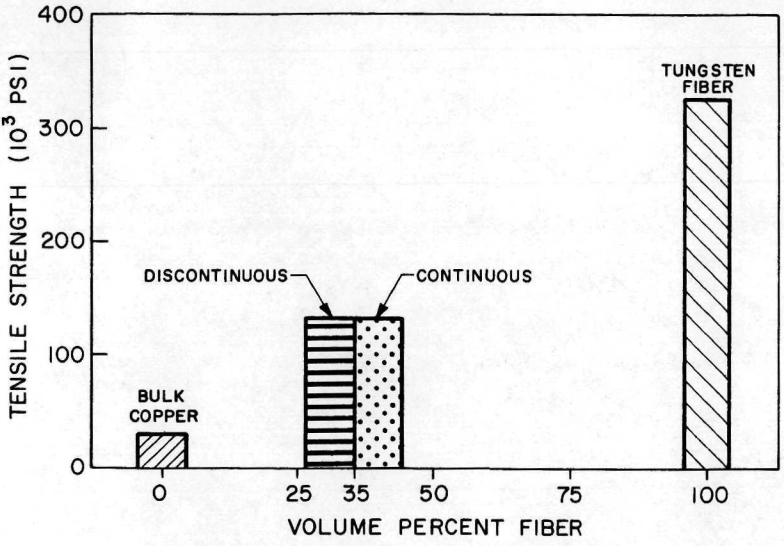

FIGURE 44.—Tensile strength of composites, continuous and discontinuous W fibers in Cu (ref. 54).

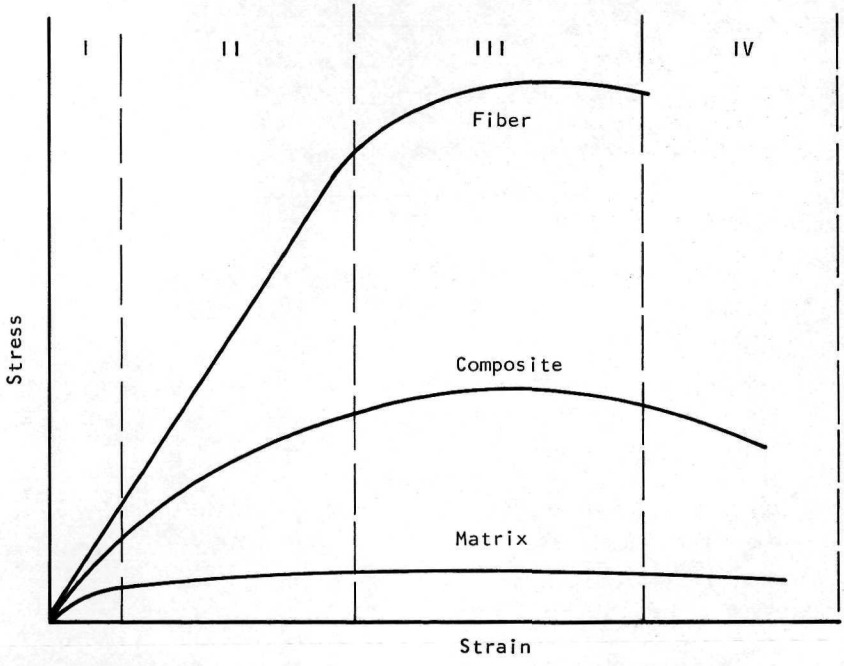

FIGURE 45.—Schematic illustration of four stages of deformation of fiber, matrix, and composite (ref. 136).

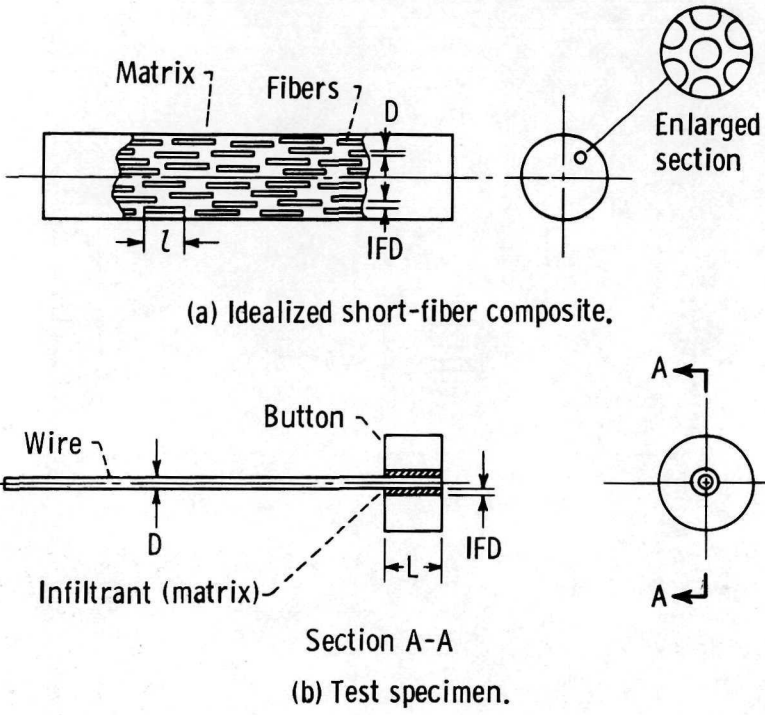

FIGURE 46.—Comparison of test specimen and short-fiber composite (ref. 139).

load on the end of the fiber whereas the actual composite loads the fiber all along its length. Even though the test apparatus does not represent the surrounding fibers accurately, the results obtained with it are indicative of the properties of a composite. Failure occurs in two ways: pullout, where the interface between the infiltrant and the fiber fails, and wire failure. Samples measuring less than the fibers' critical aspect ratio fail by pullout while those with greater values exhibit wire failure. The results can be plotted on a curve which is almost exponential with respect to the critical aspect ratio (fig. 48). This indicates that relatively short fibers can be used up to as high as 0.8 of the melting point of the matrix.

Other work on the copper-tungsten fiber system at Lewis showed the effect of fiber orientation on the strength of the composite (ref. 137). Calculations of Stowell and Liu (ref. 140) were used to calculate the relationship shown in figure 49. From this, it can be seen that the tensile strength of a composite is severely decreased when the fibers deviate as little as three degrees from

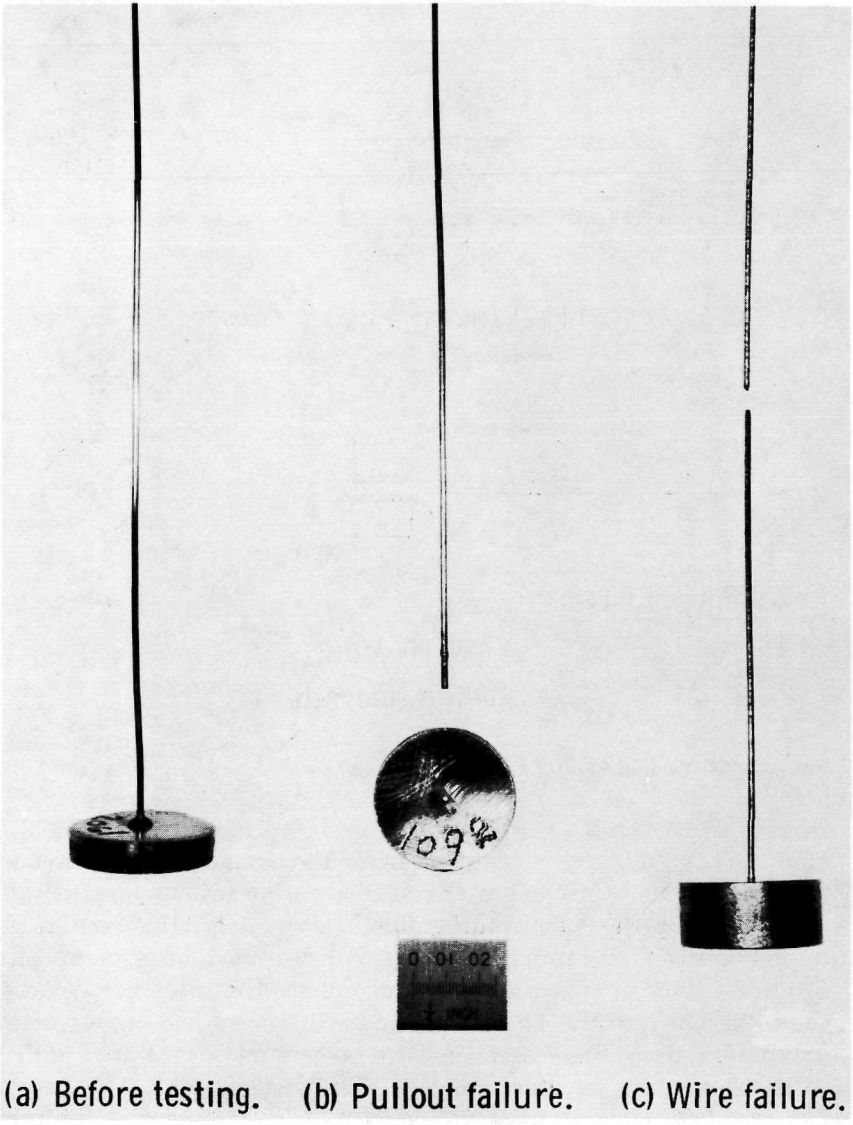

FIGURE 47.—Aspect-ratio test specimens (ref. 139).

parallel orientation at elevated temperatures. Actual tests confirmed these calculations. It was also found that alloying the copper with chromium increased the shear strength of the matrix despite its reaction with tungsten. The ability of the matrix to transfer the load was greater; and also, the tolerance for misalignment of the fibers was greater.

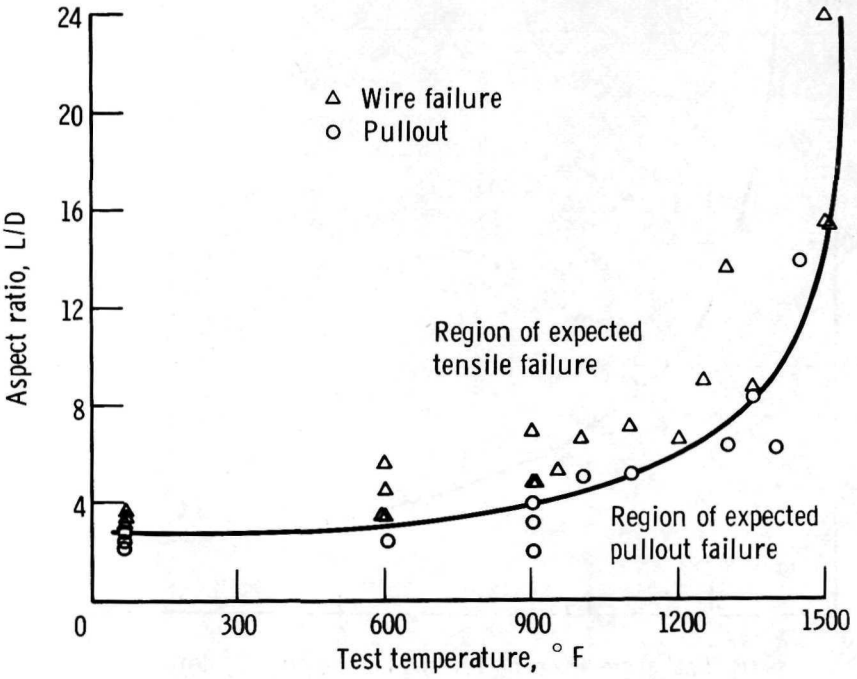

FIGURE 48.—Critical aspect ratio as function of temperature (tungsten-copper system) (ref. 139).

TUNGSTEN WIRE PROPERTIES

Part of the high strength of the tungsten wires is derived from the mechanical working process as the wire is drawn down to its final diameter. This cold-worked strength is lost if the metal is heated to the recrystallization temperature, so in subsequent steps, such as infiltration, the temperature must be carefully controlled. The ductility of the wires can be improved by the removal of surface imperfections, by electropolishing for example. A 30% improvement in room-temperature tensile strength was noted by one author (ref. 141). Another investigator raised the tensile strength 42% (from 153 000 to 219 000 psi) by electropolishing a 0.1-in. rod down to 0.01 in. (ref. 142). Heating tungsten to 1500° F in oxygen also increases the ductility (ref. 143), and the surface lattice defects are removed by the action of oxidation.

Contamination by alloying elements such as nickel, cobalt, or iron will lower the recrystallization temperature of tungsten wires (ref. 144), so the inclusion of these elements might be expected to lower the strength of a copper-tungsten composite dur-

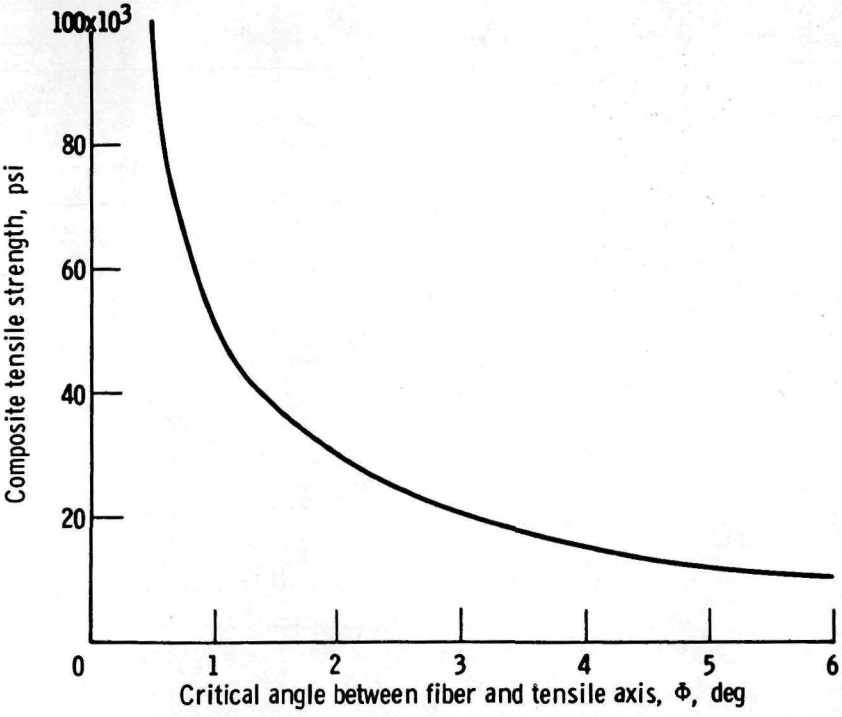

FIGURE 49.—Composite tensile strength as a function of critical angle for tungsten-fiber-copper-matrix composites at 1500° F (ref. 140).

ing and after use at high temperatures. Nickel, in particular, is a very strong contaminant for tungsten. A trace of this element such as might be rubbed off a nickel spool during a winding operation, can result in a recrystallized, brittle tungsten wire following heat-treatment. The lower limit for this embrittlement is 1200° C, however, so a medium-range composite containing nickel might be envisaged. Iron and cobalt also cause similar effects down to a 1% level, with cobalt the most damaging element (ref. 145).

It is possible that the admixture of some alloying elements could cause a synergistic effect on the properties of the final composite. This would mean that the properties would be greater than those predictable from the law of mixtures based on the strengths and volume percents of the components. Alloying at the fiber-matrix interface might improve adhesion or heal surface defects in the fibers, for example. Also, the surface-grain structure might be improved. Thus, the program at Lewis of alloying small amounts of mutually soluble metals with copper before infiltra-

tion into the tungsten fibers could have brought about greater or lesser strengths in the resulting composites.

In the investigation, a 5-mil pure-tungsten wire was used, which had a room-temperature strength of 330 000 psi after annealing at 2200° F in vacuum (ref. 134). Alloys of pure copper with nickel cobalt, aluminum, titanium, zirconium, chromium, or niobium in percentages from 1% to 33% by weight were prepared as infiltrants. The infiltration technique described previously was used to prepare the composites, and photomicrographs were made and tensile tests were run. Samples containing cobalt, aluminum, and nickel showed areas where diffusion had penetrated into the fibers. Recrystallization was evident in these areas, and the tensile strengths of the samples were reduced considerably from those of the unalloyed samples. It was found that the recrystallization of these samples acted like a brittle skin that cracked early in the tensile test, forming circumferential notches. Since tungsten is notch sensitive, premature failure was the result. Niobium and chromium seemed to form a solid-solution phase at the surface of the tungsten without any recrystallization. Only a slight reduction in strength occurred with these samples. Zirconium formed a second phase inside the tungsten fibers and considerably weakened the composite. The range and results of this program are summarized in table XVIII. The great disparity between the effect of 5% nickel and 10% nickel should be noted. This is a typical effect encountered in this program. Sectional views of single fibers from these samples can be seen in figure 50. The recrystallized areas of the 5% cobalt and the 10% nickel samples are plainly visible. No synergistic effect was noted throughout the program, and none has been reported in the literature to date (ref. 136).

Up to this point in the program, the interest had been primarily in understanding the strengthening mechanisms at work in the fiber reinforced composites. Testing consisted of short-duration, room-temperature tensile tests. But the properties at elevated temperatures are also very important since the end use of some of the materials developed would be in such applications as turbine buckets and high-temperature structural components. Petrasek investigated this question by testing the elevated-temperature tensile strengths of several samples from the previous work (ref. 146). These samples included the copper-matrix continuous tungsten-fiber composite, one containing 2% chromium, and one containing 10% nickel. The previous study had shown that chromium formed a solid solution with the tungsten which did not affect the room-temperature properties, but that nickel caused re-

TABLE XVIII.—*Room-Temperature Tensile Properties of Copper-Alloy-Tungsten-Fiber Composites (ref. 134)*

Binder material	Maximum solubility of alloying element in tungsten	Weight % of alloying element	Atomic % of alloying element	Volume % fiber	Tensile strength, psi	Reduction in area, %	Type of fracture
Pure copper	Insoluble in tungsten	0	0	65.0	225 700	----	Ductile
				70.2	238 000	----	Ductile
				75.4	249 800	----	Ductile
Copper-nickel	0.3	5	5.4	79.0	246 600	34	Ductile
				78.4	250 000	37	Ductile
				76.0	218 900	32	Ductile
		10	10.9	74.1	131 700	Nil	Brittle
				75.5	108 800	Nil	Brittle
				79.5	51 300	Nil	Brittle
Copper-cobalt	0.3	1	1.1	77.3	219 400	----	Semiductile
		5	5.4	76.0	213 200	1.5	Semiductile
				74.8	229 300	2.3	Ductile
				74.7	147 200	----	Brittle
				74.9	172 100	----	Brittle

Copper-aluminum	2.6	5	11.3	63.4	98 900	Nil	Brittle
				72.4	153 800	Nil	Semiductile
				76.1	154 500	Nil	Semiductile
		10	20.8	76.7	138 500	----	Brittle
Copper-titanium	8	10	12.8	78.2	223 700	----	Semiductile
				71.7	220 100	10	Semiductile
		25	30.7	76.3	186 700	----	Brittle
Copper-zirconium	3	10	7.2	72.8	216 000	Nil	Brittle
				78.5	255 300	Nil	Ductile
				75.6	226 900	Nil	Semiductile
				64.7	172 600	Nil	Brittle
				64.3	195 700	Nil	Semiductile
		33	25.5	75.9	106 700	Nil	Brittle
Copper-chromium	Complete solid solubility (Miscibility gap)	1	1.2	78.7	223 500	7.4	Semiductile
				77.5	228 600	25.8	Ductile
				77.2	225 900	7.5	Semiductile
		2	2.4	76.4	241 700	16.4	Ductile
Copper-niobium	Complete solid solubility	1	0.6	75.4	237 100	20.6	Ductile
				75.1	223 100	24.7	Ductile

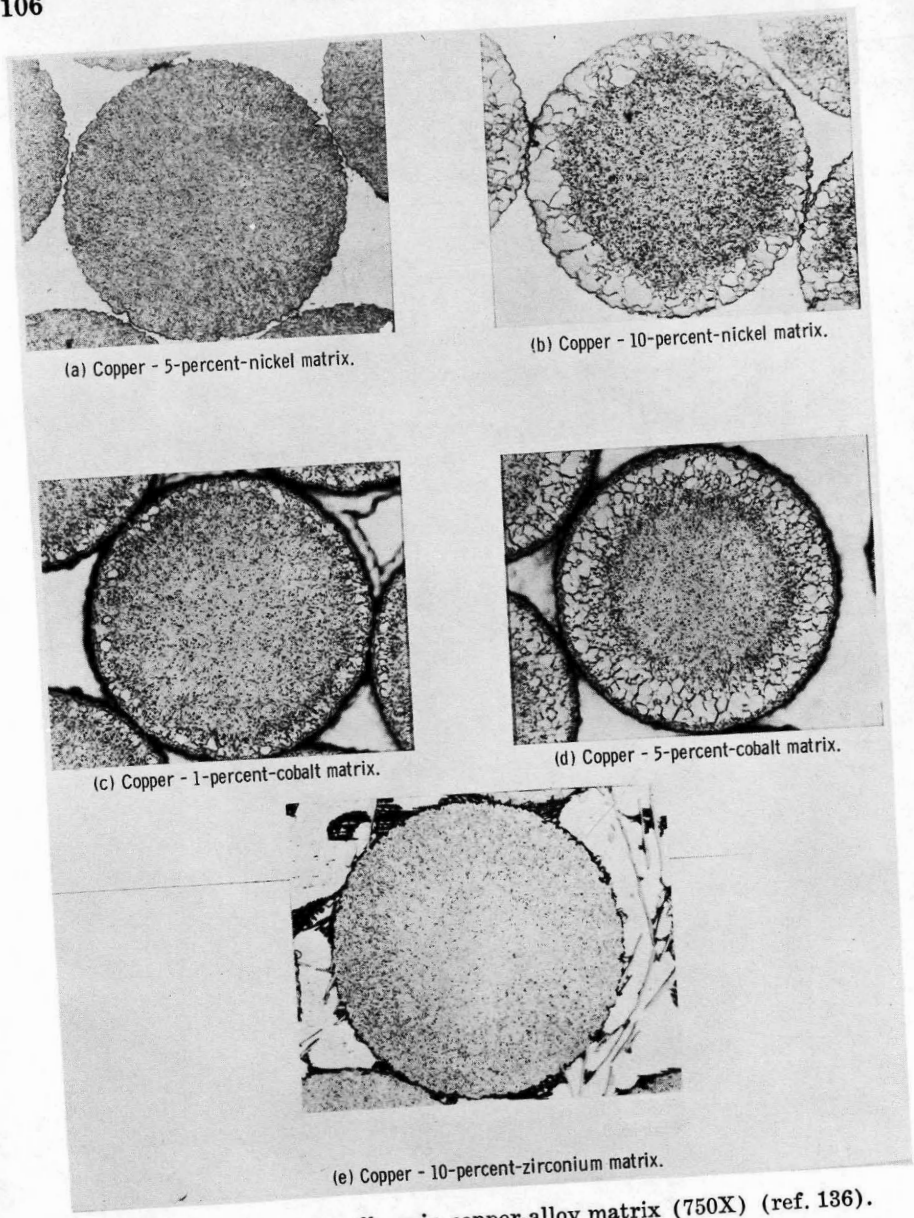

FIGURE 50.—Tungsten fibers in copper-alloy matrix (750X) (ref. 136).

crystallization which did lower the strength markedly (ref. 134). Tensile tests were run at room temperature and at 300° intervals up to 1800° F. Some of the results of these tests are illustrated in figure 51. The composites that contained only copper as an infiltrant maintained their adherence to the law of mixtures at the el-

evated temperatures, as did the specimen containing 2% chromium. The latter was also only slightly weaker than the former in all tests. In the sample containing nickel, however, a different situation was found. As in the previous program, the room-temperature strength was low; but at 300° F, a considerable improvement was noted. A probable explanation is that the ductile-brittle temperature of tungsten had been exceeded by this temperature. The strengths were still much lower than in either of the other materials.

TUNGSTEN WIRES IN NONCOPPER MATRICES

The advantages of the copper-tungsten system are principally the mutual insolubility of the constituents and the wide difference in melting points. Silver, gold, and zinc also share these properties with copper as infiltrants for tungsten, but are not adequate for future high-temperature applications. They either have too low a melting point, too high a vapor pressure, or poor oxidation resistance. Composites composed of copper-base alloys as the infiltrant cannot be considered for high-temperature applications

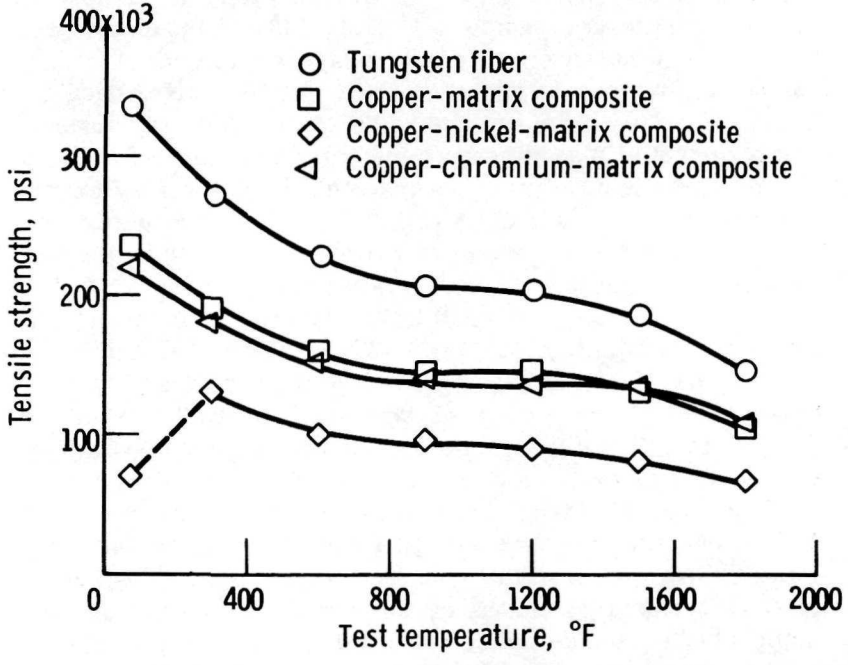

FIGURE 51.—Tensile strength as a function of test temperature for composites containing 70 volume percent fibers and for individual constituents (ref. 146).

because of the relatively low melting point of copper (1981° F). For this reason, at the same time as the copper-tungsten system was being used to characterize the parameters of fiber reinforcement, other systems were being developed for eventual use. Petrasek and Weeton experimented with tungsten fibers embedded in a niobium-nickel matrix and a nickel-iron matrix (ref. 134). Also, cobalt-base superalloys S–816 and L–605 were tried. The experimental technique was the same as described for the copper matrices except that a higher infiltration temperature (2800° F) was used. The problems encountered in this exploratory program were caused primarily by the high temperature and the reactions that occurred between the fibers and the matrix. In some cases, complete recrystallization of the fibers occurred and in others dissolution and stress cracking was evident. One possible solution to this problem is to lower the formation temperature through a powder metallurgy approach. Cratchley, for example, had coated fibers with aluminum and hot-pressed them to achieve high-strength composites (refs. 147 and 148). By making a stainless steel fiber-aluminum matrix composite in this way, strengths of 40 000 psi with 16% fiber by volume were achieved. This procedure also seemed to follow the law of mixtures.

Baskey et al applied a powder metallurgy approach to preparing fiber-reinforced composites (ref. 149). Tungsten wires of from 2- to 10-mils were oriented in layers interspaced with powdered high-temperature metals such as Nichrome, cobalt, and L–605. Hot-pressing was done at 2000° to 2300° F, considerably below the 2800° F infiltration temperature required for the same systems. The resulting composites could be worked by extrusion, swaging, forging, or rolling. Both extrusion and rolling aligned short fibers to produce superior properties in the direction of alignment. These phenomena were reported earlier by Jech et al (ref. 150), working with 0.1- to 0.25-in. molybdenum fibers embedded in titanium or Ti–6Al–4V powders. The investigators cold-pressed the randomly oriented mixture first and then vacuum-sintered it. Extrusion of the billet partially oriented the fibers, and rolling, even more so. During rolling, the fibers were elongated to as much as 6 in. in length. This process is illustrated in figure 52. The tensile properties of a composite containing 40% fiber were increased 70% at room temperature and 400% at 1400° F over the unreinforced Ti–6Al–4V. At all test temperatures, the tensile strengths of the composites were considerably higher then the unreinforced-matrix alloy.

The composites of Baskey et al (ref. 149) contained either continuous or short fibers and were tested at both room temperature

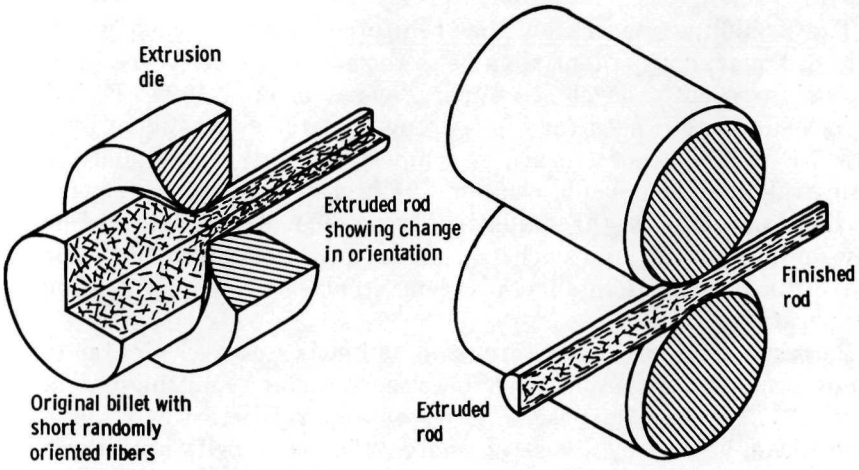

FIGURE 52.—Fabrication of fiber-reinforced metal-matrix composites by extrusion and rolling (discontinuous fibers) (ref. 150).

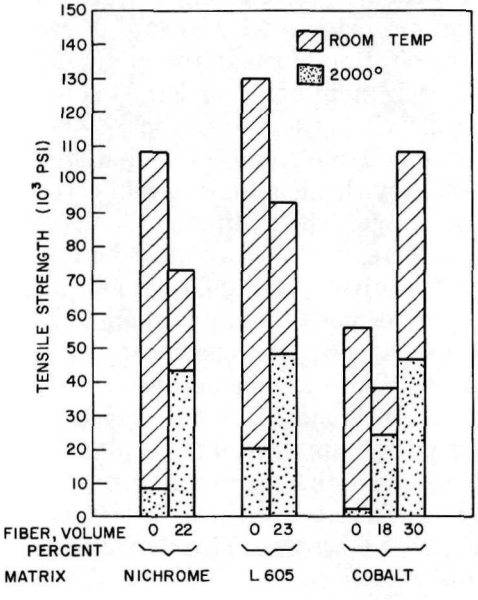

FIGURE 53.—Tensile strengths of tungsten-fiber-reinforced cobalt or nickel-base-matrix composites (ref. 149).

and at 2000° F (figure 53). In the cases of Nichrome and L–605, the addition of fibers lowered the strength of the material at room temperature. Even the much weaker cobalt matrix was further weakened (up to 18%) by the addition of fibers. At 2000° F, on the other hand, all samples containing fibers showed considerable improvement over the matrix alloys.

The preliminary work on fiber-reinforced alloys opened up an area of tremendous potential value to the aerospace field. The limit for using recently developed superalloys is around 1900° F, but there is an urgent need for high-strength materials usable at over 2000° F in advanced aircraft. A composite of refractory fibers in a superalloy matrix would combine the high-temperature strength of the former with the oxidation resistance of the latter. The powder metallurgy approach to this is important since it avoids the diffusion and solubility problems that occur at infiltration temperatures.

Petrasek et al initiated a program at Lewis Research Center to achieve maximum compatibility between the fibers and the matrix (ref. 28). For this purpose, a series of four refractory wires and four nickel-base alloys were evaluated. The composition of these materials and the relative depths of reaction into the fiber that occur are listed in table XIX. The samples were sintered and pressed and then sectioned and examined microscopically. The alloys which contained aluminum and titanium were more compatible with the fibers than the ones without these elements, probably because of the formation of a gamma prime (Ni_3Al) and an eta (Ni_3Ti) phase. Each of these precipitation-hardens the alloy and ties up three atoms of nickel for each atom of Al or Ti. This action lowers the reactivity of the matrix by lowering nickel's potential for diffusion. It is also evident from table XIX, that molybdenum-base TZM reacts severely with all matrices while the commercial tungsten is the most stable. The optimum diameter for the wires was also considered. Here, two factors must be balanced off against each other. First, a given depth of reaction has less effect as the diameter of the wire increases, and second, the strength of the wire increases as the diameter decreases. The length of time at high temperature is also a consideration, since the depth of reaction is increasing continuously. For this reason, thicker wires are required for longtime applications, despite the fact that thinner wires have more strength. A graphic comparison of these factors led the Lewis workers to conclude that 11-mil wires were the most suitable for 100-hr stress-rupture results at 2000° F, and experimental results confirmed that the best size is between 8 and 15 mils.

A slip-casting technique, which is described in chapter 2, was used to fabricate samples for this program. The samples were canned in nickel under vacuum after sintering, and isostatically hot-pressed at 2000° F for 2 hr under 20 000-psi helium. They were evaluated with the proposed aerospace applications in mind. If, for example, turbine blades were fabricated from them, the

TABLE XIX.—*Alloy Tensile Data (ref. 28)*

Types of Wires

218CS	Commercial tungsten (General Electric Co.)
NF	$W-1ThO_2$
3D	W–3Rh
TZM	Mo–0.5Ti–0.08Zr–0.015C

Matrix Materials

Alloy	Nominal composition of alloy, wt %							
	Al	Cb	Cr	Mo	Ni	Ti	W	Ta
1	----	----	20	--	55	----	25	----
2	2	----	15	--	56	2	25	----
3	----	1.25	19	4	70.5	----	4	1.25
4	4.2	1.25	15	4	66.8	3.5	4	1.25

Compatibility Studies of As-Pressed Specimens
[Fabricated by high-temperature-densification technique]

Alloy	Wire material	Depth of penetration, in.
1	218CS	0.00200
	NF	.00250
	3D	.00150
	TZM	Complete
2	218CS	0.00100
	NF	.00180
	3D	.00100
	TZM	Complete
3	218CS	0.00300
	NF	.00325
	3D	.00320
	TZM	Complete
4	218CS	0.00075
	NF	.00150
	3D	.00100
	TZM	Complete

tensile strength would need to be higher for a more dense material because of the centrifugal loading that occurs during operation. The higher density of tungsten causes a nickel composite reinforced with 70% tungsten fibers to be almost twice as heavy as unreinforced nickel, so the high-temperature advantage of this

composite would be considerably reduced. For this reason, the stress-rupture strengths of these materials were divided by a density factor in comparison with the matrix materials. Even with this correction, however, superior results were achieved especially at 2000° and 2200° F compared with the best available nickel-base superalloys such as M22 or NASA–TRW VI A (fig. 54). The useful temperatures of the composite are 140° or 170° F higher

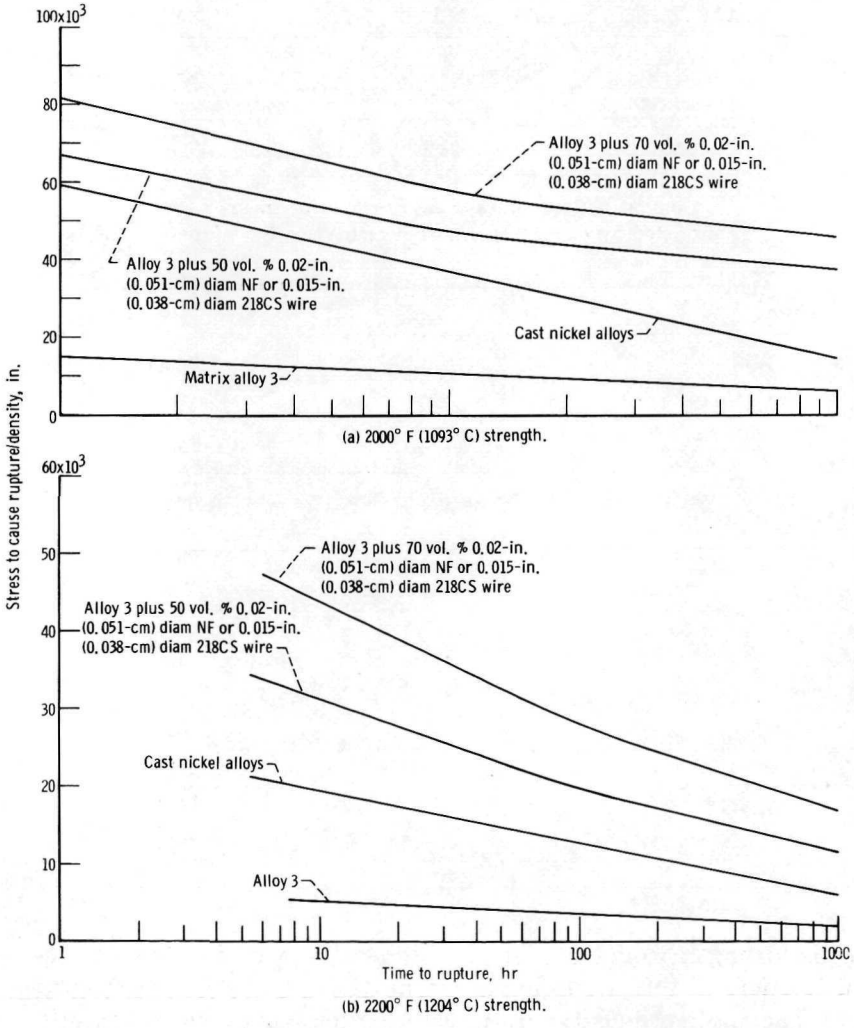

FIGURE 54.—Comparison of specific rupture strength of 50 and 70 volume percent composites (cast nickel alloys and matrix Alloy 3) (ref. 28).

than the superalloy for specific strength-to-cause-rupture in 100 hr and 1000 hr, respectively.

The results of this effort to produce a fiber-reinforced superalloy were so successful that they were awarded one of the Industrial Research Magazine IR–100 awards for 1968 (ref. 151). The NASA Tech Brief (ref. 152) gives a good summary of the award winning composite.

The only case in which it appears that the law of mixtures relationship for fiber reinforcement might have been exceeded is the explosive-bonding work of Reece (ref. 15). A typical composite of this program contains 12.2 volume % stainless-steel wires interspaced by sheets of aluminum. Compaction is achieved by first covering the lay-up with a 1.5-in. buffer plate, above which a nitroguanidine explosive charge is placed. The explosion produces a finished compact, and so is equivalent to compaction, sintering, and working. In this example, the material had yield strength of 66 500 psi, ultimate tensile strength of 67 000 psi, zero elongation, and density of 0.123 lb/in^3. The strength predicted by the law of mixtures based on 13 000-psi aluminum and 400 000- to 500 000-psi stainless steel would be roughly 50 000 psi.

WHISKER-REINFORCED COMPOSITES

The success of the fiber reinforcement program has not carried over into the efforts to incorporate whiskers into metallic composites. The ability to grow very long stable ceramic whiskers with unusually high-strength characteristics that are not destroyed by high temperatures has been known for a long time. A typical technique is that used by Gatti et al in a program of developing boron carbide whiskers for NASA (ref. 153). They evaporated B_4C powder at 1900° C and then cooled it in a graphite chimney-shaped chamber at 1700° C. Some alternate configurations of this apparatus are shown in figure 55. The tensile tests of individual whiskers yielded a wide range of values from about 200 000 to 2 000 000 psi. Size did not seem to be the determining strength factor, and microscopic examination showed growth steps on the surfaces of the weaker fibers while the strongest ones were smooth. Heat-treatments at 1500° C did not strengthen the whiskers. A value of 500 to 1 has been proposed as the desirable aspect ratio for whiskers because of the difficulty in obtaining a good bond to the matrix (ref. 154). Also, because of the extreme fineness of whiskers, this length would enable easier orientation.

Silicon carbide and alumina whiskers have been researched as reinforcements for cast cobalt alloys (ref. 155). This exploratory

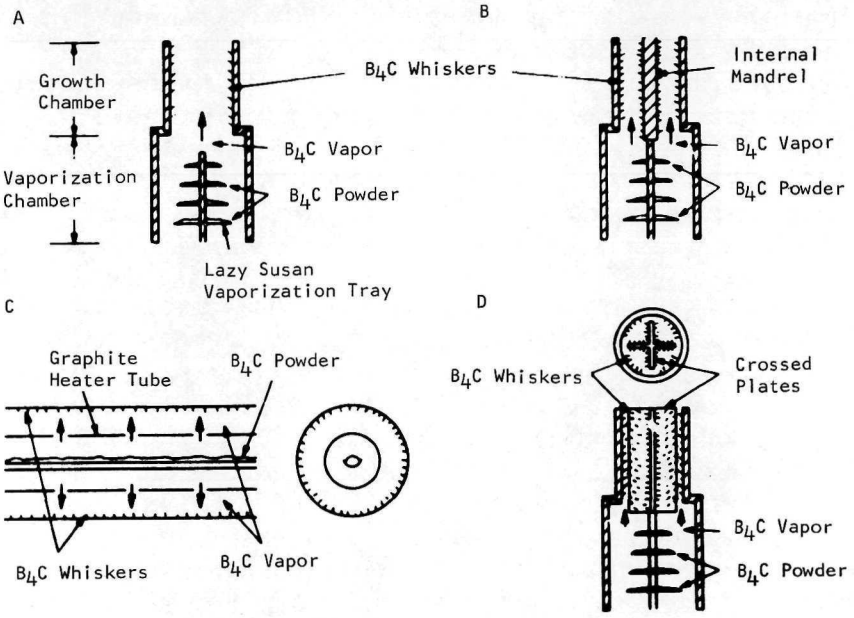

FIGURE 55.—Schematic diagrams showing the evolution of the direct-vapor process for growing B_4C whiskers (ref. 153).

effort pointed up the potential usefulness of these composites, together with their attendant problems. SiC whiskers had roughly the same strengthening effect as Al_2O_3 at about 3% of the cost. They must be protected from molten metals, however, to prevent diffusion and degradation of the fibers. This was accomplished by a carbon coating applied with an acetylene torch. Alumina whiskers were also coated because of the low contact angle of the surface and hence the difficulty in wetting. Composites containing 10% whiskers maintained the tensile strength of the matrix through the 1500° to 1800° F range where cobalt alloys usually drop sharply in strength. The addition of 25% whiskers did not produce proportionate strength increases, indicating that efficient use was not being made of the whisker strength according to the law of mixtures.

OXIDE FIBER REINFORCEMENT

The use of metal oxides as reinforcement fibers for high-temperature composites has excited interest in the past. These materials are usually chemically stable, highly refractory, and of low density. They are generally quite brittle, however, unless in a very thin or whisker form. A composite of alumina whiskers in a

silver matrix, for example, has shown a higher strength-to-weight ratio than René 41 at both room temperature and at 1600° F (ref. 156). Cratchley and Baker used silica fibers to reinforce aluminum (ref. 148). In these and other similar investigations, the oxide fibers were incorporated into the matrix alloys through various handling procedures. However, some types of handling degrade the mechanical properties of the oxides. Protective coatings have been used to avoid this problem (for example, see ref. 157), but these must be removed before incorporation into the composite unless they are to be used as alloying or bonding agents. The extrusion work of Baskey et al (ref. 149) showed that fibers could be oriented along the axis of extrusion, and exploratory work at Lewis Research Center indicated that some refractory oxide powder particles could be elongated into fibers by extrusion. Such a technique could effectively eliminate the problems of producing fine fibers and of handling them. Superior bonding would be achieved between the fiber and the matrix because of the fresh surface created during the elongation cycle. Considerable progress has been made in achieving these goals at the Lewis Research Center to date (refs. 158, 159, and 160).

Tungsten was used initially as a matrix metal (ref. 158) because of its high melting point, which permits a wide range of temperatures for processing, and its relative stiffness, which transmits the high stresses necessary to deform the oxides. The matrix should have more elongation than the fibers to transmit the load properly. This permits refractories with lower moduli and high-creep rates, such as tantalum and niobium, to be used as matrices. Zirconia, yttria, hafnia, and thoria have been successfully fiberized in preliminary experiments, as have other refractory compounds such as hafnium boride, hafnium carbide, and tantalum carbide. Tungsten powders of approximately 1-micron diam were mixed with 2-micron oxide powders and cleaned with hydrogen at 1500° F for 6 hr to reduce residual tungsten oxide prior to isostatic compaction in a rubber mold at room temperature and 30 000 psi. Sintering was done under vacuum at temperatures up to 4200° F before the billet was encased in a molybdenum can and extruded. Extrusion reduction ratios were 8 or 16 to 1 at 3700° to 4200° F. There was significant fiberizing in the cases of yttria, hafnium nitride, zirconia, and hafnia. Fibers of these materials had aspect ratios (length/diameter) of from 12.7 to 23.3. Thoria, tantalum carbide, and hafnium carbide were less successfully fiberized; their aspect ratios were 5.1 to 7.8. Improvements in strength over unreinforced tungsten were noted for all samples containing over 10% fiber. Hafnium nitride pro-

duced particularly good results, exceeding the properties of many of the better tungsten alloys.

Tantalum and niobium were next chosen as matrix candidates for *in situ* fiberizing because of their low moduli (ref. 159). The materials for the fibers were chosen to have higher moduli and similar melting points to the matrix materials. The two systems selected on this basis were tantalum reinforced with magnesium oxide and niobium reinforced with aluminum oxide. Other systems were also tried in which the softening temperature of the oxide was within the range of the experiments, even though the melting point was much higher. The fabrication of extrusion billets was similar to the earlier work, except that a higher-compaction pressure was used, and the sintering temperatures ranged from 2800° to 3700° F. The billets were canned in molybdenum and were extruded at 2800° to 3800° F with reduction ratios of 16:1 to 32:1. Each billet was examined at both ends and in the middle to detect the temperature changes that might occur as the billet pases through the die.

Another program evaluated rolling as a means for producing fibers from powder particles. Zirconia, niobium, and tantalum powders were pressed and sintered into bars, and then rolled at 3500° F with flat rolls. A series of passes through the rolls reduced the area of the compacts 25%, 50%, 75% and 90%, respectively. Metallographic examinations were conducted after each pass. This program produced a wealth of information on the mechanism of *in situ* fiberizing. For example, the best temperatures for fiberizing magnesia, thoria, or zirconia were found to range between 0.57 and 0.78 of their melting points. The amount of deformation caused by either extrusion or rolling, however, is the most important criterion. The relative resistance to deformation of the matrix is also important as a tungsten matrix will deform zirconia particles at a given temperature and achieve a reduction in area to a greater degree than either tantalum or niobium. As far as physical properties are concerned, in this exploratory work, niobium containing 20% of either thoria or zirconia showed a considerable increase in stress-rupture properties over unalloyed niobium at both 2200° and 2500° F.

More recently, Blakenship produced zirconia and urania (UO_2) fibers with aspect ratios of 200 to 1 by extruding them in tungsten tubing (ref. 160). The choice of thin-wall ⅝- or ½-in. tubing for an experimental program was made to avoid the nonhomogeneous deformation that occurs in the extrusion of bar stock. Another change from the previous work was in the relative sizes of the powders. The average particle sizes of the urania and zir-

conia were 45 microns as opposed to 0.88 microns for the tungsten powder. Cylinders were pressed from powder mixtures containing 20% oxide, sintered, and canned in special molybdenum cans (fig. 56) by powder metallurgy techniques. They were extruded in a vertical extrusion press at a nominal reduction of 18 to 1, with temperatures ranging from 2800° to 4600° F.

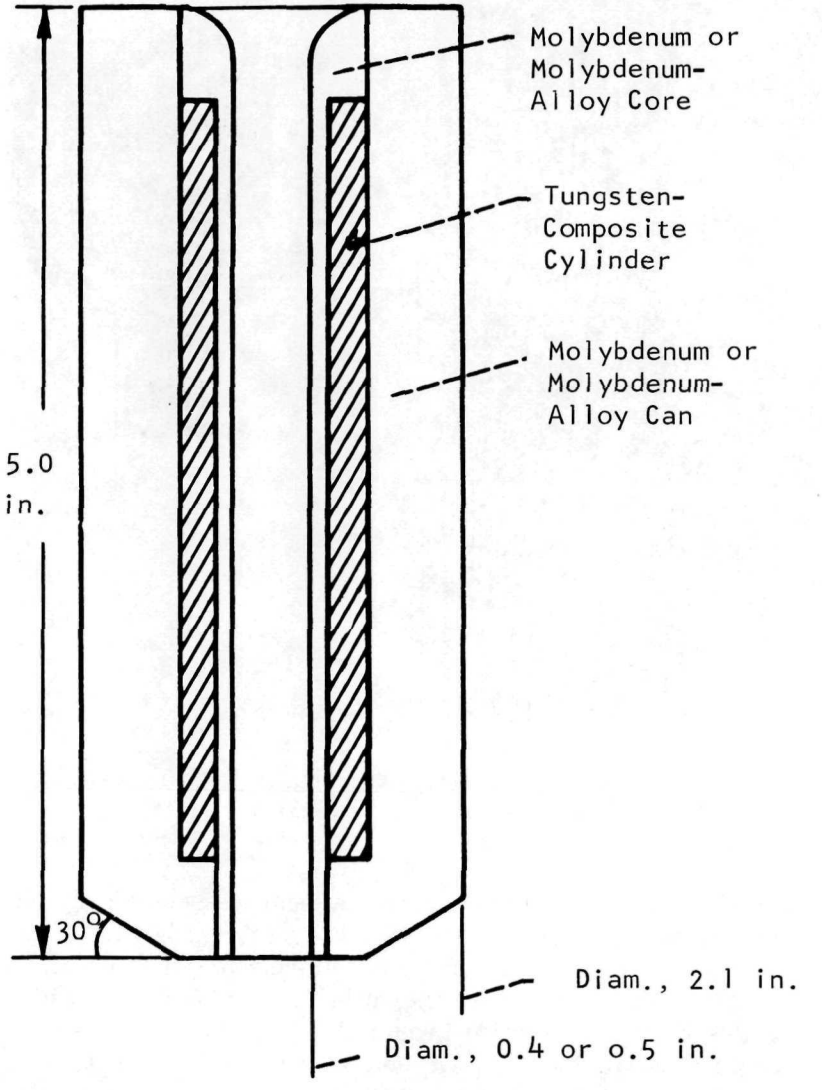

FIGURE 56.—Billet assembly for extrusion of tungsten-composite tubing (ref. 160).

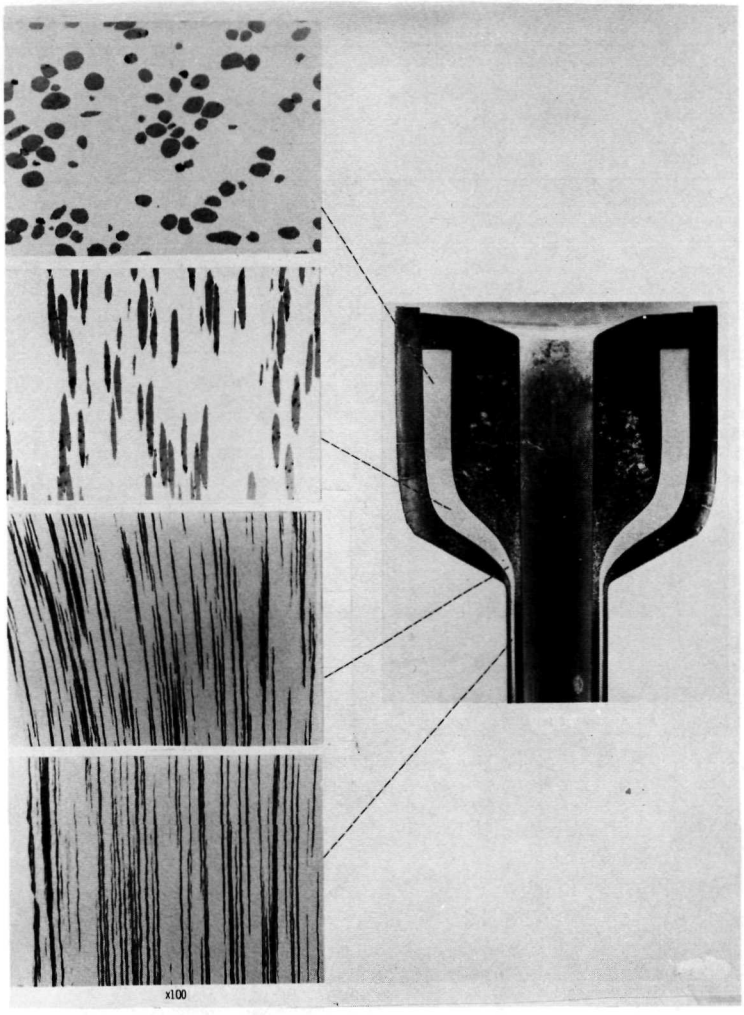

FIGURE 57.—Oxide-deformation pattern during extrusion of composite tubing (ref. 160).

After extrusion, the canning material was machined away and tensile test specimens cut out by electric-discharge machining. Examples of the amount of oxide deformation that occurs during the extrusion process are shown in figures 57. Fibers with aspect ratios of 200 to 1 were produced by extruding tungsten urania composites at 3600° F. Higher as well as lower extrusion temperatures produced shorter fibers. The optimum temperature for zirconia was 4000° F, which produced fibers having aspect ratios of 160. Tungsten with the longest urania fibers had about twice

the tensile strength (about 14 000 psi) at 3500° F of that of unalloyed tungsten. Those samples with fibers half as long exhibited only a 30% increase in strength at this temperature. The results with zirconia generally were not as satisfactory. Considering the advanced state of the conventional tungsten alloys, the potential for this type of material with alloyed matrices is very promising.

The boron-aluminum composites that are now being engineered for actual use in aircraft are merely the forerunners of a host of future materials containing fiber reinforcement. This prediction follows logically from the research results described here. It can be seen that the incorporation of fibers of very high strengths into metal matrices enables materials of high strength-to-weight ratios to be fabricated, and the strength of the materials can be oriented in directions where it is most needed. Another advantage, which might not be so obvious from this work, is an economic one. Many of the strongest fibers listed in table XVII are made from common, inexpensive materials. With the anticipated scarcity and high cost of the currently used high-strength alloying elements, the substitution of carbon, ceramic, and metallic fibers together with cheaper matrix materials will be of increasing economic and technological benefit.

Page intentionally left blank

CHAPTER 6

Some Special Powder Metallurgy Products

POROUS MATERIALS

Porous structures have manifold applications in aerospace technology. These include filters, fuel cells, heat exchangers, and even rocket engines. Structures in which pores are infiltered with a second material appear as bearings, electrical contacts, and rocket nozzles. Perforated plates, or brazed bundles of tubes are sometimes used, but the most common means of production is through the sintering of metal powders.

A pile of loose metal powder consists of more than 60% voids, with the exact amount determined by the size and shape distribution of the particles. When compacted, the porosity of the powder decreases but generally remains interconnected. Sintering causes substantial changes in the compacted mass of powder. Different sintering temperatures and duration result in variations in the strength of the compact as well as basically different porosity characteristics. The changes that are directly attributable to such sintering conditions as time and temperatures are:

1. The total porosity (total pore volume) decreases
2. The pores change their shape from irregular to rounded to circular
3. The pore-surface area decreases because of (1) and (2)
4. The number of fine pores decreases considerably
5. The number of large pores increases slightly
6. The average pore diameter increases
7. The total pore length decreases
8. The number of dead-end and closed pores increases
9. The outside pores sometimes close under conditions where inner pores still exist.

Dead-end pores and completely closed pores are highly undesirable for most applications of porous metallic structures. The orientation of the pores depends on the final use of the material desired and can be controlled by compaction. Highly-oriented pores are produced by unidirectional, conventional pressing and are perpendicular to the direction of pressing. This is also true of isostatic pressing, although the pores are more randomly ori-

ented. Extrusion produces highly-oriented pores parallel to the direction of extrusion while slip casting produces little or no orientation. The variables that need to be considered in designing porous structures are:

1. Total pore volume
2. Volume of all interconnected pores
3. Volume of all dead-end pores
4. Volume of all closed pores
5. Total surface area of all interconnected pores
6. Orientation of pores
7. Total length of all interconnected pores
8. Average diameter of interconnected pores
9. Pore-size distribution
10. Pore shape
11. Pore-shape distribution.

Special techniques have been developed for manufacturing tungsten, rhenium, iridium, tantalum, and molybdenum as well as the more conventional metals, such as nickel, copper, and stainless steel, into plates with controllable ranges of pore densities. Materials are commercially available in porosities of 6 narrow pore sizes between 1 and 3 microns, and corresponding surface densities of 8×10^6 to 1.4×10^6 pores/cm^2 are obtained (ref. 161). These are made by warm-pressing narrow-size fractions of spherical powders producing high-strength "as-pressed" plates. No binder is used, and sintering is done under high vacuum. Closely packed, mainly one-size spheres are essential to the production of uniform pore size with the desired high percentage of interconnecting pores. Areas of the porous plates can be selectively sealed with an electron beam to tolerances of 0.002 in. The electron beam can also be used for joining porous tungsten to solid tungsten, molybdenum, tantalum, or rhenium. Among the uses that are suggested for these structures are filters for high-temperature liquid metals and high-temperature, high-pressure flow-control devices, impregnated cathode bodies, and liquid-gas separators.

The liquid-gas separator is a vital part of the life-support systems in spacecraft. It must be very efficient and operable at zero gravity. Booth (ref. 162) developed such a unit which depends on the ability of sintered metal to maintain a pressure differential between the inside and outside of an apparatus, and also to draw in liquids by capillary attraction. The patented system has sintered tubes with porous fins on the outside. Coolant circulates through the tubes and wets the outside by capillary action.

Condensate forms on the fins and enters, mixing with the coolant stream which is at a lower pressure than the gas stream.

Porous tungsten is of considerable value in applications requiring the high-temperature strength plus another property which solid tungsten lacks. This property can often be supplied by infiltrating the porous tungsten with a second material such as copper or silver. Electrical contacts with high-current-carrying capacity and high resistance to spark erosion are made this way. Tungsten provides spark resistance, and copper provides good conductivity. Other examples are lubricant-impregnated, high-temperature bearings and silver-infiltrated rocket nozzles (ref. 163). The "hot-ion" rocket engine is the most prominent application of uninfiltrated porous tungsten.

Porous tungsten that is used in silver-infiltrated rocket nozzles should be controlled to at least 75% of the theoretical density to provide adequate strength of the structure. At densities above 83%, on the other hand, the interconnecting porosity becomes seriously diminished. The variables controlling this range of porosity are particle size, shape, distribution, chemistry, and sintering conditions including the effects of sintering atmosphere, temperature, and duration.

For optimum conditions, tungsten powder of slightly irregular shape with an average particle size of 3 to 7 microns and a nearly Gaussian size-distribution is required. Powders of these characteristics sinter easily to produce the desired matrix of 75% to 83% density with more than 90% interconnecting pores. The variation of porosity with particle size, shape, and compaction pressure for larger particles is shown in table XX (ref. 164). Larger particle sizes produce higher percentages of interconnecting porosity as well as larger pores.

The development of the silver-infiltrated rocket nozzle came about in 1960 after a need developed for a material that could be operated at close to the melting point of tungsten. Consideration of the available materials led to the use of pressed and sintered tungsten infiltrated with a lower melting metal that would vaporize during service and cool the nozzle (ref. 163). The principle, with silver as the infiltrated metal, is shown in figure 58; the amount of heat being absorbed in the various steps of warming to melting point, melting, and warming to boiling point is also illustrated in this figure (ref. 165). The requirements for the infiltrant are:

1. A boiling point below the operating temperature of the nozzle
2. A high heat of vaporization per unit volume

TABLE XX.—*Effect of Powder Size, Compaction Pressure, and Sintering Temperature on Sintered Porosity of Tungsten* (ref. 164)*

Powder		Compaction pressure, ksi	Sintering temperature, °F	Porosity, %	
Size, microns	Shape			Bulk	Interconnected
7.6	Irregular	10	4000	30	30
		20	4000	26	26
		25	4000	23	23
		25	4500	16	13
		40	4000	19	17
		50	4000	17	15
		50	4500	10	4
4.1	Irregular	10	4000	16	12
		25	4000	12	5
		40	4000	10	1
		50	4000	10	1
10	Spherical	10	4000	27	26
		10	4500	16	15
		25	4000	24	22
		25	4500	14	12
		40	4000	20	18
		40	4500	12	8
		50	4000	19	17
		50	4500	11	6
20	Spherical	10	4000	30	30
		25	4000	27	27
		25	4500	27	27
		50	4000	22	22
		50	4500	22	22
30	Spherical	10	4000	33	33
		25	4000	30	30
		25	4500	29	29
		40	4000	25	25
		50	4000	23	23
		50	4500	23	23

* Pressed compacts presintered in dry hydrogen for 6 hr; final sintering in vacuum for 4 hr at the temperature noted.

3. An appreciable temperature difference between the melting point and the boiling point

4. No reaction between the tungsten and the infiltrant.

Of the commonly available metals, only silver and copper filled these requirements, but, in actual tests, only silver-infiltrated

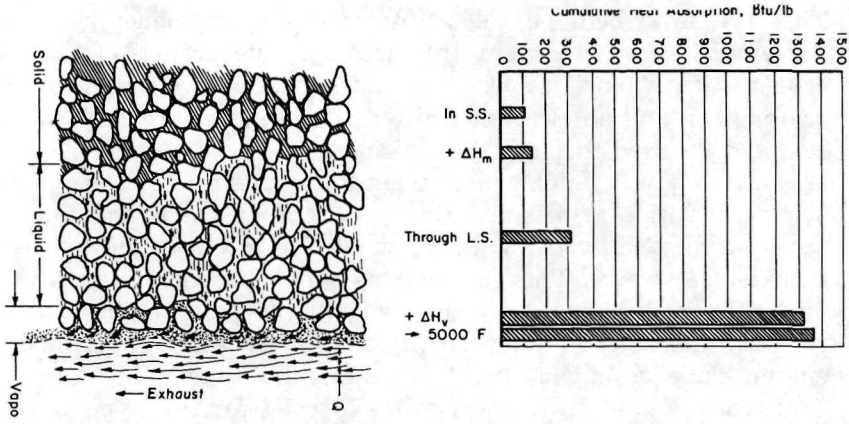

FIGURE 58.—Schematic representation of heat absorption by silver in an infiltrated tungsten-nozzle liner wall (ref. 165).

samples were successful. Workers at Virginia Polytechnic Institute prepared a mechanism for the operation of these composites and analyzed a detailed model of it (ref. 166). A liquid layer of finite thickness was observed at the surface of the composite. This was caused by the expansion of the composite when the infiltrant melted. As this layer vaporized, fresh melted infiltrant was fed to it until the vaporization rate exceeded the feed rate, depleting the layer. After this, the infiltrant vaporized from within the tungsten matrix.

Despite the successful tests of silver-infiltrated rocket nozzles, some problems still existed. At an operating temperature of 6000° F and pressures of 600 to 900 psi, which correspond to nozzle operating conditions, no substantial cooling takes place, because, at 600 psi, silver does not vaporize until it reaches 6100° F. Actually, to be effective, the nozzle must be used where the local static pressure is low enough to permit the silver to vaporize below the softening point of the tungsten matrix, about 5300° F. This pressure is 180 psi, and usually occurs only well downstream of the nozzle throat. To avoid this problem, the impregnated nozzles were coated with a thin impermeable layer of tungsten, except at certain venting regions where the local static pressure would be consistent with a coolant-vaporization temperature below the softening point of tungsten (ref. 167). In actual experiments, a coated nozzle marginally outperformed an uncoated one, but examination of the nozzle showed that the mobility of the silver was not sufficient to carry it to the vents.

The hot-ion rocket engine also depends on porous tungsten.

This engine is being developed for use in interplanetary space travel where low thrusts are required for long periods of time. It consists of a vaporizing chamber, an ionization section, an accelerator grid, and an electron emitter. Metal atoms are first vaporized and diffused through the ionization plate where they pick up a positive charge which causes them to be repelled from the plate. The acceleration grid is negatively charged and attracts the ions, accelerating and focusing them, while the electron emitter neutralizes the stream. This fast moving stream of metal atoms produces the rocket thrust by the principle of reaction. Figure 59 represents the principle of this operation. An early experimental engine using cesium as the volatile metal is shown in figure 60 (ref. 168). Currently, a mercury is favored for this type of propulsion system. Woven-wire cloth, finely spaced holes drilled in a metal sheet, closely packed wire bundles, and sintered-powder compacts made from both angular and spherical powders have all been investigated as ionizing structures; but the porous tungsten made from spherical powder appears the most satisfactory (ref. 169).

The main requirement for the ionizer of this engine is that it ionize the highest possible percentage of the metal atoms which evaporate from its surface. To avoid erosion damage to the acceleration electrodes from nonionized atoms, the surface must have a work function (i.e. the potential needed to release an electron

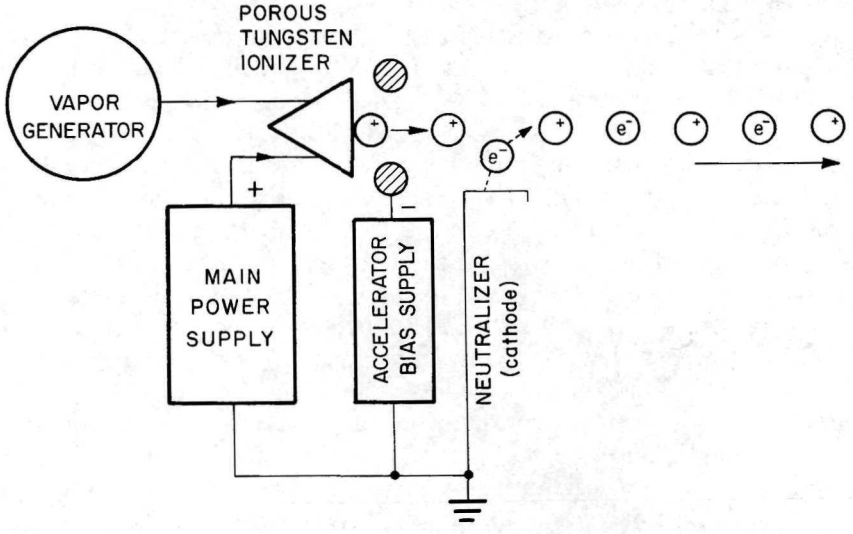

FIGURE 59.—Operation of hot ion rocket engine.

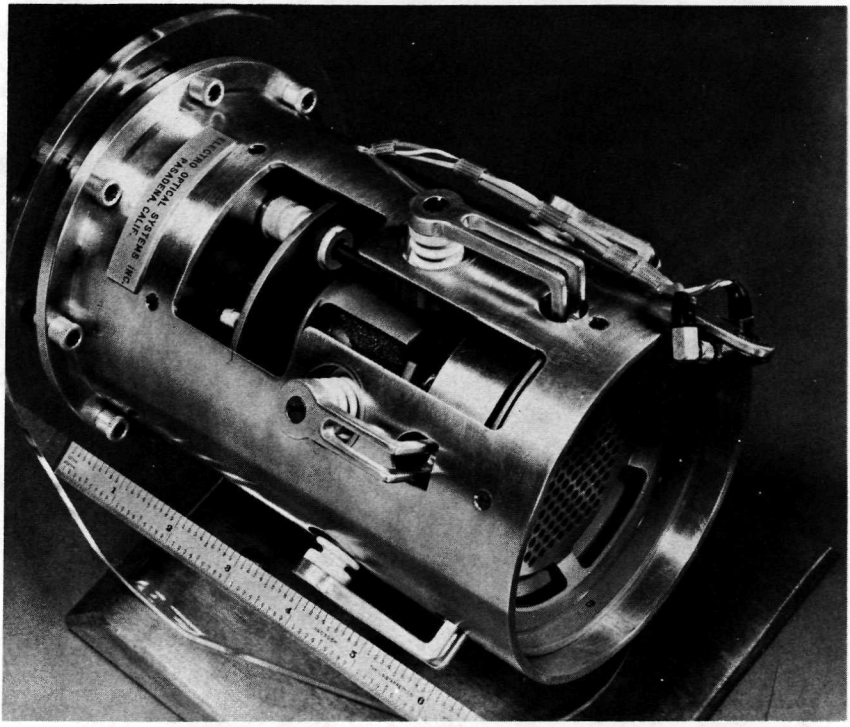

FIGURE 60.—Experimental cesium-ion rocket engine (ref. 168).

from the surface) that is higher than the ionization potential of the propellant metal. Tungsten, with a work function of 4.5 eV and a high melting point, is the best material for the purpose. High-metal-flow rates which are required for high thrusts, however, tend to flood the ionizing surface and lower the work function of the surface. When this happens, more metal is allowed to evaporate as neutral atoms. One way of combatting this is by having a surface with as many pores per unit of surface as possible to achieve a more even distribution of the evaporating metal. Unfortunately, extremely fine porous tungsten tends to sinter at the operating temperatures of the engine making the ionizer unstable and short lived; another way is to alloy the tungsten with higher-work-function metals, which will increase the repulsion of the charged metal ions. The work functions of iridium and rhenium are compared to that of tungsten in table XXI. In limited tests, a thin coating of these metals made a significant improvement in the work function of the ionizer surface and hence in the efficiency of its operation (ref. 170). After long operating periods, however, the coatings tend to diffuse into the matrix.

TABLE XXI.—*Work Functions of Refractory Metals (ref. 170)*

Metal	Work function, eV	Melting temperature
W	4.54	3410
Ir	5.30	2443
Rh	5.10	3145

To make an extremely fine porous plate of tungsten that is stable, it is necessary to have uniformly spaced and sized pores. This can be done by liquid-phase sintering with copper and nickel as the auxiliary phase (ref. 171). A ternary phase develops in which fine particles dissolve and precipitate on the particles of intermediate size. The final grains are spherical and approach single crystals in structure, so that, when the copper-nickel phase is removed, a very stable structure remains. It is vital, however, that these metals be removed completely, and a process is used involving HCl leaching followed by hot nitric acid and vacuum vaporization at 2750° F for 4 hr. Tungsten microspheres have been sintered to give more highly stable and finer pore structures than those of hydrogen-reduced powders (refs. 172, 173, and 174). The addition of tantalum to the tungsten further improved the stability of the final compacts. Tantalum was added in the form of a fine metal powder as a vapor-deposited coating and as a compound to be reduced at a later stage. This last method was the most successful.

The machining of porous tungsten shapes normally causes closure of surface pores (ref. 172). Milling is less damaging to the surface than lathe turning. Infiltration before machining and vacuum distillation of the infiltrant afterward will prevent most of this. A copper/2%-iron infiltrant was found to work well. Pure copper or silver infiltrants also allow free machining (ref. 161).

Saunders (ref. 175) studied the effects of tungsten powders of 1, 10, and 20 microns in average particle size and sintered between 2250° and 2900° F, and found that porosity varied inversely with the sintering temperature for the 1-micron powder but not with the larger sizes. Thin porous plates of 1 micron were prepared and sintered at 2750° F for 20 hr in a hydrogen atmosphere. The plates were tested successfully in an experimental cesium engine. Saunders later patented a technique for the preparation of these parts in which a fatty acid binder was used (ref. 176). An example of this procedure is: 1-micron tungsten powder containing 2% stearic acid is cold-compacted at 25 000 psi to

yield a 0.02-in. thick plate. This plate is sintered at 2750° F for 25 hr in a flowing hydrogen atmosphere. The fatty acid acts as a filler during the compaction of the fine powder, insuring a high percentage of interconnecting pores.

MATERIALS FOR ELECTRICAL APPLICATIONS

At a firing range near the Marshall Space Flight Center, explosives are being used for the fabrication of superconducting alloys. Other NASA laboratories are hot-pressing electrical contacts and sintering porous battery plates. These diverse powder-metallurgy operations make products with electrical applications.

The traditional electric motor brushes that are made from graphite for lubricity and conductivity do not work in the vacuum environment of space. Pure graphite is not a lubricant and becomes one only when water or certain other molecules are absorbed into its structure (ref. 177). A high-vacuum environment will pull out these molecules. The addition of metallic halides to graphite has been successfully used in high altitude applications, but even these compounds have sufficient vapor pressure to make them short-lived in space (ref. 178). This problem led to the initiation of research to find new electrical brush materials by the Marshall Space Flight Center. Different combinations of commutator and brush materials were tested in a vacuum similar to that found in space. The most promising one was a molybdenum disulfide (MoS_2) and copper brush on a mild-steel commutator (ref. 179).

MoS_2 has a molecular structure similar to graphite and is also a good lubricant at various temperatures. It is used, for instance, as a finely ground powdered-oil additive for engine lubrication. Unlike graphite, it does not require absorbed water or gas molecules in its structure for lubricating properties; and it should be an ideal lubricant for space environments. However, MoS_2 is a poor conductor of electricity; and metallic additives are necessary for these applications.

Much of the work concerning the development of MoS_2 brushes has been done by Ulrich and King (refs. 180 and 181). They hot-pressed combinations of MoS_2 and copper at 871° to 927° C and 3500 psi to get samples for evaluation. Those with higher percentages of MoS_2 gave better lubrication. Lifetimes of up to 700 hours in vacuum were achieved with a 90% MoS_2-10% Cu brush. Substituting silver for copper led to samples with lifetimes of several thousand hours, but in general there was a lack of reproducibility.

The experimental procedure utilizes silver powder of −325 mesh and MoS_2 in the range 0.1 to 0.2 micron. Some work has also been done with colloidal powder. The powders are mixed and placed in a graphite mold which is placed in a cold furnace. Pressure is applied before heating, and the time interval for isothermal heating is measured from the attainment of temperature to the release of pressure. The resulting compacts are machined into rectangular brushes with the long dimensions parallel to the direction of pressing. Compacts containing up to 85% by volume of MoS_2 exhibit good strength, but a nonmetallic-to-metallic conductivity transition occurs when MoS_2 content exceeds 70%. This effect, which can be seen in figure 61, changes with temperature.

A composition of 55.9% MoS_2 and 44.1% silver has exhibited a good range of properties in vacuum, and its use is anticipated in future space missions (ref. 182). The new material has now reversed the original problem by providing a good brush for use in vacuum but a poor one for use under atmospheric conditions. The desirable system should be good in either place. Several alternative brush materials have been developed for vacuum use; for example, a series of hot-pressed selenide and sulfide mixtures (ref. 183), and a MoS_2-tantalum-molybdenum composite.

MoS_2 has several disadvantages for aerospace applications. It is stable at high temperatures in vacuum to 10^{-6} torr but it tends to lose sulfur in ultrahigh vacuums at high temperatures (ref. 184). In addition, it does not have good electrical conductivity, and it is not particularly stable when exposed to radiation. Lubricants based on selenium, such as niobium diselenide ($NbSe_2$) or tungsten diselenide (WSe_2), are stable to 500° C under vacuum as high as 10^{-22} torr (ref. 183), and they are metallic conductors of electricity. They are more easily oxidized in air, however, so each lubricant requirement must be selected individually. A comparison of the properties of Ag–MoS_2 and Ag–$NbSe_2$ is shown in table XXII (ref. 185). In mounting these brushes, the compaction direction should be parallel to the sliding direction because some variation in hardness usually exists from end to end. The brushes are easily brazed or soldered without the special coatings that would be required for MoS_2 brushes.

Migration of silver during sintering or hot pressing causes poor reproducibility of the wear lifetimes of MoS_2-silver brush materials. Temperatures as low as 1700° F cause variations in the electrical conductivity across the surface of the compacts. Explosive compaction provides a means of consolidating these materials without heat. Reece (ref. 15) has made some compacts of molybdenum and MoS_2 in this manner for use as vacuum brushes.

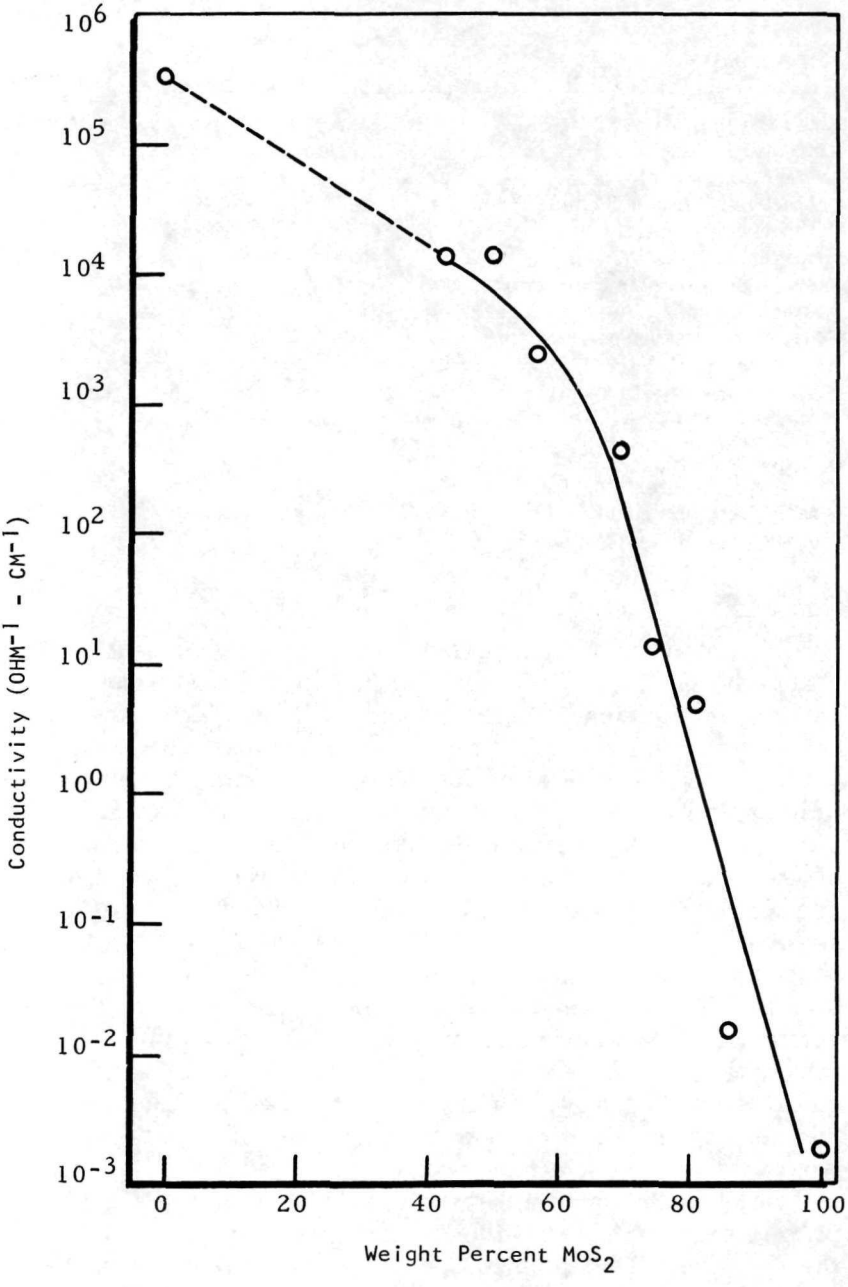

FIGURE 61.—Conductivity as a function of composition of MoS_2–Ag hot-pressed at 927° C and 3500 psi (ref. 180).

TABLE XXII.—*Comparison of Ag–MoS_2 and Ag–$NbSe_2$ Brushes in High Vacuum at Low Speeds (ref. 185)*

Composition	85–15 Ag–MoS_2*	85–15 Ag–$NbSe_2$*
Wt. loss, g/cm²/hr	4.2×10^{-8}	5.5×10^{-8}
Ring wear	Light	Light
Average contact drop, mV	70	30
Contact resistance, milliohms	2.3	1.2
Contact temp., °C	67	53
Space temp., °C	40	35
Average % increase in contact roughness after 1000 hr	81%	18%
Contact drop frequency variation, V	0.05–.20	0.03–.06

* Noise levels below 1 microvolt at 125–250 kc were measured, but are not to be considered accurate due to low sliding speeds.
Current density: 13 A/cm²
Speed: 0.0125 ft/min
Brush pressure: 300 g/cm²
Temperature: ambient
Vacuum: 10^{-8} torr
Rings: coin silver

By instantaneously compacting and sintering, essentially no change in the distribution of either material can take place. Compactions comprising 10%, 20%, and 30% by weight MoS_3 have been made, with the 20% sample being the most successful.

The primary purpose of Reece's experimental work was improving the compositions of superconductors so that they have higher transition temperatures than the present limits. Examples of these compositions are: $GaNb_3Sn$ (18.0° K), GaV_3 (16.8° K), and Nb_3Sn (18.0° K). By improving the structure through explosive compaction, it may be possible to raise the superconductivity-transition temperature above 20° K. Dr. Gunther Otto of Marshall Space Flight Center and Dr. Upendra Roy of the University of Alabama are also working on this program. Explosive compaction enables a large series of compositions to be evaluated quickly and efficiently with close control of compaction pressures and detonation velocities. The set-up consists of a container of nitroguanidine into which a copper tube filled with the metallic powders has been placed. Pressures up to 3 million psi can be applied to the sample, depending on how much explosive is placed in the container. The samples are made by mixing fine elemental powders of tin and niobium in a 1 to 3 ratio based on their atomic weights. Compaction produces an intermetallic lattice which determines the degree of superconductivity. Lower-pres-

sure experiments have not produced a large amount of the required structure, but as the pressure is increased, the lattice structure improves. Other systems such as Nb_3Au, Nb_3Al, and Nb_3Ta have also been tried.

The nickel cadmium storage battery, currently in commercial use as a rechargeable self-contained power supply for tools and appliances, is of great interest to NASA. Because it can be recharged thousands of times, and because of its light weight and long shelf life, it is a good candidate for the power supply in aerospace vehicles. The heart of the nickel cadmium battery is a nickel plaque, which is over 80% porous and filled with an active form of cadmium. Integral contact between these active constituents is essential. The efficiency of the cell is determined by the number of charge-discharge cycles it can sustain and the percentage of discharge in each cycle. Problems arise with high-discharge rates because the cadmium in the interior of the plaque usually lacks sufficient contact with the electrolyte to react completely. In 1964, it was reported that commercially available cells exhibited less than 10% of their theoretical efficiency because of the relatively large area of electrode surface that failed to react (ref. 186).

To improve the accessibility of the internal pores in these cells, NASA has sponsored research in several forming techniques to produce the initial porous nickel plaque. The commercial method of production is to compact lightly and sinter nickel carbonyl powder to give a material with a porosity of 80%, but which has random pore sizes, not all of which can be filled with active cadmium. Also, since the cadmium impregnation procedure can be lengthy and expensive, a thorough study of the entire powder-metallurgy process has been initiated by NASA. A comprehensive bibliography on the subject was published as the initial effort of this program (ref. 187) followed by a study of the powders commercially available for the production of these cells (ref. 188). Results of this study emphasized the value of the scanning electron microscope to observe the surface characteristics and particle shapes of nickel powders. The study also indicated the need to study fabricated nickel plaques to determine the effects of different fabrication techniques and variations in pore structure.

Fibrous nickel has been substituted for the normally used powder in a project for the Lewis Research Center (ref. 189). Flat fibers with average widths of 65 microns, thicknesses of 2 to 3 microns, and lengths of 540 microns were felted into mats and sintered at various temperatures up to 2150° F for 20 min. Excellent porous plaques were obtained with porosities as high as

90% and acceptable tensile strengths of better than 300 psi. The resulting large-internal surface areas coupled with controllable high porosities indicate a promising potential for this technique.

A nonpowder metallurgical technique for the production of nickel battery plaques is also being investigated. Nickel sheets are electroformed into screens which can then be stacked in various configurations to give plaques with large-internal surface areas (ref. 190). Electroforming allows for precise control of pore shape and size, and the stacking operation produces the desired orientations. While the parameters of this method are still being investigated, it is evident that the potential to form highly efficient batteries is present. The expense of machining and stacking nickel sheets would be considerably higher than the cost of the compaction and sintering process of powder metallurgy; thus it remains to be seen whether the gain in efficiency will offset the increase in cost.

SINTERED BEARINGS

The application of powder metallurgy to the manufacture of bearings brought about a major improvement in the quality and maintenance of consumer appliances and machines. Practically every automobile, washing machine, refrigerator, and air conditioner that is produced today contains sintered bearings. The world production of these bearings amounts to more than three billion per year. The use by industry of this tremendous volume of sintered bearings is based on three factors: (1) substantial cost savings over other bearings, (2) controllability of characteristics made possible by powder metallurgy techniques, and (3) self-lubrication capacity of the bearings.

A sintered bearing is essentially a sleeve bearing with a built-in lubrication supply and distribution system. It consists of a porous-metal matrix which contains and controls a solid or liquid lubricant. The liquid-lubricated sintered bearing is the best known on the commercial market and is commonly referred to as the oilless bearing. It is practically maintenance free and replaces sleeve and ball bearings which require periodic lubrication. Its production starts with a porous-sintered compact which is sized to final dimensions before processing. The compact is then infiltrated by evacuation followed by immersion in oil which penetrates into the pores by capillary action. The solid-lubricated bearings are employed in high-temperature or high-vacuum environments. The lubricant is normally built into the bearing at the time of consolidation. Powders of metal and lubricant are mixed, pressed, and sintered.

The operation of the liquid-lubricated sintered bearing occurs through two mechanisms, hydrodynamic and boundary-film lubrication. Under the former, pressure created by the rotating motion of the shaft sustains the layer of oil between the shaft and the bearing. The load-carrying ability of the bearing is determined in part by the circumferential velocity of the shaft. Hydrodynamic pressure created by a rotating shaft builds up in the direction of the load causing oil to circulate into the bearing at this area and out in the areas of less pressure. This circulation prevents heat buildup in the areas of the most load. When the shaft is at rest, no pressure is being generated (unless an external pump is used). The lubrication is dependent upon the boundary film which in turn is dependent upon the ability of the lubricant to maintain a continuous film under load. The matrix material ideally should be both hard and soft; hard in order to wear at a low rate with a minimum of distortion over long periods, and soft to accommodate abrasive contaminants that enter most lubricated systems during their lifetimes. These particles can embed themselves into the softer matrix, preventing damage to the shaft. The ideal bearing would contain both hard and soft phases. In practice, however, because contamination is the more serious problem, bronze, soft iron, and aluminum are most frequently used as matrix materials.

The first Orbiting Solar Observatory contained sintered bronze bushings in its altitude control mechanisms and in the hinges of three equally spaced arms which carried pressurized-nitrogen jets. These jets assisted in the orientation of the satellite's instruments so that they pointed toward the sun at all times. Bronze bushings were also used in the solenoids which activated tape recorders in many of the Explorer series of satellites (ref. 191).

The solid-lubricant bearings contain lubricants which have extremely low coefficients of friction. Common, commercially used examples are the fluorocarbon polymers and graphite. In addition, there is a bearing used in heavy machinery in which a very soft metal powder, such as lead, cadmium, or tin, is sintered together with copper powder to form the bearing material. While the solubility of these metals in iron is extremely low, thus reducing the possibility of cold-welding, their primary purpose is the removal by embedment of hard, particulate contaminants. Supplementary lubrication is supplied by a pressurized oil flow. Solid-lubricated bearings, on the other hand, operate completely dry, and sometimes even in a vacuum. Their use and construction closely parallels those of the electrical brushes described previously since the requirements for both are the same, except that

electric conductivity is necessary in one case and load-bearing ability in the other.

Graphite was the first solid lubricant to be incorporated into a bearing material, but it has several drawbacks that affect its use. For example, graphite "fines" tend to coat the matrix powder during mixing and prevent effective sintering. Thus, bearings with high amounts of lubricant (over 30%) tend to be weak. Also, there is the lack of lubricity in vacuum that was described previously under electrical materials. Even at atmospheric pressure, however, graphite exhibits discontinuities in its lubricating properties. An early NACA report (ref. 192) showed that graphite was a good lubricant at room temperature and 1000° F, but showed a high coefficient of friction (over 0.2) between 200° and 900° F. The presence of an oxide film on the metal-bearing surfaces was cited as one cause for this phenomenon.

MoS_2 is an excellent substitute for graphite in electrical brushes for use in high vacuum; it also replaces graphite in many other lubricating applications. The extendable legs of the lunar module (fig. 62), which landed on the Moon July 20, 1969, were lubricated with a MoS_2-phenolic mixture.

The frictional characteristics of hot-pressed molybdenum disulfide-silver bearing materials were studied at the Lewis Research Center (then the Lewis Flight Propulsion Laboratory) more than twenty years ago (ref. 193). Cylindrical shaped riders with hemispherical tips made of powder mixtures containing from 1% to 35% MoS_2, 5% copper, and the balance silver were pressed at 1400° F in an induction-heated carbon die. The test apparatus consisted of a rotating disk on which the rider slid with loads varying from 269 to 1017 grams. The sliding velocity could be varied from 70 to 8000 ft/min. The coefficient of friction was calculated from the frictional force on the rider and velocity of rotation. The wear of the riders was also determined from measurements of the wear-spot diameter. The results of the program showed that the bearing materials function by the transfer of the lubricant from within the structure of the rider to its interface with the steel disk. This transfer results in the formation of an effective lubricating film on the steel surface. Of the bearing compositions tested, the one containing 10% MoS_2 had the best performance characteristics relative to both wear and friction. Lower concentrations of MoS_2 resulted in higher friction, greater wear, and greater surface failure by welding. Concentrations of MoS_2 above 10% showed only a slight decrease in friction, but wear increased, probably because of the lower physical strength of the material.

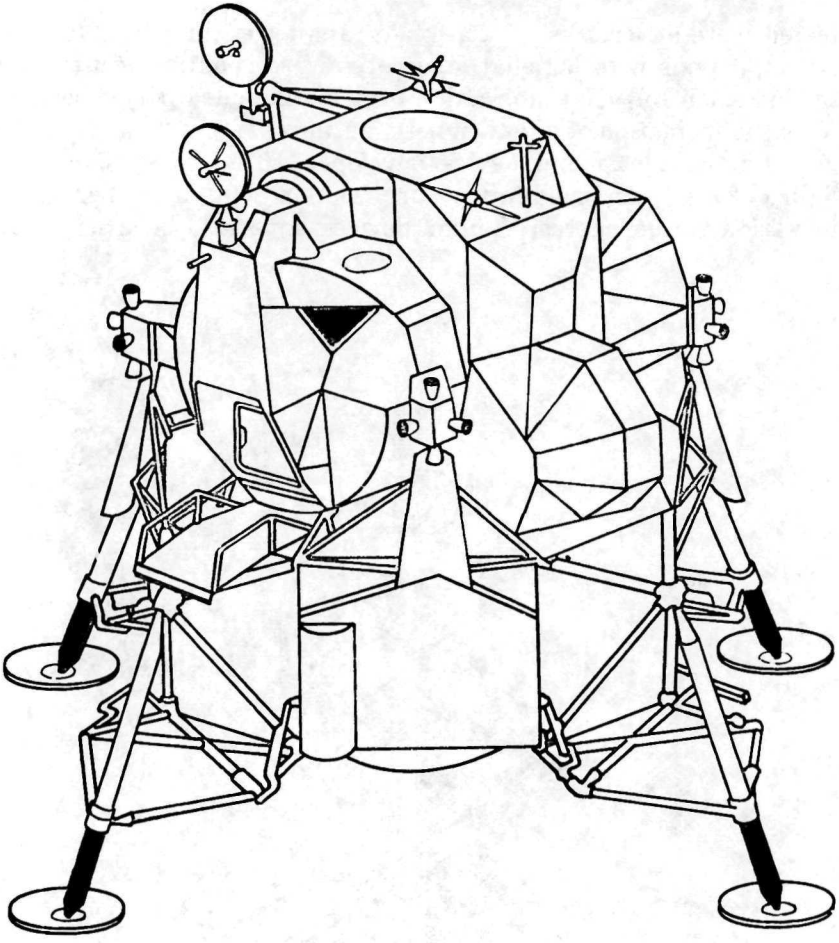

FIGURE 62.—Lunar module using MoS_2-phenolic lubricant on extendable legs.

MoS_2 is the first of a series of compounds, called lamellar solids, to be tested as solid lubricants for vacuum and high-temperature use. The requirements for a solid lubricant are thermal stability, low shear strength, surface adherence, and a lamellar structure (ref. 194). Several different kinds of materials have been tested at Lewis for these properties under various conditions (ref. 195 to 199). In an early project a wide range of compounds having lamellar structures were tested, (ref. 193) including cadmium iodide, silver sulfate, copper bromide, and tungsten sulfide. MoS_2 was the most effective lubricant in this program. It is interesting to note, however, that many of the other compounds

tested were at least as effective as graphite or zinc stearate. Not all compounds with lamellar structures were good lubricants, and the criterion for good lubrication over an extended period seemed to be the formation of a film on both mating surfaces.

A friction-measuring device developed at Lewis is shown in figure 63. It is designed to measure friction at high temperatures in various atmospheres. Similar devices have also been used for

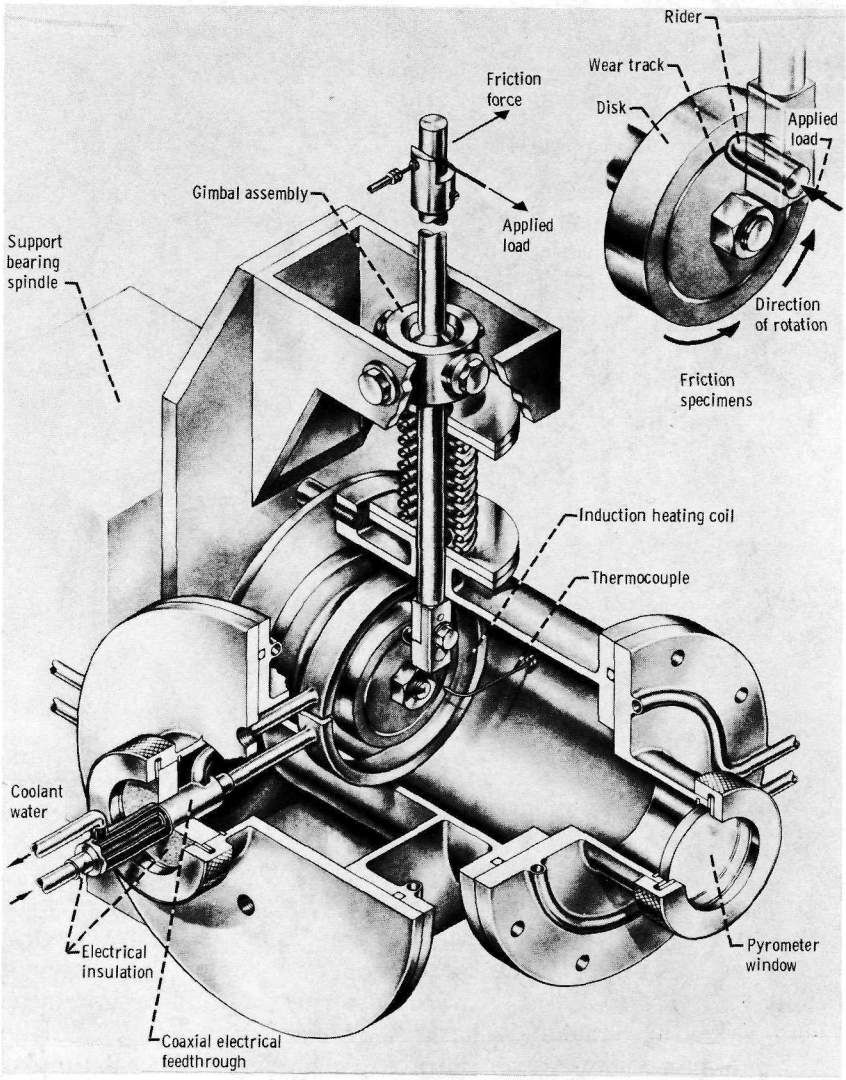

FIGURE 63.—High-temperature friction measuring apparatus (ref. 197).

ultrahigh vacuum environments (ref. 197). The same principle is applied to another device used to measure friction in liquid hydrogen (ref. 198). The friction-test apparatus consists of a rotating disk in sliding contact with a hemispherically tipped rider that is $\frac{3}{16}$ in. in diameter. A constant load of 500 g is applied to the rider which slides along a 2-in. diameter wear track on the disk. The sliding velocity can be continuously varied from 200 to 25 000 ft/sec. In the high-temperature apparatus, the disk is heated with an induction coil, and temperatures from 200° to 4000° F can be controlled and measured. Disk temperatures of 1650° F can be reached in the vacuum apparatus by heating with an electron gun mounted close to its edge. Samples are normally applied by rubbing them into the surface of the rotating disk.

The ditellurides and diselenides of both tungsten and molybdenum have been found to share the lubricity characteristics of the disulfides of these metals. Some have already been used in areas where conventional lubrication cannot be used, for example, at extremes of temperature or pressure. The stability of these materials in vacuum at elevated temperatures depends on the thermal-dissociation temperature. There is a considerable variation in the literature among the published values of these temperatures for even the most common material, MoS_2. They range from 1832° (ref. 200) to 3092° F (ref. 201). For the others, the data are still nonexistent. Brainard ran a series of thermal stability tests to verify this temperature (ref. 197). The results that he obtained are given in table XXIII. In all cases, when the temperature of the test apparatus reached the breakdown point, the pressure in the chamber would rise and an interconnected mass spectrometer would record peaks of the anion of the lubricant (Te, Se, or S). The results of frictional tests run in the same program are shown in figure 64. For all compounds except WTe_2, the

TABLE XXIII.—*Temperatures at Which Thermal Dissociation in Vacuum Was Observed by Mass Spectrometry (ref. 196)*

Lubricant	Temperature (°F)
MoS_2	2000
WS_2	1900
$MoSe_2$	1800
WSe_2	1700
$MoTe_2$	1300
WTe_2	1300

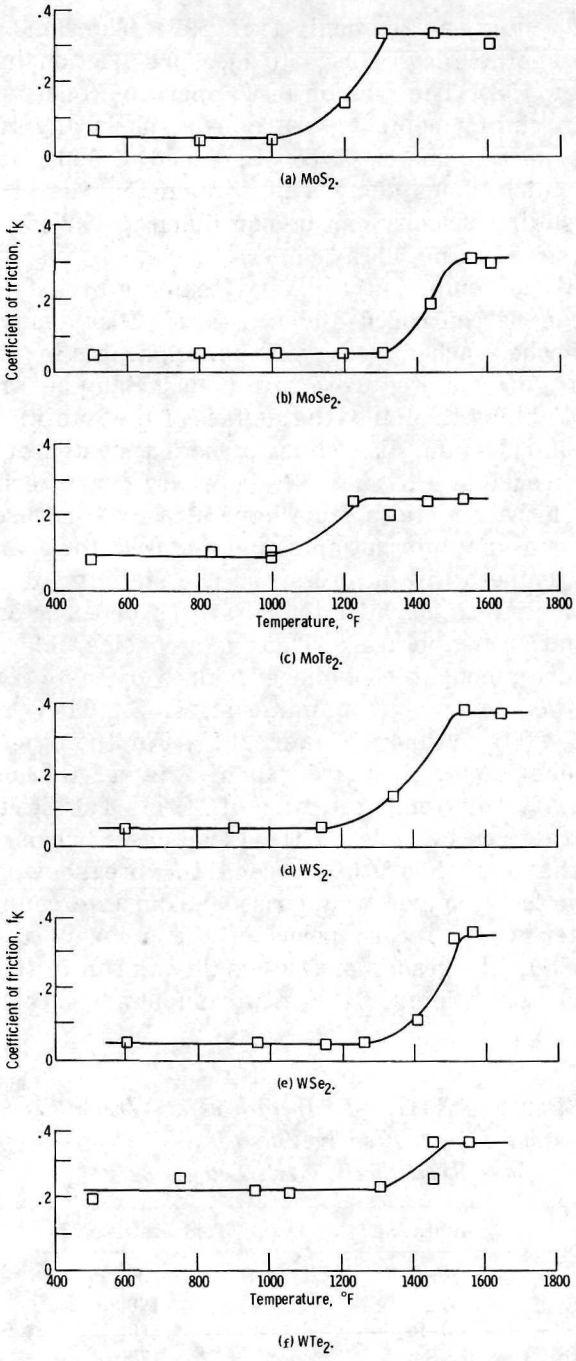

FIGURE 64.—Friction coefficients of various lubricants (ref. 196).

friction below 1200° F was low (0.04 to 0.08). Above this temperature, evaporation reduced the amount of lubricant available, and dissociation reduced it even further at higher temperatures. The diselenides of both tungsten and molybdenum provided the best performance of the series, retaining lubrication at 1400° F. At atmospheric pressures, the lubricating properties of MoS_2 are not as good as in vacuum, and various ways have been investigated to raise them. For example, a composite lubricant coating with good properties in both vacuum and air was developed for NASA. It was a composite containing MoS_2, graphite, gold powder, and a potassium silicate binder (ref. 202).

Other high-temperature lubricants that have been tried by NASA are the rare-earth fluorides such as lanthanum trifluoride, LaF_3 (ref. 196) and graphite fluoride, $(CF_x)n$ (ref. 195). The first of these preliminary programs was the more successful, showing that either cerium trifluoride (CeF_3) or LaF_3 can lubricate nickel-base superalloys in air or argon from room temperature to at least 1800° F. The coefficient of friction drops from the 0.3 to 0.4 range below 500° F to 0.1 at 1800° F. The most valuable property of these materials seems to be their ability to form films. When a sliding member is placed on such a material, it will flow into a thin adherent film on the sliding surfaces. In addition, these materials are relatively soft at room temperature and have melting points above 2200° F. Their thermal expansion coefficients are in the same range as those of the nickel-base superalloys and stainless steels. The work on graphite fluoride has been simply a feasibility study, but it has shown some favorable trends. On stainless steel at 400° C, its coefficient of friction is 0.02 to 0.15. It also has a longer wear lifetime than either graphite or MoS_2.

A wide variety of bearing composites containing lamellar solids is shown in table XXIV. These materials are used in thousands of applications over a wide range of operating conditions and environments, to include contacts, slip rings, ball and roller bearings, bushing journal and shaft bearings, valve seats, seals, and gears. The lubrication of ball or roller bearings in vacuum has been successfully accomplished by either a solid-lubricant retainer ring or by spring loading a composite insert into the outer race in such a way that it contacts the balls or rollers. A ball bearing equipped with a 75–25 Ag–WSe_2 retainer operating under low loads at speeds of 1768 rpm in a vacuum of 10^{-9} torr was estimated to have a life of 3 yr (ref. 183).

Gas-lubricated bearings derive their lubrication from the viscosity of a compressed gas. They generally have a much smaller

TABLE XXIV.—*Properties of Some Typical Composites (ref. 183)*

Composition by wt.	Density, g/cc	Typical coef. of friction	Hardness, Rockwell	Useful range from cryogenic to maximum temperature, °C	
				Vacuum	Air
90–10 Ag–$NbSe_2$	8.82–9.31	0.10–0.18	50–70 M	400	350
85–15 Ag–$NbSe_2$	8.57–9.04	0.08–0.17	50–70 M	400	350
80–20 Ag–$NbSe_2$	8.32–8.78	0.07–0.15	50–70 M	400	350
70–30 Ag–$NbSe_2$	7.85–8.28	0.06–0.14	50–70 M	400	350
80–15–5 Ag–$NbSe_2$–C	7.35–7.76	0.08–0.17	----------	Unstable [a]	350
90–10 Ag–C	6.92–7.30	0.12–0.17	----------	Unstable [a]	350
80–20 Ag–CS	5.45–5.76	0.11–0.20	----------	Unstable [a]	350
90–10 Ag–MoS_2	8.45–8.92	0.10–0.19	----------	400	260
80–20 Ag–MoS_2	7.63–8.06	0.08–0.18	----------	400	260
90–10 Ni–WS_2	7.87–8.31	0.12–0.20	90–110B	550	350
80–20 Ni–WS_2	7.72–8.14	0.08–0.15	85–105B	550	350
65–35 Ni–WS_2	7.52–7.94	0.05–0.12	75–95 B	550	350
95–5 Ni–CaF_2	7.35–7.76	0.30–0.40	60–70 B	650	650
90–10 Ni–CaF_2	6.67–7.04	0.28–0.35	65–80 B	650	650
85–15 Ni–CaF_2	6.31–6.66	0.28–0.33	70–85 B	650	650
85–15 Ag–WSe_2	9.22–9.73	0.10–0.18	60–30 M	400	350
75–25 Ag–WSe_2	9.07–9.57	0.07–0.15	60–80 M	400	350
70–20–10 Ag–PTFE–$NbSe_2$	6.14–6.48	0.06–0.15	60–80 H	260	260
70–20–10 Ag–PTFE–WSe_2	5.29–5.59	0.06–0.15	60–80 H	260	260
90–10 Ni–$NbSe_2$	7.69–8.12	0.12–0.20	90–110B	650	350
80–20 Ni–$NbSe_2$	7.38–7.79	0.08–0.18	85–105B	650	350
85–15 Ni–WSe_2	8.02–8.46	0.11–0.20	110–120B	650	350
75–25 Ni–WSe_2	8.04–8.48	0.09–0.17	95–105B	650	350
90–10 Ni–MoS_2	7.24–7.64	0.08–0.15	70–80 B	400	260
85–15 Ni–MoS_2	7.10–7.50	0.07–0.15	70–80 B	400	260
100% $NbSe_2$	5.63–5.94	0.02–0.04	low	1100	350
100% WSe_2	8.10–8.55	0.02–0.04	low	1100	350
100% WS_2	6.76–7.14	0.03–0.05	low	1100 [b]	440
100% MoS_2	4.32–4.56	0.04–0.06	low	1100 [b]	350

[a] In vacuum, graphitic component deteriorates but $NbSe_2$ permits operation to 400° C.

[b] Considerable outgassing of disulfides.

clearance between the moving parts than in a liquid-lubricated bearing and are used in very-high-speed applications such as gyroscopes. As yet, hardly any attempts have been made to use porous compacts to feed the gas into the bearing, but powder metallurgy does enter into this technology as far as the bearing material itself is concerned. During use and particularly during start-ups, these bearings may "bottom." In other words, the two parts may

come into contact. When this happens, sliding friction occurs, and a desirable material will have a high resistance to damage at these times. The material should have such properties as a low coefficient of friction, a high modulus of elasticity to resist centrifugal growth at high speeds, a low coefficient of thermal expansion, good impact resistance, and good dimensional stability. Alumina (Al_2O_3) fulfills these requirements admirably, and in addition, it is chemically inert and maintains a good surface finish. The friction and wear characteristics of alumina, made by pressing and sintering, cementation, hot-pressing, and plasma-arc deposition, were determined in one NASA project. The surface properties of the materials were first examined closely to determine their effect on the friction and wear of the bearings (ref. 203). These properties include finish, topology, grain size, preferred orientation, residual stresses, inclusion, microcracks, pits, and contaminant layers. The second part of the program evaluated the more successful bearing materials under conditions of actual use (ref. 204).

This program evaluated two proprietary materials, hot-pressed alumina and plasma-arc sprayed Al_2O_3 on a beryllium substrate. One proprietary bearing was a fine-grain, high-purity alumina made by powder compaction at room temperature followed by sintering at very high temperatures. The other was 90% alumina, 2% tungsten, and 8% fluxing agent yielding a higher density than pure Al_2O_3 with no internal voids. The hot-pressed alumina was made from 120- to 200-micron powders and had a final density of 98% theoretical. The plasma-arc sprayed material consisted of a 0.015-in. thick layer of 97% alumina-3% binder on a special beryllium substrate. Another sample was made from hot-pressed beryllium oxide. It had an irregular grain structure and large internal voids.

The tests consisted of roughness measurements, interferometry, and other surface-measurement procedures including electron microscopy. Friction and wear characteristics were measured with flat thrust-washer type specimens set up to simulate actual use. The variables were bearing stress, contact velocities, temperature, running time, and environment. Conditions causing bottoming were induced into these tests and the coefficient of friction was determined. Any damage observed was also analyzed. The more promising materials were further tested with new machining techniques designed to give extremely smooth surfaces.

Normally, ceramic surfaces have pits caused by the pullout of grains during the finishing operation. Also, voids in the matrix of the material are exposed so there is more surface roughness. An

experimental finishing technique started with surface grinding with a 400 grit to a flatness of 0.0001 in., followed by applying a 1200-grit diamond wheel, and then free abrasive machining with boron carbide particles. A 12-in. steel wheel rotating at 60 rpm was used. The specimen was mounted on a 4-in. base-plate rotating at 240 rpm and in contact with the wheel at a radius of 4 inches. Abrasive particles suspended in a suitable vehicle were periodically fed onto the specimen as it was being ground. A series of 400-, 600-, 800-, and 1000-grit sizes were used to create 2-microinch surfaces described as the ultimate in surface finishes for a ceramic.

The results of this program are summarized in table XXV. They primarily show that pressed and sintered alumina, 90 alumina-2 tungsten-8 flux, and plasma-arc deposited alumina are the most promising materials for use in high-speed bearings. Damage to surfaces during bottoming occurs more frequently on surfaces having well defined pits. The resurfacing techniques described here definitely reduced the possibility of damage. Damage also was always associated with an increase in the coefficient of friction while the other variables such as velocity, temperature, humidity, and normal force seemed to have little effect.

NUCLEAR MATERIALS

NASA's interest in nuclear power is directed towards two goals: nuclear rocket propulsion and space-station power generation. Of these, the nuclear rocket has received the most attention. The Atomic Energy Commission and the U.S. Air Force started research on this program at Los Alamos Scientific Laboratory in 1955. NASA joined the effort in 1960 with the establishment of a joint AEC-NASA office, the Space Nuclear Propulsion Office. The program was given the acronym NERVA (Nuclear Engine for Rocket Vehicle Application). Since that time, a series of successful nuclear engines have been built and tested. The most probable outcome of this program will be a nuclear-rocket third stage atop the first two stages of the Saturn V. A 65% gain in lunar payload can be expected over that available with the currently used chemical rockets. For other planned missions, such as the Mars Orbiter, the Jupiter-Saturn Flybys and the Solar Probe, the payloads could be increased even more. Orbital missions using nuclear engines would include the movement of large payloads from one orbit to another, such as in the case of reusable ferries plying between a low Earth orbit and a lunar orbit.

The nuclear rocket engine is essentially an adaptation of the

TABLE XXV.—*Properties of Sintered Ceramic Gas-Bearing Surfaces (ref. 203)*

	Coefficient of friction	Resistance to damage	Debris particles	Start-stop	Bottoming	Machinability	Dimensional stability	Density, g/cc
Hot Pressed and sintered Al_2O_3	Low	Good	Yes	Good	Poor	Good	Good	3.98
90% Al_2O_3, 2% W, 8% flux	Low	Excellent	No	Good	Good	Good	Good	4.15
Hot-Pressed Al_2O_3	High	Poor	Yes	Medium	Good	Medium	Poor	3.93
Plasma-Arc deposited Al_2O_3	Low	Good	Yes	Good	Medium	Medium	Medium	1.85(Be)
BeO	Medium	Good	No	---	---	Toxic	Poor	2.90

liquid-propellant rocket engine with the combustion chamber replaced by the nuclear reactor. The temperature required to expand the liquid propellant into a large volume of gas for propulsion is provided by the reactor core, so no actual combustion takes place. The fuel used for the engine is liquid hydrogen because it yields the highest specific impulse of any propellant at a given temperature. The specific inpulse for any fuel is the technical term for the velocity of the exhaust of a rocket engine. The higher the specific impulse, the greater the payload that can be carried. It is proportional to $(T/MW)^{\frac{1}{2}}$ where T is the operating temperature and MW the molecular weight of the exhaust gas. Hydrogen's molecular weight of 2 makes it vastly superior to chemical rockets where the combustion product might be H_2O ($MW=18$) or HF ($MW=20$). The use of this system will potentially allow payloads to be doubled over those borne by conventional rockets.

The environment in the nuclear rocket is probably more severe than in any other system built by man. The temperatures in the engine range from $-423°$ F to almost 4500° F. Intense radiation and the high vacuum of space are also present. Many unique manufacturing and materials developments have been required by this program, and powder metallurgy has played an important role. It has been applied to the manufacture of the fuel elements, the control materials, and the high-temperature supporting materials.

The operation of the nuclear engine consists of the flow of propellant from a tank through turbopumps that boost the pressure from 30 psi to approximately 1200 psi. This pressurized flow of the propellant is fed through the rocket nozzle and the nuclear reflector where it serves as a regenerative coolant. It then passes through the turbines which drive the turbopumps, through internal radiation shield, and finally through the reactor core where its temperature is increased to approximately 4250° F. The acceleration of this hot gas through the nozzle provides the thrust to the engine. A cutaway drawing of the NERVA engine is shown in figure 65.

The fuel elements being used currently are composites of discrete particles of fissionable ceramic embedded in a graphite matrix (ref. 205). Uranium, enriched with U–235 to the maximum capacity of the gaseous diffusion plant (about 92%) and converted to uranium carbide (UC_2), forms the starting material for the fuel. Free UC_2 forms low-melting eutectics with the refractory materials used in the fuel elements that would weaken the structural strength; consequently, the Atomic Energy Commission

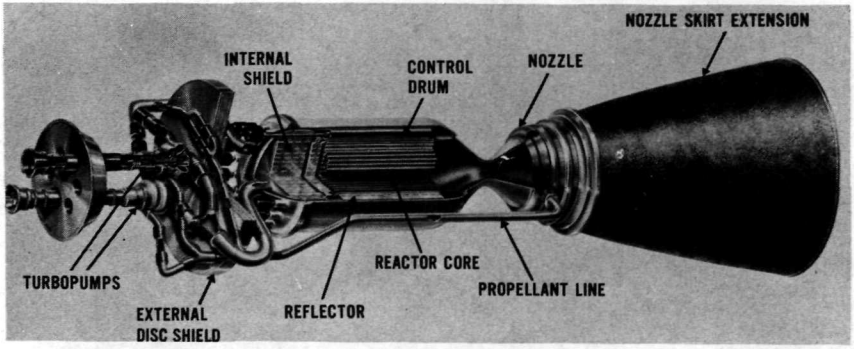

FIGURE 65.—NERVA engine.

has developed coated, spheroidized UC_2 particles (refs. 206 and 207). The fine, uniform sizes of these particles are shown in figure 66. They are prepared in fluidized beds by the pyrolytic decomposition of hydrocarbons such as acetylene or methane. Temperatures as high as 1900° C are used, but careful control of flow rates, temperatures, and contact times is necessary to regulate the density and structure of the coating. The precision and flexibility that has been developed is exemplified in figure 67 (ref. 208). Here, a triple-layered coating has been applied to a UC_2 particle for use in an experimental ultrahigh-temperature reactor. The inner layer is relatively porous to absorb the high-temperature swelling of the UC_2. The outer layer is very dense, serving to seal the particles and contain the fission gases, while the middle layer acts as a buffer between the two, preventing crack propagation (ref. 208).

Graphite is used as the matrix of the fuel elements because of its high-sublimation temperature, strength-to-weight ratio, and thermal-stress resistance. It is also an efficient neutron moderator. The chief drawback of graphite is hydrogen corrosion which occurs at high temperatures, forming methane or acetylene. This cannot be tolerated in the operating times of 1 hr or longer, which are expected from these engines, so refractory-cladding materials have been developed to separate the graphite matrices from the hydrogen stream.

Present fuel-element construction starts with spherical UC_2 particles coated with sufficient graphite to yield the correct proportion of fuel to the matrix in the final element. These are extruded into hexagonal rods about 0.75 in. across the flats and about 4 ft long, and containing 19 axial-flow channels. Careful oven curing and precision machining follow. UC_2 exposed by the

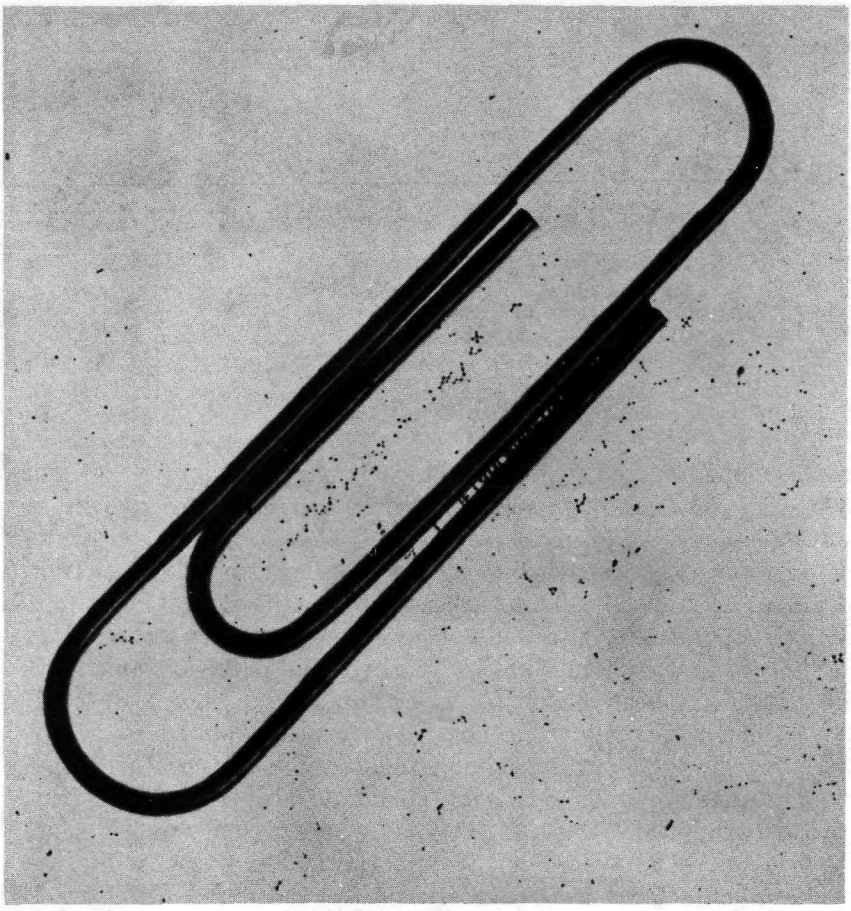

FIGURE 66.—Graphite-coated, spheroidized uranium carbide particles (ref. 205).

machining is leached away by gaseous HCl, and a refractory coating is applied.

Coating is accomplished in an apparatus similar to that in figure 68. Niobium pentachloride or zirconium tetrachloride are reduced under high temperatures by carbon to niobium or zirconium carbides. The system includes a vaporizer in which hot argon becomes saturated with the vapors of the molten salt, an induction-heated furnace containing the fuel elements where the reduction and coating takes place, and a trap for the unreacted vapors. The precise control of the temperature along the entire length of the fuel element is necessary, so a series of sight ports are lo-

FIGURE 67.—Photomicrograph (500X) of a triple-layered fuel particle (ref. 208).

cated along the axis of the apparatus for measuring optical temperature.

After coating, the rods are subjected to a series of rigorous nondestructive tests before being assembled into the final reactor core. These tests include electrical resistivity, coating thickness, dimensions, uranium content, hole location, air impedance, porosity, radiographic thickness, and density. Each rod has a serial

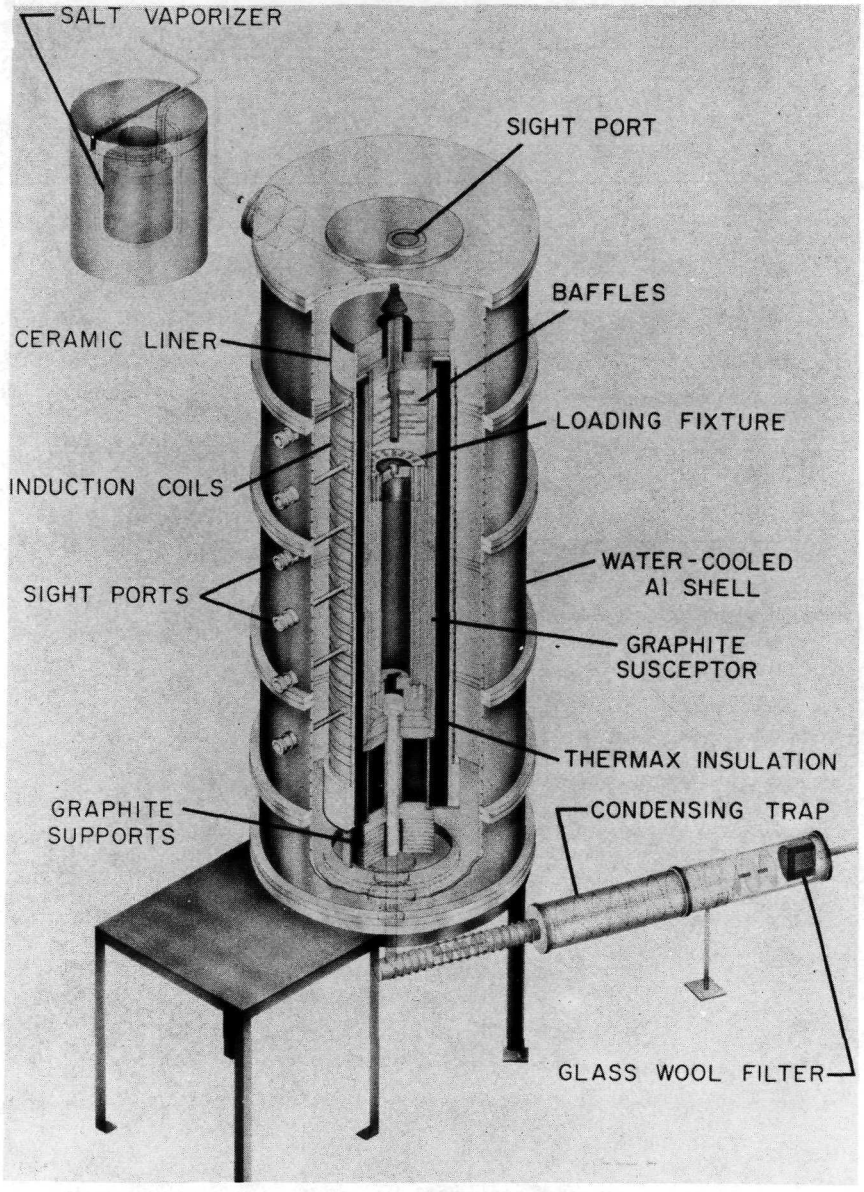

FIGURE 68.—Fuel-element coating apparatus (ref. 205).

number placed on it immediately after its initial extrusion, so that flaws can be traced back to the step where they were introduced.

The finished hexagonal fuel rods are assembled into groups of

six surrounding a tie rod. These assemblies are then packed together to form the final reactor core which must be anchored in the rocket engine to withstand the force of the flowing hydrogen. This can be done either at the cool end or the hot end. Devices screwed into the coolant holes at the cool end of the core to "hang" the elements are of questionable reliability, however, because of the brittle nature of the graphite matrix. Support from the lower end is preferred and can be accomplished by the use of cooled tie rods with refractory hot-end support.

NASA has devoted considerable efforts to developing stable high-temperature materials for such applications as the core support for the nuclear rocket (refs. 209 to 215). These materials must withstand an environment of high temperature and hot hydrogen, and those most suitable for this purpose have been refractory carbide-graphite composites. These materials comprise graphite mixed with either a single carbide or a solid solution of two or more carbides, fabricated by hot pressing. Attack by hot hydrogen is still a problem, since free carbon is present and coatings are required. The principal advantage of coated composites over coated graphite is the excellent adherence of a niobium carbide or zirconium carbide coating. These composites can withstand many cycles of reactor operation with corrosion well below that of coated graphite.

Composites of niobium carbide with graphite and a solid solution of niobium and tantalum carbides with graphite have been manufactured and tested in reactors (ref. 216). The manufacturing process starts with a mixture of refractory carbide powder and graphite flour which is loaded into an induction-heated die for vacuum hot pressing (fig. 69). The die is flushed with argon and heated to about 3000° C. A pressure of 3200 psi is gradually applied and held for 10 min. The system is then allowed to cool under atmospheric pressure. Machining of the resultant billet must be done with diamond tooling because of the hardness of the material. Ultrasonic machining has also been successfully applied. Coating is accomplished and rigorous inspection is made in the same manner as that for the fuel elements.

A nuclear reflector assembled after the machining of the individual segments is shown in figure 70 (ref. 217). The 12 large holes are for the fission-control drums while the smaller ones are coolant ducts and bolt holes. The nuclear reflector surrounds the core of the NERVA engine and reduces the number of neutrons leaking from the core. Beryllium is the best material for this purpose because of its very low atomic weight and its capacity to reflect neutrons back into the core of the reactor. This enables the

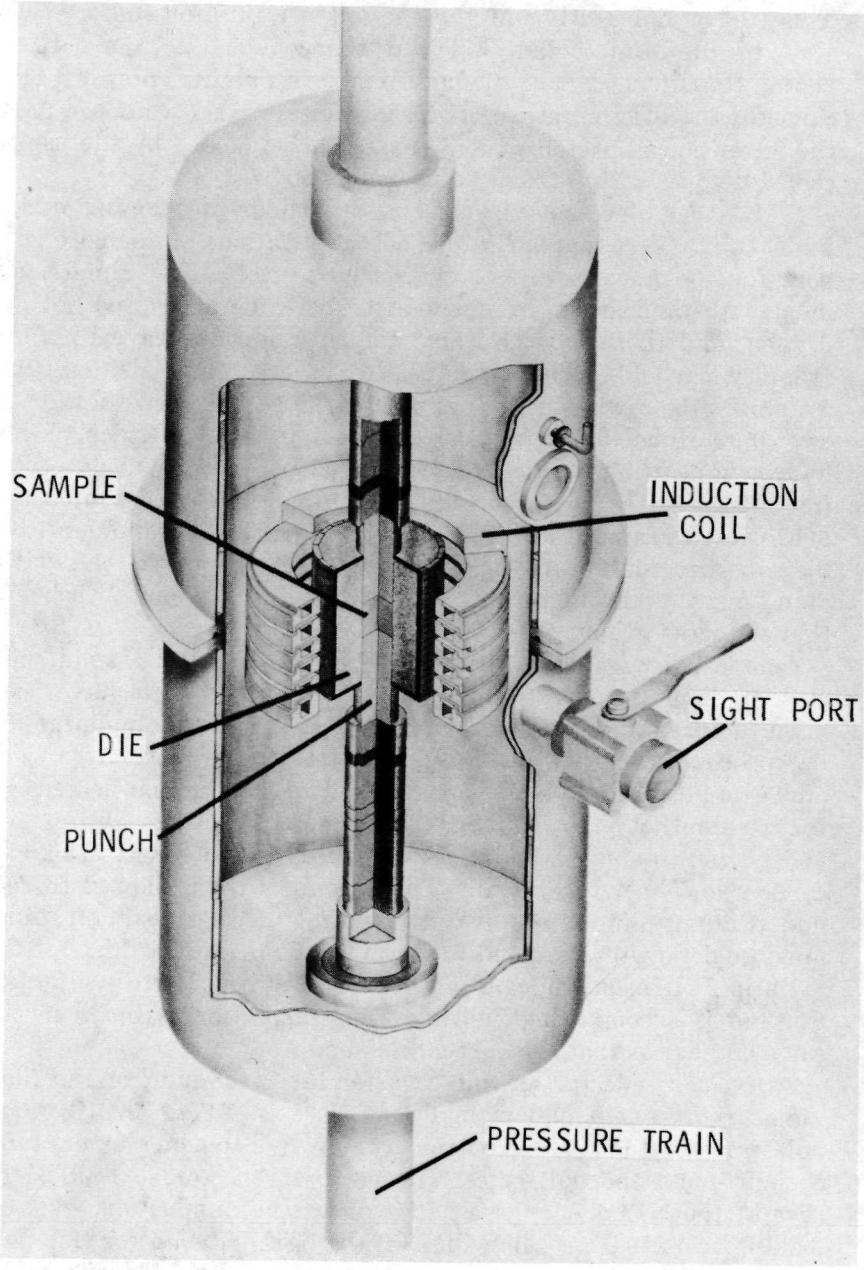

FIGURE 69.—Vacuum hot-pressing apparatus at Los Alamos (ref. 205).

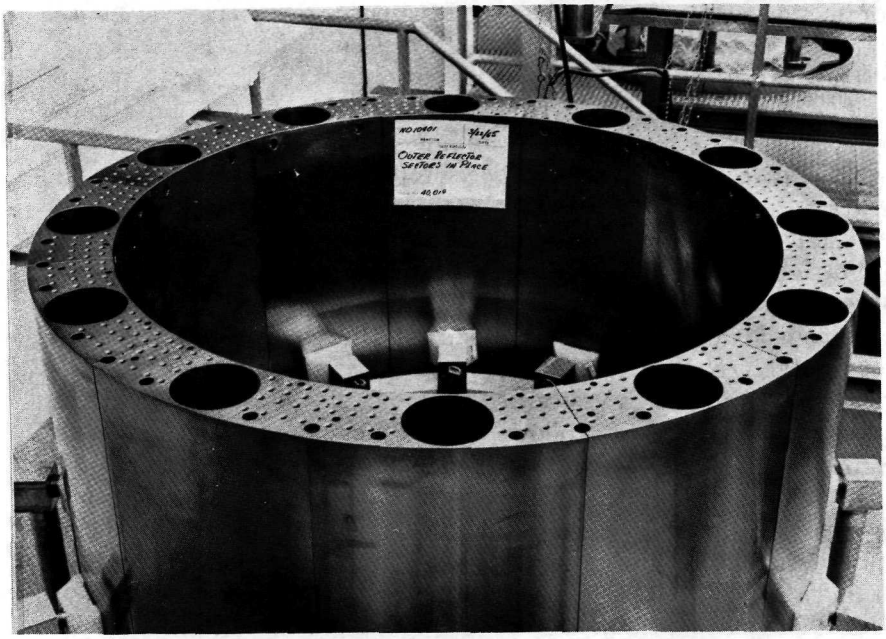

FIGURE 70.—Reflector for nuclear rocket core (ref. 217).

core size and the amount of critical fuel required to be reduced substantially. In the earlier reactors, this reflector was made up of twelve 30° sectors as shown in figure 70. In the more recent reactors, the reflectors have been made up of rings instead of sectors. In either case, titanium bolts hold the pieces together.

The entire field of beryllium metallurgy has been thoroughly considered in the manufacture of these parts. Large, homogeneous hot-pressed blocks are required. These must be sawed into uniform blanks in which large holes are drilled. Special precautions must be taken to collect all the dust produced because of its toxicity. Carbide-tipped tooling is used for all machining, and extreme precision is exercised in the formation of the final part. Finishing cuts are done in decreasing depths to reduce surface flaws to a minimum; the final cut does not exceed 0.005 in. in depth.

Twelve to eighteen fission-control drums are mounted in the reflector to increase or decrease the activity of the reactor core. One hundred and twenty degrees of the surface of each drum contains a nuclear "poison". When these surfaces are rotated towards the core, neutrons are absorbed by the poison and the reac-

tor is slowed down. Any desired irradiation level may be maintained by the amount of control surface close to the core.

The poison material used in the first few reactor tests was a commercial product made from boron carbide (B_4C) and aluminum by powder metallurgy techniques. The boron was specially processed to be high in the B^{10} isotope, which is a very strong neutron absorber, but which also is very expensive. To replace this, Los Alamos developed a material using boron carbide made from natural boron dispersed in a copper matrix (ref. 218). A higher percentage of boron was required to compensate for the diminished amount of B^{10} isotope, but the overall material was considerably cheaper and more uniform in composition. The fabrication techniques investigated included hot pressing and cold pressing with sintering followed by coining. Both materials were canned in steel, hot-rolled, and annealed before testing. The best composition for this material proved to be a mixture of fine copper powder and 15%-by-weight-B_4C powder which had been spheroidized in a plasma arc. These were mixed and hot-pressed at 950° C and 2200 psi to give a 98.5%-dense composite material. The billet was then canned and rolled to a 0.100-in. thick sheet.

High-temperature nuclear reactors are also being designed by NASA as power generation units for space stations and rockets. These impose the added requirement on the fuel matrix of low weight and structural support. For this purpose, considerable interest has been given to tungsten. Cermets containing from 20% to 50% by volume uranium dioxide in tungsten and clad with pure tungsten have been made and tested on an experimental basis (ref. 219).

The primary goal in the preparation of these composites is preventing agglomeration of the UO_2 particle. Both the mechanical and the nuclear properties of the final fuel elements are seriously affected when this happens, so a technique of rolling tungsten-coated particles was developed by NASA. UO_2 particles of 50 microns are coated with tungsten hexachloride in a fluidized bed reactor. The coated particles are then canned and formed into dense cermet plates by hot-roll compaction. After they are shaped into the desired form, the compacts are clean-annealed in hydrogen at 1350° C and then clad by vapor deposition of tungsten.

The quest for lighter-weight reactor materials for space power generation has led to the development of uranium nitride (UN) (ref. 220) and molten uranium (ref. 221) as reactor fuels. Both these materials provide a higher uranium density than UO_2, but on the other hand, they also create more problems as far as cladding and containment are concerned. The chief problem is corro-

sive attack by free uranium at elevated temperatures (ref. 222). The properties of several uranium compounds are summarized in table XXVI.

In addition to having a higher uranium concentration than UO_2, UN also has a higher thermal conductivity and a lower thermal expansivity. It has good chemical compatibility with reactor coolant materials such as lithium, a relatively high melting point (2850° C), and good dimensional stability during irradiation. At high temperatures, however, UN will decompose into nitrogen and uranium. At 1400° C, the effect is minimal; but, at higher temperatures, serious problems may develop since the free uranium will attack cladding metals such as tungsten and molybdenum. This type of corrosion, first reported by McIntosh and Bagley in 1955 (ref. 222), occurs by intergranular penetration of uranium atoms into the supporting metal. One method of avoiding the problems is to use single-crystal tungsten which has no polycrystalline interfaces. Since molten uranium exhibits a 5° to 10° contact angle on tungsten at 1200° C, it "wets" extremely

TABLE XXVI.—*Physical Properties of Nuclear Fuels*

	Compound						
	U	UO_2	UC*	UC_2	UN	U_3Si	US
Compound density	19.1	10.96	13.63	11.28	14.32	15.58	10.87
Uranium density	19.1	9.6	12.97	9.95	13.6	14.99	9.7
Melting point °C	1133	2750	2400	2575	2850	1400	2450
Thermal conductivity (cal/sec/cm/°C) Measured at °C							
20	------	------	------	-----	------	0.036	-----
100	0.065	0.018	0.06	-----	0.033	------	-----
400	0.081	0.012	0.055	-----	0.04	------	-----
700	0.104	0.008	0.050	-----	0.05	------	-----
Thermal expansion in percent Measured at °C							
200	------	0.18	0.18	-----	0.18	------	-----
400	------	0.40	0.42	-----	0.35	------	-----
500	------	0.50	0.55	-----	0.48	------	-----
600	------	0.60	0.66	-----	0.55	------	-----
800	------	0.80	0.90	-----	0.73	------	-----
1000	------	1.03	1.12	-----	0.95	------	-----
1100	------	1.20	1.35	-----	1.12	------	-----
1200	------	------	------	-----	1.50	------	-----

* Contains 5% C.

well (ref. 218). This means that, in time, molten uranium will seek out any flaws such as welds or microcracks and initiate corrosion there (ref. 221).

Desired porosity in cermet fuel elements is dependent on the amount of fuel burnup required in a reactor. Low burnups will permit containment of fission gases by high-strength, dense cermet fuels, but high burnups require substantial fuel porosity to vent gases and prevent swelling. The purpose of a project by Takkunen (ref. 221) was to specify and fabricate W–UN and Mo–UN cermets for use as fuels. Two fabrication processes were used to produce W–UN and Mo–UN cermets with densities ranging between 80% and 100% of theoretical and fuel loadings of 50% to 70% UN, which are required in reactor applications. The processes were (1) cold pressing and sintering of powder mixtures and (2) hot isostatic consolidation of metal-coated UN particles. The latter gave excellent fuel distribution and allowed higher fuel loadings, but the conventional press and sinter technique is the simplest and cheapest method and also allows for the greatest degree of variation in the porosity. In all samples, no chemical reactions were found to take place between UN and either tungsten or molybdenum at temperatures up to 2200° C, provided that nitrogen was present in the reactor atmosphere. When nitrogen is not present, liquid-phase sintering with molten uranium takes place.

References

1. ANON.: Höganäs Iron Powder Handbook. Höganäs-Billesholms AB, Höganäs, Sweden, 1958.
2. QUATINETZ, MAX; SCHAFER, ROBERT J.; AND SMEAL, CHARLES: The Production of Submicron Metal Powder by Ball Milling with Grinding Aides. Trans. AIME, vol. 221, no. 12, Dec. 1961, pp. 1105–1110.
3. ARIAS, ALAN: The Release of Hydrogen on Ball Milling Chromium in Water. NASA TN D–4569, 1968.
4. ARIAS, ALAN: The Role of Chemical Reactions in the Mechanism of Comminution of Ductile Metals into Ultrafine Powders by Grinding. NASA TN D–4862, 1968.
5. HABASI, F.; MURRY, R.J.; TOIVONEN, R.W.; GRIFFITH, V.; AND HANSON, G.T.: Ultrafine Beryllium Powder by the Amalgam Process. NASA CR–84116, 1966.
6. ARIAS, ALAN: Chromium and Nickel Powders Made by Reduction of Their Oxides With Magnesium, Lithium, or Sodium Vapors. NASA TN D–4714, 1968.
7. CHENEY, R.F.; AND SCHEITHAUER, W., JR.: Development of Cobalt-Base Dispersion Strengthened Alloys. NASA CR–54599, 1968.
8. NOEL, D.O.; SHAW, J.D.; AND GEBERT, E.B.: Production and Some Testing Methods of Metal Powders. Trans. AIME, vol. 128, 1938, p. 37.
9. OLBRICH, M.: Superfine Grinding of Metal Powders. Light Metals, vol. 7, 1944, p. 157.
10. WEETON, JOHN W.; AND QUATINETZ, MAX: Cleaning and Stabilization of Dispersion-Strengthened Materials. NASA TM X–52228, 1966.
11. DOUGLAS, A. DAVID: The Hydrogen Purification of Submicron Nickel Powder. NASA CR–54526, 1968.
12. ARIAS, ALAN: Feasibility of Producing Dispersion Strengthened Chromium by Ball-Milling in Hydrogen Halides. NASA TN D–4912, 1968.
13. NORRIS, L. FREDRICK; REINHARDT, GUSTAV; AND CREMENS, WALTER S.: Comparison of Selected Submicron Powder Blending Methods for Dispersion Alloys. NASA TN D–3834, 1967.
14. REINHARDT, GUSTAV; CREMENS, WALTER S.; AND WEETON, JOHN W.: Cold Consolidation of Metal Dispersoid Blends for Examination by Electron Microscopy. NASA TN D–3611, 1966.
15. REECE, ORVIL Y.: Explosive Bonding of Metal Matrix Composites. Paper presented at SAMPE Technical Conference (Seattle, Wash.), Sept. 1969.
16. WARD, ROBERT: Explosive Bonding Technique Emerging in NASA Plans. Metalworking News, Oct. 13, 1969, p. 27.
17. NOLAND, MICHAEL C.; GADBERRY, HOWARD M.; LOSER, JOHN B.; AND

SNEEGAS, ELDON C.: High-Velocity Metalworking. NASA SP–5062, 1967.

18. GRIPSHOVER, PAUL J.; AND HANES, HUGH D.: Porous Removable Mandrel, New Technology Disclosure. Battelle Memorial Inst., 1966.
19. ASHURST, A.N.; GOLDSTEIN, M.; AND RYAN, M.J.: Techniques for Fabricating Rocket Engine Components Containing Intricate Flow Channels. NASA CR–72588, 1969.
20. LEIPOLD, M.H.; AND NIELSEN, T.H.: Fabrication and Characterization of Hot-Isostatically Pressed Magnesium Oxide. NASA CR–88508, 1967.
21. HAUSNER, HENRY H.: Pressureless Compacting and Sintering Metal Powders. J. Metals, vol. 13, no. 10, Oct. 1961, pp. 752–758.
22. TOAZ, M.W.; DAVIES, G.F.; AND JOHNSON, R.D.: Production of Extrusion Billets of High Temperature Alloys by Powder Metallurgy. AD 253782, 1960.
23. HAUSNER, HENRY H.: Compacting and Sintering of Metal Powders Without the Application of Pressure. Agglomeration, W.A. Knepper, ed. Interscience (New York), 1962, pp. 55–91.
24. SULINSKI, HARRY V.; AND LIPSON, S.: Slip-Casting of Copper Powder. Modern Developments in Powder Metallurgy, Vol. 1, Henry H. Hausner, ed. Plenum Press (New York), 1966, pp. 266–177.
25. KURA, J.G.; BARTH, V.D.; SAFRANEK, W.H.; HALL, E.T.; MCCURDY, H.; AND MCINTIRE, H.O.: The Making of Nickel and Nickel Alloy Shapes by Casting, Powder Metallurgy, Electroforming, Chemical Vapor Deposition, and Metal Spraying. NASA TM X–53430, 1965.
26. KURA, J.G.; BARTH, V.D.; AND MCINTIRE, H.O.: Shaping of Precipitation Hardening Stainless Steels by Casting and Powder Metallurgy. NASA SP–5086.
27. FISCHER, G.W.; ET AL.: Complex Shapes by Slip Casting. General Electric Co. Rep. R65 FPD 185 (Air Force Materials Lab. TR–65–257).
28. PETRASEK, DONALD W.; SIGNORELLI, ROBERT A.; AND WEETON, JOHN W.: Refractory-Metal-Fiber Nickel-Base-Alloy Composites for use at High Temperatures. NASA TN D–4787, 1968.
29. DIENES, G.J.: Defects in Solids and Current Concepts of Radiation Effects. Effects of Radiation on Materials, Reinhold Pub. Corp. (New York), 1957, pp. 1–47.
30. HAUSNER, HENRY H.: Powder Metallurgy in Nuclear Reactor Construction. International Atomic Energy Agency (Vienna), 1961, p. 66.
31. WEHNER, G.K.: Investigation of Sputtering Effects on the Moon's Surface. NASA CR–88738, 1967.
32. CLARKIN, PHILIP A.; WEETON, JOHN W.; AND SIKORA, PAUL F.: Effects of Variations in Carbon Content, Heat Treatment, and Mechanical Working on the Stress-Rupture Properties of a Liquid-Phase-Sintered High-Temperature Alloy. Trans. AIME, vol. 224, no. 2, Feb. 1962, pp. 116–120.
33. GYORGAK, CHARLES A.: Extrusion at Temperatures Approaching 5000° F. NASA TN D–3014, 1965.
34. VILES, FREDERICK J., JR.; CHAMBERLIN, RICHARD I.; AND BOYLER, GEORGE W., JR.: Survey and Analysis of Health Hazards Resulting from Ultrafine Metal and Metal Oxide Powders. NASA CR–72492, 1966.

35. MOSS, R.G.: Review of Beryllium Technology for Spacecraft Applications. NASA CR–96319, 1967.
36. DUDAS, J.H.; AND DEAN, W.A.: The Production of Precision Aluminium Powder Metallurgy Parts. Light Metal Age, vol. 27, no. 5–6, June 1969, pp. 18–24.
37. ANON.: High Strength Sintered Aluminum Parts Arrive. Metalworking Production, vol. 113, no. 25, June 1969, p. 7.
38. CARMICHAEL, R.L.: Non Ferrous Metals and the Chemical Engineer, Part I: Titanium. Chemical Engineering, vol. 73, No. 1966, pp. 109–114.
39. BUNSHAH, R.F.; MARGOLIN, H.; AND CADOFF, I.B.: Titanium Powder Metallurgy. Precision Metal Molding, vol. 14, no. 4, May 1956, pp. 38–40.
40. DAVIES, G.F.: State of the Art for Titanium Powder Metallurgy. Precision Metal, vol. 26, no. 2, Feb. 1968, pp. 38–40.
41. TUFFIN, WILSON B.: Titanium Alloy Powders. Precision Metal, vol. 26, no. 2, Feb. 1968, pp. 31–32.
42. FRIEDMAN, GERALD: Properties of Powdered Titanium Alloys. NASA CR–72469, 1968.
43. FRIEDMAN, GERALD: Powder Metallurgy of Titanium. Lecture no. 12, New York Univ. Course in Titanium, Sept. 1969.
44. MURPHY, E.A.; HORNAK, M.B.; AND O'ROURKE, R.G.: Developing Technology to Forge Unclad Beryllium. U.S. Air Force Materials Lab. TR–65–30, 1965.
45. RUMMLER, D.R.: Mechanical Properties and Column Behavior of Thin-Wall Be-38A1 Alloy Tubing. NASA TN D–5145, 1969.
46. WILLIAMS, R.F.; AND INGELS, S.W.: Fabrication of Beryllium—A Survey of Current Technology. NASA TM X–53453, 1966.
47. JONES, G.H.; AND WOOD, C.M.: Fabrication of a Beryllium Test Panel. NASA TM X–53529, 1966.
48. ANON.: Beryllium Fabrication Methods Development Program: Thermal Treatment. NASA CR–61659, 1965.
49. LOWE, J.N.: Beryllium Technology. J. Brit. Interplanetary Soc., vol. 22, no. 5, May 1969, pp. 314–325.
50. ANON.: 2 Years Off, But Air Force Pushes for Beryllium. Metalworking News, Feb. 2, 1970, p. 16.
51. BOHMAN, G.; AND FUCHS, W.A.: Beryllium Box Beam Development Program. Fairchild Hiller Rept. FHR–3249, X66–19531, 1966.
52. GLACKEN, JAMES J.; GOWEN, EDWARD F., JR.; AND KEENEY, CORNELIUS J., JR.: Development of Fastener Technology for Beryllium Point Drive Bolts and Blind Fasteners. NASA CR–61236, 1968.
53. RUMMLER, DONALD R.; AND WICHOREK, GREGORY R.: Design, Fabrication, and Tests of Tubular Beryllium and BE-38Al Alloy Truss-Type Structures. NASA TN D–5254, 1969.
54. DEUTSCH, G.C.; AND AULT, G.M.: Powder Metallurgy Materials for Rockets, Missiles, and Space Vehicles. Pulvermetallurgie in der Atomkerntechnik, F. Benesovsky, ed. Metallwerk Plansee AG. (Reutte/Tirol). 1962.
55. CHARTERS, A.C.: A Preliminary Investigation of High Speed Impact: The Penetration of Small Spheres into Thick Copper Targets. NACA RM A–58 B26, 1958.

56. SUMMERS, J.L.: Investigation of High Speed Impact and Impact at Oblique Angles. NASA TN D–94, 1959.
57. DIERSING, R.J.; HANES, H.D.; AND HODGE, E.S.: Fabrication of Beryllium-Clad Tubular-Hypervelocity-Impact Targets by Gas-Pressure Bonding. NASA CR–54058, 1963.
58. DIERSING, R.J.; CARMICHAEL, D.D.; HANES, H.D.; AND HODGE, E.S.: Gas-Pressure Bonding of Stainless Steel-Reinforced Beryllium-Hypervelocity-Impact Targets. NASA CR–54222, 1964.
59. DACHS, LOUIS L.: Beryllium Disks Sop Up C–5A-Size Brake Heat Loads. Space/Aeronautics, vol. 51, no. 5, May 1969, pp. 88–90.
60. DACHS, LOUIS L.: What About Beryllium? Space/Aeronautics, vol. 49, no. 6, June 1968. pp. 70–78.
61. WALKER, P.: P/M Shipments Keeping Pace with '69; Capacity Rising. Metalworking News, vol. 11 (511), April 20, 1970, p. 4.
62. KURA, J.G.; BARTH, V.D.; HALL, E.T.; SAFRANEK, W.H.; AND MCINTIRE, H.O.: The Making of Stainless Steel Shapes by Casting and Powder Metallurgy. NASA TM X–53577, 1967.
63. FRECHE, JOHN C.; WATERS, WILLIAM J.; AND ASHBROOK, RICHARD L.: Evaluation of Two Nickel-Base Alloys, Alloy 713 C and NASA TAZ–8A, Produced by Extrusion of Prealloyed Powders. NASA TN D–5248, 1969.
64. WATERS, WILLIAM J.; and FRECHE, JOHN C.: A High Strength Nickel-Base Alloy with Improved Oxidation Resistance up to 2200°F. J. Eng. Power, vol. 90, no. 1, Jan. 1968, pp. 1–10.
65. CLARKIN, PHILIP A.; WEETON, JOHN W.; AND SIKORA, PAUL F.: Influence of Certain Composition and Fabrication Variables on the Stress-Rupture Properties of a Cobalt-Base Alloy Consolidated by Powder Metallurgy. NASA TN D–1221, 1962.
66. TRIFFLEMAN, BERNARD H.: Development of Procedures for Producing Dispersion Strengthened Cobalt Base Alloys by the Flash Drying Selective Reduction Process. NASA CR–54516, 1967.
67. GYORGAK, C.A.: Burst Testing of Tungsten Tubing at Temperatures from 3000° to 4500° F (1650° to 2480° C). NASA TM X–1843, 1969.
68. MCINTYRE, RULUFF D.: Tungsten-Nickel-Copper Ternary Alloys for High-Temperature Applications. NASA TN D–3015, 1965.
69. HALL, ROBERT W.; AND SIKORA, PAUL F.: Tensile Properties of Molybdenum and Tungsten from 2500° to 3700° F. NASA Memo 3–9–59E, 1959.
70. SIKORA, PAUL F.; AND HALL, ROBERT W.: High-Temperature Tensile Properties of Wrought Sintered Tungsten. NASA TN D–79, 1959.
71. SIKORA, PAUL F.; AND HALL, ROBERT W.: Effect of Strain Rate on Mechanical Properties of Wrought Sintered Tungsten at Temperatures Above 2500°F. NASA TN D–1094, 1961.
72. TAYLOR, J.L.; AND BOONE, DONALD H.: Tensile Properties of Tungsten from 2500 to 5400° F in Vacuum. Trans. Quart., vol. 56, no. 3, Sept. 1963, pp. 643–655.
73. BURNETT, Paul L.; AND JENSEN, GERALD A.: Some Effects of Tungsten Powders on Plasma-Sprayed and Sintered Structures. Paper presented at ASD-NASA Refractory Composites Working Group Meeting (Dayton, O.), June 1962.
74. MILLS, R.G.; LINDGREN, J.R.; AND WEINBERG, A.F.: An Evaluation of Vapor-Deposited Tungsten Tubing. NASA CR–54277, 1964.

75. SCHMIDT, F.S.; AND OGDEN, H.R.: The Engineering Properties of Tungsten and Tungsten Alloys. Rept. DMIC 191, Battelle Memorial Institute Sept. 1963.

76. SIKORA, PAUL F.: High-Temperature Tensile and Stress-Rupture Properties of Some Alloys in the Tungsten-Molybdenum System. NASA TN D–1087, 1962.

77. FOYLE, FRED A.; MCDONALD, GLEN E.; AND SAUNDERS, NEAL T.: Initial Investigation of Arc-Melting and Extrusion of Tungsten. NASA TN D–269, 1960.

78. HERBELL, THOMAS P.; HOFFMAN, CHARLES A.; AND WEETON, JOHN W.: Effect of Cladding on Extrudability and Properties of Powder Metallurgy Tungsten. NASA TN D–3941, 1967.

79. KLOPP, WILLIAM D.; AND RAFFO, PETER L.: Effects of Purity and Structure on Recrystallization, Grain Growth, Ductility, Tensile, and Creep Properties of Arc-Melted Tungsten. NASA TN D–2503, 1964.

80. RAFFO, PETER L.; AND KLOPP, WILLIAM D.: Mechanical Properties of Solid-Solution and Carbide-Strengthened Arc-Melted Tungsten Alloys. NASA TN–3248, 1966.

81. RUBENSTEIN, L.S.: Effects of Composition and Heat Treatment on High-Temperature Strength of Arc-Melted Tungsten-Hafnium-Carbon Alloys. NASA TN D–4379, 1968.

82. KLOPP, WILLIAM D; AND WITZKE, WALTER R.: Mechanical Properties of Arc-Melted Tungsten-Rhenium-Hafnium-Carbon Alloys. NASA TN D–5348, 1969.

83. RAFFO, PETER L.: Exploratory Study of Mechanical Properties and Heat–Treatment of Molybdenum-Hafnium-Carbon Alloys. NASA TN D–5025, 1969.

84. RAFFO, PETER L.: Thermomechanical Processing of Molybdenum-Hafnium-Carbon Alloys. NASA TN D–5645, 1970.

85. LESSMANN, G.G.: The Comparative Weldability of Refractory Metal Alloys. Welding Research Supplement, Welding Journal, vol. 45, no. 12, Dec. 1966, pp. 540s–560s.

86. MOORE, T.J.; AND WATSON, G.K.: Evaluation of Welding Techniques for Tungsten–Uranium Dioxide Composites. NASA TM X–1405, 1967.

87. JAPKA, J.E.; AND GORDON, E.: Joining of Tungsten-Uranium Dioxide Composites by Gas Tungsten-Arc Brazing. NASA CR–54841, 1966.

88. MOORE, T.J.; AND ADAMS, D.W.: A Procedure for Furnace Brazing Butt Joints in Tungsten-Uranium Dioxide Cermet Cylinders at 3000° C. NASA TM X–1815, 1969.

89. CRISCIONE, J.M.; REXER, J.; AND FENISH, R.G.: High-Temperature Protective Coatings for Refractory Metals. NASA CR–74327, 1965.

90. REXER, J.: High-Temperature Protective Coatings for Refractory Metals. NASA CR–95569, 1968.

91. STETSON, A.R.; AND WIMBER, R.T.: Slurry Applied Duplex Coatings for Tantalum and Columbium Alloys. Paper presented at the 13th Meeting of the Refractory Composites Working Group (Seattle, Wash.), July 1967.

92. SHOEMAKER, H.E.; AND STETSON, A.R.: Silicide Coatings for Tantalum and Columbium Alloys. NASA CR–72519, 1968.

93. ANON.: The Promise of Composites. Materials in Design Engineering, Sept., 1963, pp. 79–126.

94. THRUSH, PAUL W.: A Dictionary of Mining, Mineral, and Related Terms. U.S. Department of the Interior, 1968.
95. IRMANN, R.: Sintered Aluminum with High-Temperature Characteristics. Tech. Rundschau, vol. 19, 1949, pp. 1–4.
96. ZEERLEDER, A.V.: Über Sintern Aluminum Legierungen. Zeitschrift Für Metallkunde, vol. 41, 1970, pp. 228–231.
97. ANSELL, G.S.: Proposed Mechanism for the Strengthening of Sintered-Aluminum-Powder-Type Alloys. Trans. AIME, vol. 215, 1959, pp. 249–250.
98. GRANT, N.J.; AND PRESTON, O.: Dispersed Hard Particle Strengthening of Metals. Trans, AIME, vol. 209, 1957, p. 349.
99. CREMENŞ, WALTER S.: Use of Submicron Metal and Nonmetal Powders for Dispersion Strengthened Alloys. Ultrafine Particles, W.E. Kuhn, ed., John Wiley & Sons, Inc., 1963, pp. 457–478.
100. BRUCKART, W.L.; CRAIGHEAD, C.M.; AND JAFFEE, R.I.: WADC Tech. Rep. 54–398, Jan. 1955.
101. ZWILSKY, K.M.; AND GRANT, N.J.: Copper-Silica and Copper-Alumina Alloys of High-Temperature Interest. Trans. AIME, vol. 209, 1957, p. 1197.
102. GRANT, NICHOLAS J.: Oxide-Dispersion Strengthened Alloys, NASA SP–143, 1967.
103. MANNING, C.R., JR.; ROYSTER, R.M.; AND BRASKI, D.N.: An Investigation of a New Nickel Alloy Strengthened by Dispersed Thoria. NASA TN D–1944, 1963.
104. SCHAFER, ROBERT J.; QUATINETZ, MAX; AND WEETON, JOHN W.: Strength and High-Temperature Stability of Dispersion Strengthened Nickel–MgO Alloys. Trans. AIME, vol. 221, 1961, pp. 1099–1104.
105. ANSELL, G.S.; AND ARNOLD, P.E.: Internal Friction Behavior of an Aluminum-Aluminum-Oxide SAP-Type Alloy. Trans. AIME, vol. 221, Feb. 1961, pp. 206–207.
106. CREMENS, WALTER S.: PhD Thesis, MIT, 1957.
107. QUATINETZ, MAX; SCHAFER, ROBERT J.; AND SMEAL, CHARLES R.: The Production of Submicron Metal Powders by Ball Milling with Grinding Aids. Ultrafine Particles, W.E. Kuhn, ed., John Wiley & Sons, Inc., 1963, pp. 271–296.
108. WILCOX, B.A.; AND CLAUER, A.H.: High-Temperature Dispersion-Strengthened Nickel Alloys. NASA CR–72367, 1968.
109. NELSON, R.C.; AND WIDMER, R.: Development of Dispersion-Strengthened Nickel-Molybdenum, Nonoxidation Resistant Alloys. NASA CR–85779, 1966.
110. RASMUSSEN, J.R.; AND GRANT, N.J.: Thoria Dispersion-Strengthened Nickel and Nickel-Molybdenum Alloys Produced by Selective Reduction. Powder Metallurgy. no. 15, vol. 8, 1965.
111. MCCULLOUGH, H.M.; AND ORTNER: Development of a Dispersion-Strengthened Nickel-Base Alloy Using the High-Intensity Arc Process. NASA CR–85780, 1967.
112. ANON.: The Development of Dispersion-Strengthened Nickel-Base Corrosion-Resistant Alloys. NASA CR–54580, 1967.
113. HILL, V.L.; MISRA, S.K.; AND WHEATON, H.L.: Development of Ductile Claddings for Dispersion-Strengthened Nickel-Base Alloys. NASA CR–72522, 1967.

114. SAMA, L.; LAWTHERS, D.D.; AND PEPINO, G.T.: Development of Ductile Claddings for TD-Nickel Turbine-Vane Applications. NASA CR–72521, 1968.

115. SIMS, C.T.: The Case for Chromium. J. Metals, vol. 15, no. 2, Feb. 1963, pp. 127–132.

116. GRANT, NICHOLAS J.: Research on Mechanisms of Alloy Strengthening. NASA CR–95871, 1968.

117. SCRUGGS, DAVID M.: Modified Chromium for Unprotected Structures. ARS Journal, vol. 31, no. 11, Nov. 1961, pp. 1527–1533.

118. KLOPP, WILLIAM D.: Recent Developments in Chromium and Chromium Alloys. NASA TM X–1867, 1969.

119. ABRAMS, E.F.; ALEXANDER, J.A.; SHAVER, R.G.; AND WITHERS, J.C.: The Development of Dispersion-Strengthened Chromium Alloys. NASA CR–54610, 1967.

120. WAKEFIELD, GENE F; AND HUMPHRIES, RICHARD D.: Determining Feasibility of Chemical Vapor Deposition Process for the Production of Dispersoid-Strengthened Chromium Alloys. NASA CR–72448, 1968.

121. ALLEN, R.E.: Dispersion-Strengthened Chromium Alloys. NASA CR–54491, 1969.

122. ALLEN, B.C.; MAYKUTH, D.J.; AND JAFFEE, R.I.: The Recrystallization and Ductile-Brittle Transition Behavior of Tungsten. J. Inst. Metals, vol. 90, 1961.

123. RATLIFF, J.L.; MAYKUTH, D.J.; OGDEN, H.R.; AND JAFFEE, R.I.: Tungsten-Sheet Alloys with Improved Low-Temperature Ductility. Trans. AIME, vol. 230, 1964, pp. 490–500.

124. HERBELL, THOMAS P.; WEETON, JOHN W.; AND QUATINETZ, MAX: Structure and Properties of Tungsten-Base Powder Metallurgy Composites. NASA TN D–3610, 1966.

125. KING, GEORGE W.: An Investigation of the Yield Strength of a Dispersion-Hardened W-3.8 vol % ThO_2 Alloy. Trans. AIME, vol. 245, Jan. 1969, pp. 83–89.

126. GRANT, NICHOLAS J.: Research on Mechanisms of Alloy Strengthening. NASA CR–82972, 1966.

127. GRANT, NICHOLAS J.: Research on Mechanisms of Alloy Strengthening. NASA CR–93409, 1967.

128. GRANT, NICHOLAS J.: Research on Mechanisms of Alloy Strengthening. NASA CR–87992, 1967.

129. GRANT, NICHOLAS J.: Dispersion Strengthening. Proceedings of the 12th Sagamore Army Materials Research Conference, Syracuse Univ. Press, 1966.

130. KORMAN, SAMUEL: Some New Metal and Metal-Ceramic Composites. NASA SP–5060, 1966.

131. JECH, ROBERT W.; MCDANELS, DAVID L.; AND WEETON, JOHN W.: Fiber-Reinforced Metallic Composites. Paper presented at the 6th Sagamore Ordnance Materials Research Conference on Composite Materials and Composite Structures, Aug. 1959.

132. MCDANELS, DAVID L.; JECH, ROBERT W.; AND WEETON, JOHN W.: Metals Reinforced with Fibers. Metal Progress, vol. 78, no. 12, Dec. 1960, pp. 118–121.

133. MCDANELS, DAVID L.; JECH, ROBERT W.; AND WEETON, JOHN W.: Stress-Strain Behavior of Tungsten-Fiber-Reinforced Copper Composites. NASA TN D–1881, 1963.

134. PETRASEK, DONALD W.; AND WEETON, JOHN W.: Alloying Effects on Tungsten-Fiber-Reinforced Copper Alloy or High Temperature Alloy Matrix Composites. NASA TN D–1568, 1963.

135. PETRASEK, DONALD W.; AND WEETON, JOHN W.: Effects of Alloying on Room-Temperature Tensile Properties of Tungsten-Fiber Reinforced Copper-Alloy Composites. Trans. AIME, vol. 230, Aug. 1964, pp. 977–990.

136. WEETON, JOHN W., AND SIGNORELLI, ROBERT A.: Fiber-Metal Composite Materials. NASA TN D–3530, 1966.

137. PETRASEK, DONALD W.; SIGNORELLI, ROBERT A.; AND WEETON, JOHN W.: Metallurgical and Geometrical Factors Affecting Elevated Temperature-Tensile Properties of Discontinuous-Fiber Composites. NASA TN D–3886, 1966.

138. WEETON, JOHN W.; AND SIGNORELLI, ROBERT A.: Fiber Reinforced Metal Composites under Study at Lewis Research Center. Paper presented at the 14th Refractory Composite Working Group Meeting, Wright-Patterson Air Force Base, O., May, 1968.

139. JECH, ROBERT W.; AND SIGNORELLI, ROBERT A.: The Effect of Interfiber Distance and Temperature on the Critical Aspect Ratio in Composites. NASA TN D–4548, 1968.

140. STOWELL, E.Z.; AND LIU, T.S.: On the Mechanical Behavior of Fiber-Reinforced Crystalline Materials. J. Mech. Phys. Solids, vol 9, no 4, 1961, pp 242–260.

141. DAVIS, G.L.: Recrystallization of Tungsten Wires. Mettalurgia, vol. 58, Oct. 1958, pp. 177–184.

142. SEDLATSCHEK, K; AND THOMAS, D.A.: The Effect of Surface Treatment on the Mechanical Properties of Tungsten. Powder Metallurgy Bulletin, vol. 8, no. 1–2, June 1957, pp. 35–40.

143. STEPHENS, JOSEPH R.: Effect of Oxygen on Mechanical Properties of Tungsten. NASA TN D–1581, 1963.

144. THOMAS, B.: Embrittlement of Tungsten Wires. Nature, vol. 171, Aug. 1955, p. 360.

145. DAVIS, G.L.: Embrittlement of Tungsten Wires by Contaminants. Nature, vol. 181, Apr. 1958, p. 1198.

146. PETRASEK, DONALD W.: Elevated-Temperature Tensile Properties of Alloyed Tungsten Fiber Composites. NASA TN D–3073, 1965.

147. CRATCHLEY, D.: Factors Affecting the UTS of a Metal/Metal-Fibre-Reinforced System. Powder Met., vol. 11, 1963, pp. 59–72.

148. CRATCHLEY, D.; AND BAKER, A.A.: The Tensile Strength of a Silica-Fibre-Reinforced Aluminum Alloy. Metallurgia, vol. 69, no. 414, 1964, pp. 153–159.

149. BASKEY, R.H.; DAVIES, G.F.; AND SCHWOPE, A.D.: Fiber-Reinforced, Sintered Composites. Vol. II, Applications of Modern Developments In Powder Metallurgy, H. H. Hausner, ed., Plenum Press, 1966, pp. 330–346.

150. JECH, R.W.; WEBER, E.P.; AND SCHWOPE, A.D.: Fiber-Reinforced Titanium Alloys. Reactive Metals, vol. 2 of Metallurgical Soc. Conferences, W.R. Clough, ed., Interscience, 1959, pp. 109–119.

151. ANON.: Industrial Research, Dec. 1968, p. 60.

152. ANON.: Tungsten Fiber-Reinforced Nickel Superalloy. NASA Tech Brief 68–10369, Oct. 1968.

153. GATTI, A.; FEINGOLD, E.; GEBHARDT, J.J.; BERRY, J.M.; AND CORDUA,

V.A.: Study of the Growth Parameters Involved in Synthesizing Boron Carbide Filaments. General Electric Rept. 214–1B6, 1966.

154. WEETON, JOHN W.; AND SIGNORELLI, ROBERT A.: Fiber-Reinforced Metal Composites Under Study at Lewis Research Center. NASA TM X–52444.
155. ANON.: Investigation of Fiber-Strengthened-Cast Cobalt-Base Alloys. NASA CR–87811, 1967.
156. SUTTON, WILLARD H.; AND CHRONE, JAUN: Development of High-Strength, Heat-Resistant Alloys by Whisker Reinforcement. Metals Eng. Quarterly, vol. 3, no. 1, March 1963, pp. 44–51.
157. ARRIDGE, R.G.C.; BAKER, A.A.; AND CRATCHLEY, D.: Metal-Coated Fibres and Fibre Reinforced Metals. J. Sci. Instruments, vol. 41, 1964, pp. 259–261.
158. QUATINETZ, MAX; WEETON, JOHN W.; AND HERBELL, THOMAS P.: Studies of Tungsten Composites Containing Fibered or Reacted Additives. NASA TN D–2757, 1965.
159. JECH, ROBERT W.; WEETON JOHN W.; AND SIGNORELLI, ROBERT A.: Fibering of Oxides in Refractory-Metal Matrices. NASA TN D–3923, 1967.
160. BLAKENSHIP, CHARLES P.: Oxide Deformation and Fiber Reinforcement in a Tungsten Metal-Oxide Composite. NASA TN D–4475, 1968.
161. ANON.: Controlled Porosity Powder Metallurgy. Brochure of Hughes Research Laboratories.
162. BOOTH, FRANKLIN W.: Condenser-Separator. U.S. Patent 3,420,069, 1969.
163. MATT, R.E.; AND WARGA, J.J.: Development of Silver Infiltrated Tungsten Nozzles for Uncooled Rocket Motors. Paper presented at the 5th Plansee Seminar, Reutte/Tyrol, June 1964.
164. GESSNER, F.B.; SWARTZKOPF, P.; AND WEISERT, E.D.: Self-Cooled Rocket Nozzles. AF339657–9166, 1962.
165. BARTH, V.D.; AND MCINTIRE, H.O.: Tungsten Powder Metallurgy. NASA SP–5035, 1965.
166. CRAWFORD, MARTIN; GESSNER, F.B.; AND BERRY, MAURICE R., JR.: An Analysis of the Transient Behavior of Infiltrated Tungsten Composites Including the Effect of the Melt Layer. NASA CR–103231, 1969.
167. PRICE, JOSEPH: Design, Fabrication, and Evaluation of Tungsten Encapsulated Silver-Infiltrated Porous Tungsten Rocket Nozzle Inserts. NASA CR–66759, 1969.
168. MICKELSEN, WILLIAM R.; AND KAUFMAN, HAROLD R.: Status of Electrostatic Thrustors for Space Propulsion. NASA TN D–2172, 1964.
169. TODD, H.H.; AND TEEM, J.M.: Surface Ion Source Phenomena and Technology, Part II, Porous Materials and Technology. Electro-Optical Systems, Inc. Rept. no. 16, 1963.
170. TURK, R.R.; AND MCKEE, W.E.: Alloy Ionizer Fabrication. NASA CR–54677, 1966.
171. GRAHM, JOHN W.; AND MALIK, RAJ K.: Development of Large-Size Finished Porous Tungsten Ionizers. NASA CR–54189, 1965.
172. LACHANCE, M.; AND KUSKEVICS, G.: Ionizer-Reservoir Development Studies Electro-Optical Systems, Inc. Rept. no. 2150, 1963.

173. LaChance, M.; Kuskevics, G.; and Thompson, B.: Porous Ionizer Development and Testing. NASA CR–54016, 1964.

174. LaChance, M.; Thompson, B.; Todd, H.; and Kuskevics, G.: Development of Composite Ionizer Materials. NASA CR–54188, 1965.

175. Saunders, Neal T.: Experimental Method of Producing Tungsten for Ion Rocket Engines. NASA TN D–864, 1961.

176. Saunders, Neal T.: Method of Producing Porous Tungsten Ionizers for Ion Rocket Engines. U.S. Patent 3,141,769, 1964.

177. Bryant, P.J.; Gutshall, P.L.; and Taylor, L.H.: A Study of Mechanisms of Graphite Friction and Wear. J. Wear, vol. 7, no. 1, 1964, p. 118.

178. Elsey, H.M.: Treatment of High Altitude Brushes by Application of Metallic Halides/Trans, Electrical Eng., vol. 64, Aug. 1945, pp. 276–579.

179. Horton, J.C.: Electrical Contacts in Vacuum (A) Brushes. Status Rept. no. 1, MSFC TP–S&M–61–19, 1961.

180. Ulrich, Donald R.; and King, Harry M.: The Kinetics of the Sintering of Hot-Pressed Molybdenum Disulfide and Molybdenum Disulfide-Silver Compositions and the Effect on the Electrical Conduction Processes. NASA TM X–53111, 1964.

181. Ulrich, Donald R.: An Analysis of the Variation in Wear Life of Hot Pressed Molybdenum Disulfide-Silver Electrical Contact Brushes in Vacuum. NASA TM X–53146, 1964.

182. Horton, J.C.: Electrical Contacts in Vacuum (A) Brushes. Status Report no. 2. MSFC MTP–P&VE–M–62–17, 1962.

183. Magie, P.M.: Self-Lubricating Composites. Bemol, Inc. Tech. Data Rept. 208, Mar., 1966.

184. Bowen, P.H.: Analytical and Experimental Study of Adapting Bearings for Use in an Ultrahigh Vacuum Environment AEDC–TDR–62–51, 1962.

185. Magie, Peter M.: A Review of the Properties and Potentials of the New Heavy Metal Derivative Solid Lubricants. Paper presented at the 21st ASLE Annual Meeting (Pittsburgh, Pa.), May, 1966.

186. Saunders, Neal T.; et al.: Conference on New Technology, Lewis Research Center (Cleveland, O.), June 1964, p. 64.

187. Halpert, Gerald H.; and Webster, W.H.: Bibliography of Secondary Aerospace Batteries and Battery Materials. NASA SP–7027, 1969.

188. Halpert, Gerald H.: Nickel Powders and Plaques for Nickel-Cadmium Cell Plates. NASA TM X–63425, 1968.

189. Bidler, J.L.; and Fisher, J.L.: Preparation and Evaluation of Fiber-Metal-Nickel Battery Plaques. NASA CR–54777, 1965.

190. McCallum, J.; Schaer, G.R.; Trevethan, D.G.; Faust, C.L.: Development of Large-Internal-Surface-Area Nickel-Metal Plaques. NASA CR–54831, 1965.

191. Stafford, W.H.; and Croft, R.M.: Artificial Satellites and Successful Space Probes, 1957–1960. NASA TN D–601, 1961.

192. Peterson, Marshall B.; and Johnson, Robert L.: Friction Studies of Graphite and Mixtures of Graphite with Several Metallic Oxides and Salts at Temperatures to 1000° F. NACA TN–3657, 1956.

193. Johnson, Robert L.; Swikert, Max.; and Bisson, Edmund E.: Friction and Wear of Hot-Pressed Bearing Materials Containing Molybdenum Disulfide. NACA TN–2027, 1950.

194. BISSON, EDMUND E.; AND ANDERSON, WILLIAM J.: Advanced Bearing Technology. NASA SP–38, 1964.

195. FUSARO, ROBERT L.; AND SLINEY, HAROLD E.: Preliminary Investigation of Graphite Fluoride $(CF_x)_n$ as a Solid Lubricant. NASA TN D–5097, 1969.

196. SLINEY, HAROLD E.: Rare Earth Fluorides and Oxides—An Exploratory Study of Their Use as Solid Lubricants at Temperatures to 1800° F (1000° C). NASA TN D–5301, 1969.

197. BRAINARD, WILLIAM A.: The Thermal Stability and Friction of the Disulfides, Diselenides, and Ditellurides of Molybdenum and Tungsten in Vacuum (10^{-9} to 10^{-6} Torr). NASA TN D–5141, 1969.

198. WISANDER, DONALD W.; AND JOHNSON, ROBERT L.: Friction and Wear of Nine Selected Polymers with Various Fillers in Liquid Hydrogen. NASA TN D–5073, 1969.

199. PETERSON, MARSHALL B.; AND JOHNSON, ROBERT L.: Friction of Possible Solid Lubricants with Various Crystal Structures. NACA TN 3334, 1954.

200. BOES, DAVID J.: New Solid Lubricants—Their Preparations, Properties, and Potential for Aerospace Applications. Trans. IEEE, Aerospace, vol. 2, no. 2, April 1964, pp. 457–466.

201. TOULOUKIUN, Y.S., ED.: Thermophysical Properties of High Temperature Solid Materials, vol 5. Macmillan Co., 1967, p. 691.

202. HOPKINS, VERN; GADDIS, D.H.; HUBBELL, R.D.; AND HOLM, F.W.: Research on Bearing Lubricants for Use in High Vacuum. NASA CR–58039, 1964.

203. RUTHERFORD, JOHN L.; AND SWAIN, WILLIAM B.: Research on Materials for Gas Lubricated Gyro Bearings. NASA CR–80000, 1966.

204. RUTHERFORD, JOHN L.; AND SWAIN, WILLIAM B.: Alumina Bearing in Gas Lubricated Gyros. NASA CR–88597, 1967.

205. SHEIB, WALTER S., JR.: Some Applications of Chemical Engineering in the Nuclear Rocket Program. Paper presented at the 62nd AICHE Annual Meeting (Washington, D.C.), Nov., 1969.

206. BARD, R.J.; ET AL.: Pyrolytic Carbons Deposited in Fluidized Beds at 1200° to 1400° C from Various Hydrocarbons. Carbon, vol. 6, 1968, pp. 616.

207. BOKROS, J.C.; AND SCHWARTZ, A.S.: A Model to Describe Neutron-Induced Dimensional Charges in Pyrolytic Carbon. Carbon, vol. 5, 1967, pp. 481–492.

208. BARD, R.J.; AND TAUB, J.M.: Coated Particle Fuel for UTREX. Paper presented at the AIME Nuclear Metallurgy Symposium in High-Temperature Nuclear Fuels (Delavar, Wisc.), 1966

209. HARADA, Y.: Graphite-Metal Composites. NASA CR–77114, 1966.

210. HARADA, Y.: Metal Carbide-Graphite Composites. NASA CR–89079, 1967.

211. HARADA, Y.: Metal Carbide-Graphite Composites. NASA CR–97616, 1968.

212. HARADA, Y.: Metal Carbide-Graphite Composites. NASA CR–92793, 1968.

213. HARADA, Y.: Metal Carbide-Graphite Composites. NASA CR–100842, 1969.

214. NORTON, J.T.; AND LEWIS, R.K.: Properties of Nonstoichiometric Metallic Carbides. NASA CR–67380, 1964.

215. LEIPOLD, M.H. AND BECHER, P.F.: Fabrication and Characterization of Hot-Pressed Tantalum Carbide. NASA CR–90036, 1967.
216. RILEY, ROBERT E.; ET AL., Carbide-Graphite Composites—Second Progress Rept. LA–3652–MS, Los Alamos Scientific Laboratory, 1967.
217. SLIVKA, WILLIAM R.: Manufacture and Design Technology NERVA Program. Paper presented at the Propulsion and Energetics Panel of AGARD-NATO (London, England), Apr. 6, 1969.
218. KEIL, R.W.; RILEY, R.E.; AND SHEINBERG, H.: Feasibility Study for the Fabrication of Cu-B_4C Sheet. LA–3570–MS, 1965.
219. BUZZARD, ROBERT J.: High-Temperature Creep-Rupture Properties of a Tungsten-Uranium Dioxide Cermet Produced from Coated Particles. NASA TM X–1625, 1968.
220. TAKKUNEN, PHILIP D.: Fabrication of Cermets of Uranium Nitride and Tungsten or Molybdenum from Mixed Powders and from Coated Particles. NASA TN D–5136, 1969.
221. TAKKUNEN, PHILIP D.: Compatibility Tests of Molten Uranium with Tungsten and Tungsten-1.5 Percent Hafnium. NASA TN D–5076, 1969.
222. MCINTOSH, A.B.; AND BAGLEY, K.Q.: Selection of Canning Materials for Reactors Cooled by Sodium/Potassium and Carbon Dioxide. J. Inst. Metals, vol. 84, 1955–6, pp. 251–270.

☆ U.S. Government Printing Office: 1972 O—438–546